STUDY OF NATURAL CONVECTIVE HEAT TRANSFER OF NANOFLUIDS IN CUBICAL ENCLOSURE

by

FARIZA TUL KOABRA
Roll no: P0409094003P, Session: April-2009

DOCTOR OF PHILOSOPHY
IN
MATHEMATICS

Department of Mathematics
BANGLADESH UNIVERSITY OF ENGINEERING AND TECHNOLOGY, DHAKA-1000, BANGLADESH
June – 2016

The thesis titled on **"Study of natural convective heat transfer of nanofluids in cubical enclosure"** by **FARIZA TUL KOABRA**, Roll no: **0409094003P**, Session April-2009 has been accepted as satisfactory in partial fulfillment of the requirement for the degree of **Doctor of Philosophy in Mathematics** on 25 June, 2016.

Board of Examiners

1. _____

Dr. Md. Abdul Alim — Chairman (Supervisor)
Professor
Department of Mathematics
BUET, Dhaka-1000

2. _____

Dr**. Noor Al Quddus** — Member (Co Supervisor)
Associate Professor
Department of Mechanical Engineering
BUET, Dhaka-1000

3. _____

Head — Member (Ex-Officio)
Department of Mathematics
BUET, Dhaka-1000

4. _____

Dr. Md. Mustafa Kamal Chowdhury — Member
Professor
Department of Mathematics
BUET, Dhaka-1000

5. _____

Dr. Md. Abdul Maleque Member
Professor
Department of Mathematics
BUET, Dhaka-1000

6. _____

Dr. Md. Quamrul Islam Member
Professor
Department of Mechanical Engineering
BUET, Dhaka-1000

7. _____

Dr. Sk. Sekender Ali Member
Professor
Department of Civil Engineering
BUET, Dhaka-1000

8. _____

Dr. Md. Abdur Razzaq Akanda Member
Professor (External)
Department of Mechanical & Chemical Engineering
Islamic University of Technology, Gazipur-1704

DEDICATION

This work is dedicated

to

My Late Father, **Md. Shahidul Islam**

Author's declaration

I am hereby declaring that the work in this dissertation was being carried out in accordance with the regulations of Bangladesh University of Engineering and Technology (BUET), Dhaka, Bangladesh .The work is also original except where indicated by and attached with special reference in the context and no part of it has been submitted for any attempt to get other degrees or diplomas.

All views expressed in the dissertation are those of the author and in no way or by no means represent those of Bangladesh University of Engineering and Technology, Dhaka. This dissertation has not been submitted to any other University for examination either in home or abroad.

_____

FARIZA TUL KOABRA

Date: 25th June - 2016

Acknowledgements

At first all praise belongs to almighty Allah, the most merciful, benevolent to mankind and His action.Without His will kindness and mercy, the completion of this work would have never been possible.

It is my pleasure to thank those who made this research possible. I would like to express my sincere gratitude to my supervisor Dr. Md. Abdul Alim, Professor, Department of Mathematics, Bangladesh University of Engineering and Technology, Dhaka for his valuable guidance and advice. He has been very supportive and patient throughout the progress of my thesis.

I would like to express my appreciation and heartfelt indebtedness to my co supervisor Dr.Noor Al Quddus, Associate Professor, Department of Mechanical Engineering, BUET, for his constant support and generous help.

I would like to convey my deeply indebted to Prof. Dr. Md. Mustafa Kamal Chowdhury, Prof. Dr. Md. Abdul Maleque and the other members of my doctoral committee for their time and advice and all other teachers and concerned of this department for their thoroughly help and liberal co-operation in providing me all necessary help from the department during my course of Ph.D. Degree.

Finally, my family has played an integral role in my studies. I would like to thank my parents for always believing in me and to whom I owe everything. I am extremely fortunate to have my husband Dr. Md. Salim Kaiser, whose smile encouragements and endless patience have kept me going through it all. It would not have been possible to carry out this study successfully without the continuous inspiration and encouragement from Dr. Salim.

Abstract

This thesis reports a study on natural convection heat transfer and fluid flow in a square cavity and cubical enclosure filled with Cu–Water nanofluid which is investigated numerically. The current geometry is analyzed numerically using finite element method. One vertical wall of the cavity is hot, the opposite one is cold and the rest of the walls are adiabatic. In this thesis, a finite element method for steady-state incompressible natural convection flows has been developed. The physical problems are represented mathematically by different sets of governing equations along with the corresponding boundary conditions. The non-dimensional governing equations are discritized by using Galerkin weighted residual method of finite element formulation. The numerical results are reported for the effect of Rayleigh numbers from 10^3 to 10^6, solid volume fractions 0, 0.02, 0.05, 0.08, 0.1, 0.15, 0.2 and average Nusselt number. The results of this investigation reveal that heat transfer rate is always higher for nanofluid than base fluid. Also clear water moves rapidly than nanofluid. The effects of coefficient of heat transfer are analyzed.

In addition natural convection of Cu-water nanofluid in a square cavity with circular disk is investigated numerically. Also natural convection of Cu-water nanofluid in a cubical cavity is investigated. The variable thermal conductivity and variable viscosity models are compared to both the Maxwell-Garnett model and the Brinkman model. It is found that at high Rayleigh numbers the average Nusselt number is more sensitive to the viscosity models than to the thermal conductivity models.

The results show highest heat transfer enhancement in the conduction dominated flow regime, where the enhanced thermal properties of nanofluids play an important role. When convection is the dominant heat transfer mechanism, using nanofluids yields a smaller increase in heat transfer efficiency. The obtained results are presented in terms of streamlines and isotherms, heat transfer characteristics, Nusselt numbers for various Rayleigh numbers and for different solid volume fractions of nanoparticles. The results show that the Nusselt numbers increase with the increasing of Rayleigh numbers.

Comparisons with previously reported investigations are performed and the results show excellent agreement.

CONTENTS

Board of Examiners ..... **ii**
Author's declaration ..... **v**
Acknowledgements ..... **vi**
Abstract ..... **vii**
Nomenclature ..... **x**
List of tables ..... **xii**
List of figures ..... **xii**

CHAPTER 1 ..... **1**
Introduction **1**
1.1General 1
1.2 Nanofluid 4
1.3 Heat transfer mechanism 4
1.4 Convection 5
1.5 Some definitions 7
1.5.1 Thermal conductivity 7
1.5.2 Flow with in an enclosure 8
1.5.3 Boussinesq approximation 8
1.6 Dimensionless parameters 9
1.7 Computational details 11
1.8 Finite element method 13
1.9 The reason for finite element solution 15
1.10 FEM for viscous incompressible flow 18
1.11 Motivation 19
1.12 Main objectives of the work 20

CHAPTER 2 ..... **21**
Literature Review **21**

CHAPTER 3 ..... **29**
Theoretical Description **29**
3.1Mathematical Model 29
3.1.1 Mathematical Model of cubical cavity 29
3.1.2 Mathematical model of square cavity 31
3.1.3 Mathematical model of sqare cavity under magnetic field 32
3.1.4 Mathematical model of cubical cavity under magnetic field 33
3.2 Algorithm 35
3.3 Solution of system of equations 36
3. 4 Thermo physical properties 38

CHAPTER 4 39
Natural Convection of Cu-water Nanofluid in Square Cavity 39
4.1 Physical Model of Square Cavity 39
4.2 Model Validation 39
4.1.1 Natural convection of air filled in square cavity 39
4.1.2 Natural convection of Cu-water nanofluid in square cavity 40
4.1.3 Natural Convection of air in Square Cavity 41
4.2 Natural Convection of Cu-Water Nanofluid in Square Cavity 41
4.3 Natural convection of Cu-water nanofluid in square cavity with a circular disk. 49
4.3 .1 Adiabatic circular disk 49
4.3.2 Cold circular disk 56
4.3.3 Heated circular disk 62
4.4 Natural convection of Cu-water nanofluid in square cavity with a circular disk under a magnetic field 71

CHAPTER 5 79
Natural Convection of Cu-water Nanofluid in Cubical Cavity 79
5.1Introduction 79

CHAPTER 6 92
Natural convection of Cu-water nanofluid in cubical enclosure with circular cylinder 92
6.1 Introduction 92
6.2 Results and discussion 92
6.2.1 Cubical enclosure with adiabatic circular cylinder 92
6.2 .2 Cubical enclosure with heated circular cylinder 100

CHAPTER 7 110
MHD Natural Convection of Cu-Water Nanofluid in Cubical Cavity with Circular Cylinder 110
7.1 Introduction 110
7.2 Results and discussion 111

CHAPTER 8 125
Conclusions 125
8.1Extension of this work 127

References 128

Nomenclature

Cp	specific heat at constant pressure [J kg $^{-1}$K $^{-1}$]
d	diameter of disk [m]
g	gravitational acceleration [ms $^{-2}$]
h	convective heat transfer coefficient [Wm $^{-2}$K^{-1}]
k	thermal conductivity of fluid [Wm^{-1}K^{-1}]
H	length of the cavity [m]
Nu	Nusselt number
p	pressure
q	heat flux [Wm^{-2}]
P	non-dimensional pressure
Pr	Prandtl number
Ra	Rayleigh number
T	fluid temperature [K]
u	velocity in x-direction [ms $^{-1}$]
U	dimensionless horizontal velocity
v	velocity in y-direction [ms $^{-1}$]
V	dimensionless vertical velocity
U, V, W	Dimensionless velocity component in X, Y,Z direction [-]
u , v,w	velocity components in x, y,z direction [ms^{-1}]
X, Y,Z	Dimensionless Cartesian co-ordinates [-]
x , y,z	Cartesian co-ordinates [m]

Greek symbols

α	thermal diffusivity [m^{2}s $^{-1}$]
β	coefficient of thermal expansion [K^{-1}]
ϕ	nanoparticles volume fraction
θ	dimensionless fluid temperature
μ	dynamic viscosity of the fluid [m^{2}s^{-1}]
ν	kinematic viscosity of the fluid [m^{2}s^{-1}]

ρ density of the fluid [kgm^{-3}]

σ Electrical conductivity of the fluid

Subscripts

h Hot Wall

c Cold wall

s Solid Particle

nf Nanofluid

avg Average

List of tables

3.1 Thermo-physical properties of water and Cu nanoparticle. 38

4.1 Average Nusselt number for the hot wall of the air filled square cavity obtained by various studies are shown and compared with present study for different Rayleigh numbers 40

4.2 Comparison of average Nusselt number calculated on hot wall in Cu-water nanofluid filled square cavity with Khanafer et al. (2003) 40

4.3 Comparison of average Nusselt number obtained with the computer code and those of Fusegi et al. (1991) and Frederick et al. (2000) for air (Pr = 0.71) 41

List of figures

4.1 Schematic diagram of the physical system. 38

4.2 Streamlines and Isotherm patterns for φ=0 at different Rayleigh numbers. 43

4.3 Streamlines and Isotherm patterns for φ=0.05 at different Rayleigh numbers. 44

4.4 Streamlines and Isotherm patterns for φ=0.1 at different Rayleigh numbers. 45

4.5 Streamlines and Isotherm patterns for φ=0.15 at different Rayleigh numbers. 46

4.6 Streamlines and Isotherm patterns for φ=0.2 at different Rayleigh numbers. 47

4.7 Variation of average Nusselt number with different Rayleigh numbers for different volume fractions 48

4.8 Schematic view of a square cavity with a circular disk 49

4.9	Streamlines and Isotherm patterns for pure water for φ=0 at different Rayleigh numbers.	52
4.10	Streamlines and Isotherm patterns for Cu–water nanofluid for φ=0.05 for different Rayleigh numbers.	53
4.11	Streamlines and Isotherm patterns for Cu–water nanofluid for φ=0.1 for different Rayleigh numbers.	54
4.12	Streamlines and Isotherm patterns for Cu–water nanofluid for φ=0.15 for different Rayleigh numbers.	55
4.13	Streamlines and Isotherm patterns for Cu–water nanofluid for φ=0.2 for different Rayleigh numbers.	56
4.14	Streamlines and Isotherm patterns of pure water for φ=0 at different Rayleigh numbers.	58
4.15	Streamlines and Isotherm patterns of Cu–water nanofluid for φ=0.05 at different Rayleigh numbers.	59
4.16	Streamlines and Isotherm patterns of Cu–water nanofluid for φ=0.1 at different Rayleigh numbers.	60
4.17	Streamlines and Isotherm patterns of Cu–water nanofluid for φ=0.15 at different Rayleigh numbers.	61
4.18	Streamlines and Isotherm patterns of Cu–water nanofluid for φ=0.2 at different Rayleigh numbers.	62
4.19	Streamlines and Isotherm patterns of pure water for φ=0 at different Rayleigh numbers.	64
4.20	Streamlines and Isotherm patterns of pure water for φ=0.05 at different Rayleigh numbers.	65
4.21	Streamlines and Isotherm patterns of pure water for φ=0.1 at different Rayleigh numbers.	66
4.22	Streamlines and Isotherm patterns of pure water for φ=0.15 at different Rayleigh numbers.	67

4.23	Streamlines and Isotherm patterns of pure water for φ=0.2 at different Rayleigh numbers.	68
.4.24(a)	Average Nusselt number for different volume fraction of adiabatic circular disk.	70
4.24 (b)	Average Nusselt number for different volume fraction of cold circular disk.	70
4.24 (c)	Average Nusselt number for different volume fraction of heated circular disk.	71
4.25	Schematic view of the square cavity with a circular disk	72
4.26	Streamlines and isotherms patterns for Cu-water nanofluid for Ha=10 at φ = 0.1 for Ra =10^3 - 10^6.	76
4.27	Streamlines and isotherms patterns for Cu-water nanofluid for Ha=50 at φ = 0.1 for Ra =10^3 - 10^6.	77
4.28	Streamlines and isotherms patterns for Cu-water nanofluid for Ha=100 at φ = 0.1 for Ra =10^3 - 10^6.	78
4.29 (a)	Variation of the average Nusselt number with Hartmann numbers for different volume fractions φ = 0,0.05,0.1,0.15,0.2	79
4.29 (b)	Variation of the average Nusselt number with Hartmann numbers for different Rayleigh numbers Ra =10^3 - 10^6 for φ = 0.2	79
5.1	Schematic diagram of Cubical cavity	80
5.2	Contour plot of Cu-water Nanofluid of φ = 0.1 in 3D enclosure at Z=0.5 and square cavity for different Rayleigh Numbers.	83
5.3	Distribution of average Nusselt number in the z- direction(---)Nuavg (z) and (—) Nuoverall (three dimensional); • ,Nuavg (z) (two dimensional);(a) Ra=10^3; (b) Ra=10^4;(c) Ra=10^5; (d) Ra=10^6	85
5.4	Slice Plot of Cu-water nanofluid for Ra = 10^3 - 10^6 at φ=0.02	86
5.5	Iso surface Plot of Cu-water nanofluid for Ra = 10^3 - 10^6 at φ=0.02	87

5.6	Slice Plot of Cu-water nanofluid for Ra = 10^3 - Ra= 10^6 at φ=0.05	88
5.7	Iso surface Plot of Cu-water nanofluid for Ra = 10^3 - Ra= 10^6 at φ=0.05	89
5.8	Slice Plot of Cu-water nanofluid for Ra = 10^3 - Ra= 10^6 at φ=0.1	90
5.9	Iso surface Plot of Cu-water nanofluid for Ra = 10^3 - Ra= 10^6 at φ=0.1	91
6.1	Schematic diagram of Cubical cavity with adiabatic cylinder	93
6.2	Slice Plot of pure water for Ra = 10^3 - Ra= 10^6 at φ=0	95
6.3	Iso surface Plot of pure water for Ra = 10^3 - Ra= 10^6 at φ=0	96
6.4	Slice Plot of Cu-water nanofluid for Ra = 10^3 - Ra= 10^6 at φ=0.05	97
6.5	Iso surface Plot of Cu-water nanofluid for Ra = 10^3 - Ra= 10^6 at φ=0.05	98
6.6	Slice Plot of Cu-water nanofluid for Ra = 10^3 - Ra= 10^6 at φ=0.1	99
6.7	Iso surface Plot of Cu-water nanofluid for Ra = 10^3 - Ra= 10^6 at φ=0.1	100
6.8	Variation of average Nusselt number for different volume fractions φ =0, 0.02, 0.05, 0.08, 0.1 with Rayleigh numbers Ra=10^3- 10^6.	101
6.9	Slice Plot of Cu-water nanofluid for Ra = 10^3 - Ra= 10^6 at φ=0.1	103
6.10	Iso surface Plot of Cu-water nanofluid for Ra = 10^3 - Ra= 10^6 at φ=0.1	104
6.11	Slice Plot of Cu-water nanofluid for Ra = 10^3 - Ra= 10^6 at φ=0.05	105
6.12	Iso surface Plot of Cu-water nanofluid for Ra = 10^3 - Ra= 10^6 at φ=0.05	106
6.13	Slice Plot of Cu-water nanofluid for Ra = 10^3 - Ra= 10^6 at φ=0.08	107
6.14	Iso surface Plot of Cu-water nanofluid for Ra = 10^3 - Ra= 10^6 at φ=0.08	108
6.15	Streamlines and Isotherms Plot of Cu-water nanofluid for Ra = 10^3 - 10^6 at φ=0.1	109
6.16	Variation of average Nusselt number for different volume fractions φ =0, 0.02, 0.05, 0.08, 0.1 with Rayleigh number Ra=10^3- 10^6.	110
7.1	Schematic diagram of Cubical cavity with adiabatic cylinder	111
7.2	Slice Plot of pure water for Ra = 10^3 - 10^6 at φ=0	115

7.3	Iso surface Plot of pure water for Ra = 10^3 - 10^6 at φ=0	116
7.4	Slice Plot of Cu-water nanofluid for Ra = 10^3 - 10^6 at φ=0.02	117
7.5	Iso surface Plot of Cu-water nanofluid for Ra = 10^3 - 10^6 at φ=0.02	118
7.6	Slice Plot of Cu-water nanofluid for Ra = 10^3 - 10^6 at φ=0.05	119
7.7	Iso surface Plot of Cu-water nanofluid for Ra = 10^3 - 10^6 at φ=0.05	120
7.8	Slice Plot of Cu-water nanofluid for Ra = 10^3 - 10^6 at φ=0.08	121
7.9	Iso surface Plot of Cu-water nanofluid for Ra = 10^3 - 10^6 at φ=0.08	122
7.10	Slice Plot of Cu-water nanofluid for Ra = 10^3 - 10^6 at φ=0.1	123
7.11	Iso surface Plot of Cu-water nanofluid for Ra = 10^3 - 10^6 at φ=0.1	124
7.12	Variation of average Nusselt number for different volume fractions φ = 0, 0.02, 0.05, 0.08, 0.1 with Rayleigh numbers Ra = 10^3 - 10^6.	125

CHAPTER 1

Introduction

1.1 General

Heat transfer is that science which seeks to predict the energy transfer which may take place between material bodies as a result of a temperature difference. The science of heat transfer seeks not merely to explain how heat energy may be transferred, but also to predict the rate at which the exchange will take place under certain specified conditions.

The phenomenon of heat transfer was known to human being even in the primitive age when they used to use solar energy as a source of heat. Heat transfer in its initial stage was conceived with the invention of fire in the early age of human civilization. Since then its knowledge and use has been progressively increasing each day as it is directly related to the growth of human civilization. With the invention of stream engine by James watt in 1765 A. D., the phenomenon of heat transfer got its first industrial recognition and after that its use extended to a great extent and spread out in different spheres of engineering fields. In the past three decades, digital computers, numerical techniques and development of numerical models of heat transfer have made it possible to calculate heat transfer of considerable complexity and thereby create a new approach to the design of heat transfer equipment.

The study of the universe has led to the realization that all physical phenomena are subject to natural laws. The term natural might well be used to describe the framework or system of fundamental and universal importance within this system is the mechanisms for the transfer of heat. Heat transfer is a branch of applied thermodynamics. It estimates the rate at which heat is transferred across the system boundaries subjected to specific temperature differences and the temperature distribution of the system during the process. Whereas classical thermodynamics deals with the amount of heat transferred during the process. Heat transfer processes have always been an integral part of our environment.

The study of temperature and heat transfer is of great importance to the engineers because of its almost universal occurrence in many branches of science and

engineering. Although heat transfer analysis is most important for the proper sizing of fuel elements in the nuclear reactors cores to prevent burnout, the performance of aircraft also depends upon the case with which the structure and engines can be cooled. The design of chemical plants is usually done on the basis of heat transfer analysis and the analogous mass transfer processes. The transfer and conversion of energy from one form to another is the basis to all heat transfer process and hence, they are governed by the first as well as the second law of thermodynamics. Heat transfer is commonly associated with fluid dynamics. The knowledge of temperature distribution is essential in heat transfer studies because of the fact that the heat flow takes place only wherever there is a temperature gradient in a system. The heat flux which is defined as the amount of heat transfer per unit area in per unit time can be calculated from the physical laws relating to the temperature gradient and the heat flux.

Natural convection is a mechanism or type of heat transfer in which the fluid motion is not generated by any external source (like a pump, fan, suction device, etc.) but only by density differences in the fluid occurring due to temperature variations. In natural convection, fluid surrounding a heat source receives heat, becomes less dense and rises. Heat transfer creates a cycle called convection current where a warm fluid is replaced by a cooler one. Two heat transfer mechanisms commonly researched are natural convection and forced convection. Natural convection is a mechanism that moves fluids away from areas of high temperature towards areas of low temperature. This occurs because the fluid touching the high temperature area is gaining energy and becoming less dense, this makes that part of the fluid move upward in the body of fluid. As the higher temperature fluid moves up the lower temperature, therefore more dense, fluid from the top moves down under the force of gravity to take its place. Forced convection is a mechanism that induces movement of a fluid by the application of an external force. Examples of the devices used to apply the external force are a fan or pump. Typically forced convection is used to increase heat transfer of a system when natural convection does not provide adequate heat transfer.

One of the relevant ways to enhance the heat transfer is by adding solid nanoparticle with high thermal conductivity in the fluid. The resulting fluid is a suspension of the solid nanoparticle in the base fluid which is called a “nanofluid”. Nanofluids are

engineered colloidal suspensions of nanoparticles in a base fluid. The nanoparticles used in nanofluids are typically made of metals, oxides, carbides, or carbon nanotubes. Common base fluids include water, ethylene glycol and oil. Nanofluids have novel properties that make them potentially useful in many applications in heat transfer, including microelectronics, fuel cells, pharmaceutical processes, and hybrid-powered engines, Engine cooling/vehicle thermal management, domestic refrigerator, chiller, heat exchanger, and nuclear reactor, in grinding, in machining, in space, defense and ships, and in boiler flue gas temperature reduction by Bejan,A.(2004). They exhibit enhanced thermal conductivity and the convective heat transfer coefficient compared to the base fluid. Natural convection fluid flow and heat transfer are encountered in a number of engineering and industrial applications such as cooling of electronic equipment, solar energy, and geophysics by Ostrach, S. (1988). A major limitation against enhancing the heat transfer in such engineering systems is the inherently low thermal conductivity of the commonly used fluids, such as, air, water and oil. Nanofluids were introduced in order to circumvent the above limitation. There are a number of very recent studies, using conventional numerical methods, on the natural convection heat transfer in cavities filled with nanofluids.

A high-resolution, finite element numerical study is reported on three-dimensional steady-state natural convection of Cu-water nanofluid for four Rayleigh numbers in a cubical enclosure which is heated differentially at one side walls. The left vertical wall of cubical enclosure was heated and the right vertical wall was cold. The details of the three-dimensional flow and thermal characteristics were described by Fusegi, T. *et. al* (1991). The vastly expanded hardware capabilities together with such advanced computational techniques will enable us to implement the three-dimensional numerical simulations of the flow and heat transfer properties in the enclosure. These numerical results will allow proper verification of the published paper. It is also significant that by cross-checking the results, the extent of the applicability of the earlier two-dimensional results to actual three-dimensional systems will be illuminated by Ozoe, H.and Okada, K. (1989).

There are some mechanisms which explain the enhancement of thermal conductivity in nanofluids such as interfacial layer at the particle or liquid interface, Brownian motion of the particles, nanoparticles clustering, temperature and nanoparticles size

or shape. The utilization of the nanofluids as a convenient way to access the better performance of systems has been investigated by numerous researchers in the past several years. There are a number of very recent studies, using conventional numerical methods, on the free convection heat transfer in square cavity filled with nanofluids. Few works has considered the three-dimensional natural convection which gives a more realistic presentation of the fluid motion and the heat exchange within the cavity by Frederick, R. L. and Quiroz, F. (2000).

1.2 Nanofluid

The fluid with solid-sized nanoparticles suspended in them is called “nanofluid”. In other words, Nanofluid is a fluid containing nanometer-sized particles, called nanoparticles. It is well known that 1 Nano-meter = 10^{-9}m. Also, a nanoparticle is defined as the smallest unit that can still behave as a whole entity in terms of properties and transport. Suspensions of nanoparticles (i.e., particles with diameters < 100 nm) in liquids, termed nanofluids, show remarkable thermal and optical property changes from the base liquid at low particle loadings. Nanofluids have been studied for at least 15 years and have shown promise to enhance a wide range of liquid properties. Applications of nanoparticles in thermal field are to enhance heat transfer from solar collectors to storage tanks, to improve efficiency of coolants in transformers etc. To determine the effectiveness of nanofluids in solar applications, their ability to convert light energy to thermal energy must be known. That is, their absorption of the solar spectrum must be established. The efficiency of these collectors is limited by the absorption properties of the working fluid, which is very poor for typical fluids used in solar collectors. It has been shown that mixing nanoparticles in a liquid (nanofluid) has a dramatic effect on the liquid thermophysical properties such as thermal conductivity. Nanoparticles also offer the potential of improving the radiative properties of liquids, leading to an increase in the efficiency of absorption solar collectors.

1.3 Heat transfer mechanism

Heat is the form of energy that can be transferred from one system to another as a result of temperature difference. The science that deals with the determination of the rates of such energy transfers is the heat transfer. The transfer of energy as heat is

always from the higher temperature medium to the lower temperature one, and heat transfer stops when the two mediums reach the same temperature.

Heat can be transferred in three different mechanisms or modes: conduction, convection and radiation. All modes of heat transfer require the existence of a temperature difference, and all modes are from the high temperature medium to a lower temperature one. In reality, the combined effect of these three modes of heat transfer control temperature distribution in a medium. Below we give a brief description of convection mode.

1.4 Convection

Convective heat transfer is the heat transfer mechanism affected by the flow of fluids. The amount of energy and matter is conveyed by the fluid can be predicted through the convective heat transfer. The convective heat transfer bifurcates into two branches; the natural convection and the forced convection. Forced convection regards the heat transport by induced fluid motion that is forced to happen. This induced flow needs consistent mechanical power. But natural convection differs from the forced convection through the fluid flow driving force that happens naturally. The flows are driven by the buoyancy effect due to the presence of density gradient and gravitational field. The density difference gives rise to buoyancy effects due to which the flow is gyrated. Buoyancy is due to the combined presence of the fluid density gradient and the body force. As the temperature distribution in the natural convection depends on the intensity of the fluid currents that is dependent on the temperature potential itself, the qualitative and quantitative analysis of natural convection heat transfer is very difficult. Numerical investigation instead of theoretical analysis is more needed in this field. Two generes of natural convection heat transfer phenomena can be observed in the nature. One is that external free convection that is caused by the heat transfer interaction between a single wall and a very large fluid reservoir adjacent to the wall. Another is that internal free convection which befalls within an enclosure. The thermo-fluid fields developed inside the cavity depend on the orientation and geometry of the cavity. Reviewing the nature and the practical applications, the enclosure phenomena can loosely be organized into two classes. One of these is enclosure heated from the side which is found in solar collectors, double wall insulations, laptop cooling system and air circulation

inside the room and another one is enclosure heated from below which is happened in geophysical system like natural circulation in the atmosphere, the hydrosphere and the molten core of the earth.

Convective heat transfer or, simply, convection is the study of heat transport processes affected by the flow of fluids. Convective heat transfer, clearly, is a field at the interface between two older fields-heat transfer and fluid mechanics. Before reviewing the foundations of convective heat transfer methodology, it is worth reexamining the historic relationship between fluid mechanics and heat transfer at the interface. Especially during the past 100 years, heat transfer and fluid mechanics have enjoyed a symbiotic relationship in their parallel development. Convection is that mode of heat transfer where energy exchange occurs between the particles by convection current. It may be explained as; when fluid flows over a solid body or inside a channel while temperatures of the fluid and the solid surface are different, heat transfer between the fluid and the solid surface takes place as a consequences of the motion of the fluid relative to the surfaces; the mechanism of heat transfer called convection. In the diversity of the studies related to heat transfer, considerable effort has been directed at the convective mode, in which the relative motion of the fluid provides an additional mechanism for the transfer of heat and materials. Convection is inevitably coupled with the conductive mechanism, since though the fluid motion modifies the transport process, the eventual transfer of heat from one fluid element to another in its neighborhood is through conduction.

The convection mode of heat transfer is further divided into two basic processes. If the motion of the fluid arises due to an external agent, such as the externally imposed flow of fluid stream over a heated object, the process is termed as forced convection. The fluid flow may be the results of, for instance, a fan, a blower, the wind or the motion of the heated object itself. Such problems are very frequently encountered in technology where heat transfer to, or from, a body is often due to an imposed flow of a fluid at a temperature different from that of the body. It has wide applications in compact heat exchanger, central air conditioning system, cooling tower, gas turbine blade, internal cooling passage, chemical engineering process industries, nuclear reactors and many other cases. If, on the other hand, no such externally induced flow is provided and the flow arises “naturally” simply due to the effect of a density

difference, resulting from a temperature difference, in a body force field, such as gravitational field, the process is termed as natural or free convection. The density deference gives rise to buoyancy effects due to which the flow is generated. A heated body cooling in ambient air generates such a flow in the region surrounding it. Similarly, the buoyant flow arising from heat rejection to the atmosphere and to other ambient media, Heat transfer by free convection occurs in many engineering applications, such as heat transfer from hot radiators, refrigerator coils, transmission lines, electric transformers, electric heating elements and electronic equipment etc.

The convection heat transfer that is neither dominated by pure forced nor pure free convection, but is rather a combination of the two is referred as combined or mixed convection. The buoyancy forces that arise as the results of the temperature differences and which cause the fluid flow in free convection also exist when there is a forced flow. The effects of these buoyancy forces are however; usually negligible when there is a forced flow. In some cases, however, these buoyancy forces do have a significant influence on the flow and consequently on the heat transfer rate. In such cases, the flow about the body is a combination of forced and free convection; such flows are referred to as mixed convection. For example, heat transfer from one fluid to another fluid through the walls of pipe occurs in many practical devices. In this case, heat is transferred by convection from the hotter fluid to the one surface of the pipe. Heat is then transferred by conduction through the walls of the pipe. Finally, heat is transferred by convection from the other surface to the colder fluid.

1.5 Some definitions

Some basic definitions that are related to the current study are presented below.

1.5.1 Thermal conductivity

Thermal conductivity of a material can be defined as the rate of heat transfer through a unit thickness of the material per unit area per unit temperature difference. Therefore the thermal conductivity of a material is a measure of the ability of the material to conduct heat. A high value for thermal conductivity indicates that the material is a good heat conductor, and a low value for thermal conductivity indicates that the material is a poor heat conductor or insulator. For example the materials such as copper and silver that are good electric conductors are also good heat conductors,

and have high values of thermal conductivity. Materials such as rubber, wood are poor conductors of heat and have low conductivity values. The rate of heat conduction through a medium depends on the geometry of the medium, its thickness, and the material of the medium, as well as the temperature difference across the medium.

1.5.2 Flow with in an enclosure

The flow within an enclosure consisting of two horizontal walls, at different temperatures, is an important circumstance encountered quite frequently in practice. In all the applications having this kind of situation, heat transfer occurs due to the temperature difference across the fluid layer, one horizontal solid surface being at a temperature higher than the other. If the upper plate is the hot surface, then the lower surface has heavier fluid and by virtue of buoyancy the fluid would not come to the lower plate. Because in this case the heat transfer mode is restricted to only conduction. But if the fluid is enclosed between two horizontal surfaces of which the upper surface is at lower temperature, there will be the existence of cellular natural convective currents which are called as Benard cells. For fluids whose density decreases with increasing temperature, this leads to an unstable situation.

1.5.3 Boussinesq approximation

The governing equations for convection flow are coupled elliptic partial differential equations and are, therefore, of considerable complexity. The major problems in obtaining a solution to these equations lie in the inevitable variation of density with temperature, or concentration, and in their partial, elliptic nature. Several approximations are generally made to considerably simplify these equations. Among them Boussinesq approximation attributed to Boussinesq (1903) is considered here. In flows accompanied by heat transfer, the fluid properties are normally functions of temperature. The variations may be small and yet be the cause of the fluid motion. If the density variation is not large, one may treat the density as constant in the unsteady and convection terms, and treat it as variable only in the gravitational term. This is called the Boussinesq approximation.

1.6 Dimensionless parameters

The dimensionless parameters can be thought of as measures of the relative importance of certain aspects of the flow. Some dimensionless parameters related to our study are discussed below:

Grashof number *Gr*

The flow regime in free convection is governed by the dimensionless Grashof number, which represent the ratio of the buoyancy force to the viscous forces acting on the fluid, and is defined as

$$Gr = \frac{g\,\beta\,L^3\left(T_w - T_\infty\right)}{\nu^2}$$

where g is the acceleration due to gravity, β is the volumetric thermal expansion coefficient, T_w is the wall temperature, T_∞ is the ambient temperature, L is the characteristic length and ν is the kinematics viscosity. The Grashof number plays the same role played by the Reynolds number in free convection. As such, the Grashof number provides the main criterion in determining whether the fluid flow is laminar or turbulent in free convection. For vertical plates, the critical value of the Grashof number is observed to be about 10^9. Therefore, the flow regime on a vertical plate becomes turbulent at Grashof numbers greater than10^9.

Prandtl Number *Pr*

The relative thickness of the velocity and the thermal boundary layers is best described by the dimensionless parameter Prandtl number, defined as

P_r = Molecular diffusivity of momentum / Molecular diffusivity of heat = υ/α

It is named after Ludwig Prandtl, who introduced the concept of boundary layer in 1904 and made significant contributions to boundary layer theory. The Prandtl numbers of fluids range from less than 0.01 for liquid metals to more than 100,000 for heavy oils. Note that the Prandtl number is in the order of 10 for water. The Prandtl numbers of gases are about 1, which indicates that both momentum and heat dissipate through the fluid at about the same rate. Consequently the thermal

boundary layer is much thicker for liquid metals and much thinner for oils relative to the velocity boundary layer.

Nusselt Number *Nu*

The Nusselt number represents the enhancement of heat transfer through a fluid layer as a result of convection relative to conduction across the same fluid layer, and is defined as

$Nu = hL / k$

where k is the thermal conductivity of the fluid, h is the heat transfer coefficient and L is the characteristics length. The Nusselt number is named after Wilhelm Nusselt, who made significant contributions to convective heat transfer in the first half of the twentieth century, and it is viewed as the dimensionless convection heat transfer coefficient. The larger Nusselt number indicates a large temperature gradient at the surface and hence, high heat transfer by convection. A Nusselt number of $Nu = 1$, for a fluid layer represents heat transfer across the layer by pure conduction. To understand the physical significance of the Nusselt number, consider the following daily life problems. We remedy to forced convection whenever we want to increase the rate of heat transfer from a hot object.

Rayleigh Number *Ra*

The Rayleigh number (Ra) for a fluid is a dimensionless number associated with buoyancy-driven flow, also known as free convection or natural convection. When the Rayleigh number is below a critical value for that fluid, heat transfer is primarily in the form of conduction, when it exceeds the critical value of heat transfer is primarily in the form of convection.The Rayleigh number is named after Lord Rayleigh and is defined as the product of the Grashof number,which describes the relationship between buoyancy and viscosity within a fluid, and the Prandtl number, which describes the relationship between momentum diffusivity and thermal diffusivity. Hence the Rayleigh number itself may also be viewed as the ratio of buoyancy and viscosity forces multiplied by the ratio of momentum and thermal diffusivities.

1.7 Computational details

A commercial finite element package was used to obtain the solutions. A triangular Lagrangian mesh was used. A total 12,000 elements or more was used for most cases. Relatively finer mesh was used at the corners and near round surfaces. The model was discretized with weak formulation to obtain the results. The system takes the equations and approximates them into a system of ordinary differential equations and then uses standard numerical solving techniques to solve the problem. The COMSOL computer program used in this project is a finite element program. A typical finite element program consists of a pre-processor, a mesh generator, a processor or solver, and a post-processor. The pre-processor part of the program consists of building a model of the item to be analyzed and the application of boundary conditions. The boundary conditions consists of any constraints or loads being applied in the statics or dynamics region or any velocity or temperature conditions for the fluid dynamics and heat transfer aspects. In additions to boundary condition definition, the properties of the materials involved are also defined, and many programs have a library in which the properties of common materials are stored and able to be used for definition. The mesh generator breaks up the model into elements which are geometric bodies that produce the stiffness or material properties of part of the structure. The element geometry is defined by nodal locations. These elements can be modified to be smaller or larger or coarser or more refined. The mesh created from the model applies the geometric and boundary conditions as well as the material properties to the entire structure. The processor portion of the finite element program has the equations of heat transfer, fluid flow, as well as solid property equations in order to solve the defined model. In the COMSOL program there are three different types of non-linear solver which can be used for this purpose. How the solver develops a solution can also be modified by increasing or decreasing the tolerance of convergence that is required for a solution to be obtained, or by changing the order in which the solver solves the equations. The equation of continuity has been used as a constraint due to mass conservation and this restriction may be used to find the pressure distribution. The continuity equation is automatically fulfilled for large values of this constraint. Then the velocity components (U, V) and temperature (θ) are expanded using a basis set.

The governing equations in fluid dynamics and heat transfer, including conservation forms of the Navier-Stokes equations as derived from the first law of thermodynamics, expressed in terms of the control volume or surface integral equations, which represent various physical phenomena. To visualize these thermo fluid flow scenarios, an approximate numerical solution is needed, which can be obtained by the CFD (Computational Fluid Dynamics) code. The partial differential equations of fluid mechanics and heat transfer are discretized in order to obtain a system of approximate algebraic equations, which then can be solved on a computer. The approximations are applied to small domains in space and/ or time so the numerical solution provides results at discrete locations in space and time. Much accuracy of experimental data depends on the quality of the tools used; the accuracy of numerical solution is dependent on the quality of discretization used. CFD computation involves the creation of a set numbers that constitutes a realistic approximation of a real life system. The outcome of computation process improves the understanding of the behavior of a system. Thereby, engineers need CFD codes that can produce physically realistic results with good accuracy in simulations with finite grids. Contained within the broad field of computational fluid dynamics are activities that cover the range from the automation of well established engineering design methods to the use of detailed solutions of the Navier-Stokes equations as substitutes for experimental research into the nature of complex flows. CFD have been used for solving wide range of fluid dynamics problem. It is more frequently used in fields of engineering where the geometry is complicated or some important feature that cannot be dealt with standard methods. The complete Navier-Stokes equations are considered to be the correct mathematical description of the governing equations of fluid motion. The most accurate numerical computations in fluid dynamics come from solving the Navier-Stokes equations. The equations represent the conservation of mass and momentum.

There are several discritization methods available for the high performance numerical computation in CFD.

- Finite volume method (FVM)
- Finite element method (FEM)

- Finite difference method (FDM)
- Boundary element method (BEM)
- Boundary volume method (BVM)

In the present numerical computation, galerkin finite element method (FEM) is used.

1.8 Finite element method

The finite element method (FEM) is a powerful computational technique for solving problems that are described by partial differential equations. The basic idea of the finite element method is the domain is broken into a set of finite elements that are generally triangular or quadrilaterals. The distinguishing feature of FE methods is that the equations are multiplied by a weight function before they are integrated over the entire domain. In the simplest FE methods, the solution is approximated by a linear shape function within each element in a way that guarantees continuity of the solution across element boundaries. Such a function can be constructed from its values at the corners of the elements. The weight function may be the same of different form. This approximation is then substituted into the weighted integral of the conservation law the equations to be solved are derived by requiring the derivative of the integral with respect to each nodal value to be zero; this corresponds to selecting the best solution within the set of allowed functions. The result is a set of nonlinear algebraic equations.

Mathematical model of physical phenomena may be ordinary or partial differential equations, which have been the subject of analytical and numerical investigations. Analytical solutions of these equations involve closed form expressions that give us the variation of the dependent variables continuously throughout the domain. On the other hand, for most of these equations there are no available analytical methods to find their solutions. In contrast, there are available numerical methods to solve these equations. Numerical solutions of these equations can give answers at only discrete points in the domain. In addition, numerical methods give us approximate solution of these differential equations. To obtain an approximate solution numerically, one has to use a discretization technique that approximates the differential equations by a

system of algebraic equations at only discrete points in the domain, which can then be solved on a computer.

The first step to numerically solve a mathematical model of physical phenomena is its numerical discretization. This means that each component of the differential equations is transformed into a “numerical analogue” which can be represented in the computer and then processed by a computer program, built on some algorithm. There are many different methodologies devised for this purpose in the past and the development still continues. In this thesis the finite element method (FEM) has been used to solve the differential equations.

Since COMSOL is a finite element solver, a basic understanding of the finite element method is necessary to work within the program. The in-depth complexities of the program finite element method would take far too long to explain, but this section provides a brief explanation as to what the finite element method is. The most basic explanation of the finite element method is a technique for solving a numerical solution to a boundary value problem described by a differential equation. The differential equation itself is used to describe some aspect of engineering, for this project, incompressible fluid flow. Specific boundary conditions determine what the solutions to those equations must be on the boundary of the shape in question. In order to numerically solve the problem, the geometry in which the equation will be solved must be broken down into a stiffness matrix. The stiffness matrix is a series of points within the boundaries of the geometry. The equations will be solved on each of these individual points. Once the points are set in place, they are connected to one another. For a two dimensional area these connections sometimes form rectangular mesh elements, other times they form triangular mesh elements. COMSOL almost always uses a triangular connectivity pattern. These points and their connections are what give the “mesh” its visible mesh-like quality.

The finite element method is based on the idea that a continuous function may be approximated by solving it at discrete points. In this case, those points are the individual elements that are comprised of three nodes. For a simplified example, assume that there is a governing equation for a two dimensional model with one unknown. There are two functions necessary to solve this, and any other, finite

element problem. The first is the interpolation function. Each finite element has its own interpolation function to approximate what is happening within that particular element, based on the governing equation for the full model. The second necessary function is the shape function. Shape functions are usually the coefficients in the interpolation function and are unique to each node within the element. The solution of the shape function is such that if it were for each node within one element, the value of the function will be one at one node and zero at every other node in the element. There are as many shape functions within an element as there are nodes. Each node will cause one of the shape functions to equal one at that particular node and zero at every other node. Consequently, part of the interpolation function is solved at each node individually. The solutions are then added together to find the value of the variable in the interpolation function for that mesh element. Since the solutions for finite element analysis are based for these individual meshes elements, the space between the nodes directly affects the accuracy of the solution. The closer the nodes are, the smaller the mesh area of the mesh elements will be and the smaller the distance across which the governing equation must be approximated. So, the more refined the mesh, the better the solution. However, the more mesh elements present, the more equations must be solved and the greater the computing power required to arrive at a solution.

1.9 The reason for finite element solution

The analysis of flow and heat transfer in thermodynamics can be performed either theoretically or by experimental means. Experimental investigation of such problem could not gain that much popularity in the field of thermodynamics because of their limited flexibility and applications. For every change of geometry body and boundary condition, it needs separate investigation, involving separate experimental requirement/ arrangement, which, in turn makes it unattractive, especially, from the time involved as well as economical point of views. The theoretical investigation, on the other hand, can be carried out either by analytical approach or by numerical approach. The analytical methods of solution are not of much help in solving the practical problems. This is mainly due to the very involvement of a large number of variables, complex geometrical bodies and boundary conditions, and arbitrary boundary shapes. General closed form solutions can be obtained only for very ideal

cases and the results obtained for a particular problem, usually with uniform boundary conditions. For two-dimensional thermodynamics problems, mathematical model involve partial differential equations are required to be solved simultaneously with some boundary conditions. Therefore, there are no alternatives except the numerical methods for the solution of the problems of practical interest. In the field of numerical analysis, the major numerical methods in use are the method of finite difference (FD), finite volume (FV) and finite element (FE).

Finite element method is an ideal numerical approach for solving a system of partial differential equations. The finite element method produces equations for each element independently of all other elements. Only when the equations are collected together and assembled into a global matrix are the interactions between elements taken into account. Despite these ideal characteristics, the finite element method dominates in most of the computational fluid dynamics (CFD). The present research is an attempt to bring the FE technique again into light through a novel formulation of two dimensional incompressible thermal flow problems. As the formulation establishes a priority of finite element technique over the FD and FV method, the philosophy and approach of the three methods are recapitulated here in brief. The finite difference method relies on the philosophy that the body is in one single piece but the parameters are evaluated only at some selected points within the body, satisfying the governing differential equations approximately, where as the finite volume method relies on the philosophy that the body is divided into a finite number of control volumes (CVs), On the other hand, in the finite element method, the body is divided into a number of elements. The relative advantages and disadvantages of the finite element method are shown below:

Finite Element Method

Advantages

a) Finite element method works when all other method fails.

b) It is very good in managing complex geometrical bodies and boundaries.

c) There are many commercial packages such as ANSYS, FEMLAB, COMSOL for analyzing practical problems.

Disadvantages

a) The body is not in one piece, but it is an assemblage of elements connected only at nodes.

b) Variations of parameters over individual elements are assumed to be simple like polynomial of limited order.

c) Finite element solution is highly dependent on the element type.

Accurate and reliable prediction of complex geometry is of great importance to meet the severe demand of greater reliability as well as economic challenge. It is noted that these complex geometries occur most frequently in CFD. Presented methods have a common feature: they generate equations for the values of the unknown functions at a finite number of points in the computational domain. But there are also several differences. The finite difference and the finite volume methods generate numerical equations at the reference point based on the values at neighboring points. The finite element method takes care of boundary conditions of Neumann type while the other two methods can easily apply to the Dirichlet conditions. The finite difference method could be easily extended to multidimensional spatial domains if the chosen grid is regular (the cells must look cuboids, in a topological sense). The grid indexing is simple but some difficulties appear for the domain with a complex geometry. For the finite element method there are no restrictions on the connection of the elements when the sides (or faces) of the elements are correctly aligned and have the same nodes for the neighboring elements. This flexibility allows us to model a very complex geometry. The finite volume method could also use irregular grids like the grids for the finite element methods, but keeps the simplicity of writing the equations like that for the finite difference method. Of course, the presence of a complex geometry slows down the computational programs. Another benefit of the finite element method is that of the specific mode to deduce the equations for each element that are then assembled. Therefore, the addition of new elements by refinement of the existing ones is not a major problem. For the other methods, the mesh refinement is a major task and could involve the rewriting of the program. But for all the methods used for the discrete analogue of the initial equation, the obtained system of simultaneous equations must be solved. That is why, the present work

emphasizes the use of finite element techniques to solve flow and heat transfer problems. The details of this method are explained in the following section.

1.10 FEM for viscous incompressible flow

Viscous incompressible thermal flows have been the subject of my investigation. The problem is relatively complex due to the coupling between the energy equation and the Navier-Stokes equations that govern the fluid motion. These equations comprise a set of coupled nonlinear partial differential equations that is difficult to solve especially with complicated geometries and boundary conditions. The finite element method is one of the numerical methods that have received popularity due to its capability for solving complex structural problems. The method has been extended to solve problems in several other fields such as in the field of heat transfer, computational fluid dynamics, electromagnetic, biomechanics etc. In spite of the great success of the method in these fields, its application to fluid mechanics, particularly to convective viscous flows, is still under intensive research. This is due to the fact that the governing partial differential equations for general flow problems consist of several coupled equations that are inherently nonlinear. Accurate numerical solutions thus require a vast amount of computer time and data storage. One-way to minimize the amount of computer time and data storage used is to employ an adapting meshing technique. The technique places small elements in the regions of large change in the solution gradient to increase solution accuracy, and at the same time, uses large elements in the other regions to reduce the computational time and computer memory.

As the first step toward accurate flow solutions using the adaptive meshing techniques, this chapter develops a finite element formulation suitable for analysis of general viscous incompressible thermal flow problems. The formulation evaluated in this chapter will be used with the adaptive meshing technique in the future. The chapter starts from the Navier-Stokes equations together with the energy equation to derive the corresponding finite element equations. The computational procedure used in the development of the computer program is described.

The major steps involved in finite element analysis of a typical problem are:

- Discretization of the domain into a set of finite elements (mesh generation).
- Weighted-integral or weak formulation of the differential equation to be analyzed.
- Development of the finite element model of the problem using its weighted-integral or weak form.
- Assembly of finite elements to obtain the global system of algebraic equations.
- Imposition of boundary conditions.
- Solution of equations.
- Post-computation of solution and quantities of interest.

1.11 Motivation

From the literature review it is mentioned that a very few numerical works have been done introducing temperature dependent thermal conductivity and viscosity properties of nanofluid. In spite of that there is a large scope to work with nanofluid flow and heat transfer by analyzing these properties. In this paper, we investigated numerically the effect of variable thermal conductivity and viscosity across the nanofluid in square cavity and cubical cavity.

The present theoretical study may be useful guide for research and experiments on heat transfer in closed enclosure using nanofluids to enhance thermal efficiency. The results obtained in this thesis are likely to be helpful in applications including manufacturing, chemical and pharmaceutical processes, medical treatments, cosmetics, modeling solar thermal receivers, refrigerator and electronic cooling process etc.

The knowledge of natural convection heat transfer has many significant engineering applications; for example, geothermal engineering, solar-collectors, cold storage performance, thermal insulation of buildings, nuclear reactors, electrical, microelectronic equipments containers and in many other design problems convective heat transfer is predominant. Therefore for that reason, necessary numerical studies are still required to modify a mathematical model comprising of Navier-Stokes, continuity and energy equations dictating convective heat transfer of

nanofluids and to carry out the validation of the present numerical technique by comparing with the previous works which forms the basis of the motivation behind selecting the present work.

1.12 Main objectives of the work

The objective of this study is to investigate natural convection heat transfer in a closed enclosure filled with water based nanofluid and the effects of nanoparticles on the flow field, temperature distribution and heat transfer coefficient. Results will be presented for different non-dimensional governing and physical parameters in terms of streamlines, isotherms, heat transfer rate as well as the average Nusselt number in the cavity. The specific objectives of the present research work are:

- To study a finite element model comprising of Navier-Stokes, continuity and energy equations dictating convective heat transfer of water based nanofluid in cubical enclosure.
- To validate for natural convection of water based nanofluids in a square cavity against established numerical results.
- To validate the present model by investigating the natural convection flow of water based nanofluids in cubical enclosure
- To analyze the flow and thermal characteristics of water based nanofluids confined square cavity with various heating patterns of walls.
- To study the effects of governing parameters namely Rayleigh number, Prandtl number, solid volume fraction on heat transfer parameters such as average Nusselt number and isotherms to evaluate heat transfer rate in cubical enclosure.
- To carry out MHD effects of Cu-water nanofluid of both square and cubical enclosure.
- To compare the results between square cavity and cubical enclosure.

CHAPTER 2

Literature Review

Natural convection in cubical and square cavities has received considerable attention because of its importance in several thermal engineering problems, for example, in the design of electronic devices, solar thermal receivers, uncovered flat plate solar collectors having rows of vertical strips, geothermal reservoirs, etc. During the past two decades, several experiments and numerical calculations have been presented for describing the phenomenon of natural convection in square and cubical cavities. Those studies have been focused to study the effect on flow and heat transfer for different Rayleigh numbers, solid volume fraction of nano particles.

Nanofluid has been under extensive analysis in the last decade due to its potential in heat transfer enhancement related application. Nanometer sized particles finely dispersed in a base fluid is known as nanofluid which exhibits higher heat transfer coefficient than that of base fluid by Xuan,Y.M. and Li, Q. (2000).This phenomenon profoundly opens up doors for application of nanofluid in micro-cooling, nano-scale drug delivery and energy conversion. An extensive review on recent works on nanofluid can be found very helpful for the researchers working related to the subject by Mahmoodi, M. (2011). Many experimental studies have been conducted as well as many theoretical studies (both numerical and analytical). Most theoretical work considered nanofluid as a single phase solution and formulate the problem in Eulerian frame of reference. Particle concentration of nanofluid has also been investigated in some analysis. Effect of Brownian motion was showed to be important in few cases. Magnetic field was shown to influence the heat transfer characteristics of nanofluid by Ghasemi, B.*et al*.(2011).

Ravnik, J.*et al.*(2010) carried out a boundary element method (BEM) analysis of free convection in a cubic cavity filled with nanofluids. Ha, M.Y. and Jung, M. J. (2000) solved three-dimensional, steady, conjugate heat transfer of natural convection and conduction in a cubical volume for Ra=10^3,10^4 and 10^5. Frederick, R. L.and Quiroz, F. (2000) analyzed convection flows in a cubical cavity and focused on the transition from conduction to convection regime as the Rayleigh number is increased from 10^5 to 10^7. Ahmed , G. R. and Yovanovich, M. M. (1992) obtained numerical and

experimental data for $10^3 \leq \mathrm{Ra} \leq 10^6$ and Prandtl number of Pr= 0.72 in a cube shaped box with discreet heat sources. Some investigation has been done on the natural convection around an obstacle in a cavity. Lee , J. R. and Ha, M. Y. (2005) have numerically studied the natural convection in a horizontal cavity with a conducting body. They investigated the effect of conductivity of central obstacle on flow pattern and heat transfer. Another study has been done by Sheikhzadeh *et al*. (2011). They have investigated the effects of Prandtl number on the steady magneto-convection around a centrally located adiabatic body inside a square cavity. Abu-nada *et al*. (2009) investigated numerically the effect of Cu-water nanofluid on natural convection heat transfer in an inclined cavity. They used the inclination angle as a control parameter for flow and heat transfer in the cavity and studied the problem in various inclination angle, Rayleigh numbers and solid volume fractions and found that the effect of the nanoparticles on Nusselt number is more pronounced at low volume fraction that at high volume fraction. Khanafer *et al.* (2003) performed a numerical study of laminar natural convection in a square cavity. They have used three theoretical models for prediction of viscosity and thermal conductivity of nanofluids and deduced that the variances within different models have substantial effects on the results. They also found that the heat transfer increases with solid volume fraction of the nanofluid capacity.

Natural convection under the influence of a magnetic field is of great importance in many industrial applications such as crystal growth in liquid, cooling of nuclear reactor, electronic package, microelectronic devices, and solar technology. In the case of free convection of an electrically conducting fluid in the presence of a magnetic field, there are two body forces: buoyancy force and Lorentz force. They interact with each other and can influence heat and mass transfer. Thus, it is important to study the detailed characteristics of transport phenomena in such a process to have a better product with improved design. Magneto hydrodynamic natural convection in a vertical cylindrical cavity with a sinusoidal upper wall temperature was investigated by Kakarantzas et al. (2009).They concluded that the increase of Hartmann number results in a damping of the fluid motion, and thus heat conduction progressively dominates over convection heat transfer. Rudraiah et al. (1995) investigated numerically the effect of a magnetic field on natural convection

in a rectangular enclosure. They found that the magnetic field decreases the rate of heat transfer. Sheikholeslami *et al.* (2012) studied the natural convection in a concentric annulus between a cold outer square and heated inner circular cylinders in the presence of a static radial magnetic field. They reported that the average Nusselt number is an increasing function of the nanoparticle volume fraction parameter and Rayleigh number, while it is a decreasing function of Hartmann number. Effect of magnetic field on natural convection was considered by several authors. Ghasemi *et al.* (2011) performed a numerical study of natural convection of water-Al_2O_3 nanofluid in an enclosure subjected to an external magnetic field. They concluded that the heat transfer rate increases with an increase of the Rayleigh number but it decreases with an increase of the Hartmann number. Moreover the increment of the nanofluid volume fraction leads to enhancement or deterioration of the heat transfer performance depending on the value of Hartmann and Rayleigh numbers. Sheikhzadeh, G. A. *et al.* (2011) compared stream functions, isothermal lines and velocity maps for the natural convection heat transfer in a square cavity filled with air in a numerical and experimental study for $\mathrm{Ra} = 9.08 \times 10^4 - 2.51 \times 10^5$. Jou *et al.* (2006) studied the influence of nanofluids on natural convection heat transfer in 2-D square enclosures. The transport equations were modeled using a stream function-vorticity formulation and solved by finite volume methodology. The effects of Rayleigh number and aspect ratio of the enclosure were considered and it was deduced that an enhancement in heat transfer is achieved by adding the nanoparticles to the basefluid. Tiwari *et al.* (2007) studied numerically combined convection heat transfer and fluid flow inside a two-sided lid-driven differentially heated square cavity for various Richardson number and the direction of the moving walls. They observed that the nanoparticles when immersed in a fluid enhance the heat transfer capacity of the base fluid and are able to alter the pattern of the flow field. They concluded that the heat transfer rate increases with an increase of the Rayleigh number but it decreases with an increase of the Hartmann number. Moreover the increment of the nanofluid volume fraction leads to enhancement or deterioration of the heat transfer performance depending on the value of Hartmann and Rayleigh numbers.

Recently, an increasing number of studies have been conducted on free convection in non-square geometries because of its wide applications in engineering and industry. It was found that the application of the transverse magnetic field normal to the flow direction decreases the Nusselt and Sherwood number. Koca *et al.* (2007) investigated the influence of Parndtl number on natural convection in triangular enclosures with localized heating from below. They observed that the variation of the Prandtl number affects both the flow and temperature fields in the enclosure. In addition, it was found that the heat transfer rate increases with the increasing of Prandtl and Rayleigh numbers for all cases.

Two different nanofluid models namely, the Brinkman model and the Pak and Cho correlation were employed by Nasrin *et al.* (2012). The developed equations were given in terms of the Navier Stokes and the energy equation and were nondimensionalized and then solved numerically subject to appropriate boundary conditions by the Galerkin's finite element method. Parvin *et al.* (2012) analyzed thermal conductivity variation of water-alumina nanofluid in an annulus where two thermal conductivity models namely, the Chon *et al.* model and the Maxwell Garnett model are used to evaluate the heat transfer enhancement in the annulus. R. Roslan *et al.* (2011) investigated heat transfer in a naonofluid filled trapezoidal enclosure with variable thermal conductivity and viscosity. They found that the effect of the viscosity was more dominant than the thermal conductivity and there was almost no improvement in heat transfer performance utilizing nanofluids. Tanmay Basak *et al.* (2006) presented the effects of thermal boundary conditions on natural convection flows within a square cavity. The system of equations of motion is derived by using the governing mass, momentum and energy equations.

Based on literature reviews, despite a large number of numerical studies on free convection of nanofluids inside rectangular and square cavities with different boundary conditions, but there is no study on natural convection of Cu-Water nanofluid in cubical enclosure. This problem may be occurred in a number of technical applications such as solar collectors, heat exchangers, and cooling of electronic equipment and chips using nanofluids. Studies on natural convection using nanofluids are very limited and they are related with differentially heated enclosures. The buoyancy-driven heat transfer in square cavities filled with air with partially

active vertical walls was studied numerically by Valencia, A.and Frederick,R.L. (1998). Aminossadati *et al.* (2005) numerically investigated the flow and temperature fields in an inclined enclosure simulating an inclined electronic device. They showed that placing the enclosure at different orientations significantly affected the heat transfer rate.

Natural convection flow analysis in enclosures has many thermal engineering applications, such as cooling of electronic devices, energy storage systems and fire-safe compartment. In the numerical domain, a big progress has been made on the natural convection in complex geometries by Yang, Y. (2005). For many years a lot of attention has been paid to the problems of natural convection in enclosure. However, the limitations of numerical tools and experimental techniques restrict investigators within the approximation of a two dimensional model even though fluid motion is three dimensional in nature. Bessnov *et al*. (1997) have suggested a benchemark numerical solution for the three dimensional natural convection in cubical enclosure. Three dimensional laminar flow has been also studied by Mallinson *et al.* (1977) and Lee *et al.* (1988) for enclosures of the length aspect ratio. Lankhorst *et al*. (1988) computed steady flows for numbers of Rayleigh ranging from 10^6 to 10^8. Fusegi *et al.* (1991) made a three dimensional flow analysis on natural convection in a differentially heated cubical enclosure, the detailed structures of the fields were scrutinized by using high-resolution computational results over the range of Rayleigh numbers studied, $10^3 \leq Ra \leq 10^6$, they clarified three dimensional structures of flow, vorticity and temperature in the cavity; they also compared their numerical results with the experimental measurements as studied by Bilsk *et al*.(1986). The complexity of such problems increases when the hot surface of the cubical enclosure becomes wavy. Adjlout *et al*. (2002) have also investigated the two dimensional natural convection in an inclined cavity with hot wavy wall. They simulated the fluid and heat transfer with ADI scheme; one of their interesting results was a decrease of the averaged heat transfer compared with the mean Nusselt number of the square cavity. They showed that the thermal boundary layer is considerably affected by wavy wall and they recommended investigating the hot wall geometry optimisation. Natural convection in three dimensional rectangular enclosures had been analyzed numerically by T. Lee *et al* (1995), the effect of the Rayleigh number was mainly

investigated. The results showed that the temperature distribution imposed on the wall reinforced the axial flow and magnified the three dimensional effect. Three dimensional structures in laminar natural convection in a cubic enclosure were investigated experimentally by Hiller *et al.* (1989). The Rayleigh numbers ranged from 10^4 to 2×10^7 and the Prandtl numbers from 5.8 to 6×10^3. They showed the velocity and vorticity fields and compared the experimental observations with numerical calculations found in the literature. H .Gunes (1992) studied numerically three dimensional natural convection cooling in enclosures and vertical channels with spatially periodic heat sources in his thesis. It was established that the convection reduces the maximum operating temperature for all configurations. Joshi Yu .E (1997) carried out a numerical study of a three dimensional laminar natural convection in a vented enclosure. They presented the local and overall heat transfer from the heat source and the substrate, in terms of Nusselt numbers and the surface temperatures to illustrate the vent effects. Akrour *et al.* (2000) made numerically a three dimensional steady flow on natural convection in a differentially heated cubical enclosure. The variation of Nusselt numbers on the hot and cold walls were also presented to show the overall heat transfer characteristics inside the enclosure. They found that the three dimensional data demonstrate reasonable agreement with the experimental measurement. Natural convection heat transfer associated to fluid dynamics phenomena was studied extensively by Corzo *et al.* (2011). The results presented revealed a good agreement not only in 2D also in 3D and for a wide range of Ra numbers. Kürekci *et al.* (2012) made an experimentaland numerical study of laminar natural convection in a differentially heated cubical enclosure.They compared numerical and experimental results and were found to be in general agreement with each other. M. Ahmadi *et al.* (2012) carried out a numerical analysis to study the laminar natural convection in a three dimensional enclosure. Results exposed that the average Nusselt number increases by increasing in Ra, the rate of heat transfer from hot and cold sources and maximum component of velocity increase. Lahoucine *et al.* (2013) carried out the three dimensional numerical study of natural convection in a cubical enclosure with two heated square sections submitted to periodic temperatures, filled with air. The obtained results showed significant changes in terms of heat transfer and flow intensity. Sabeur *et al*. (2007)

performed a numerical investigation of the influence of the hot surface geometry on a laminar natural convection in a cubical cavity filled with air differentially heated. The results obtained showed that the hot wall geometry affects the flow and the heat transfer rate in the cavity. The mean Nusselt number decreases compared with the heat transfer in the cubical cavity. Fusegi *et al.* (1991) studied numerically a transient three dimensional natural convection in a differentially heated cubical enclosure at Rayleigh number of 10^6. They showed that the behavior of the heat transfer rate in the enclosure was considerably influenced by the presence of the internal gravity wave motion. Fusegi *et al.* (1992) also carried out a three dimensional numerical simulation of periodic natural convection in a differentially heated cubical enclosure; at the Rayleigh number of 8.5×10^6, they found that the period of the oscillations was consistent with the experimental measurements. In another study, Fusegi *et al.* (1993) made numerical simulations of natural convection in a differentially heated cubical enclosure with a partition. They scrutinized the effects of the partition geometry on the three dimensional flow properties. Silva *et al.* (2005) evaluated the effect of the aspect ratio and horizontal length of a high conductivity rectangular fin attached to the hot wall of a three dimensional differentially heated cubic enclosure in laminar natural convection, a scale analysis was used to predict the domain in which the fin geometry played a significant role. Frederick R.L. (1997) made a numerical study of natural convection of air in a differentially heated cubical enclosure with a thick fin placed vertically in the middle of the hot wall; he investigated the variation of overall Nusselt number with Rayleigh number and thermal conductivity ratio. Frederick R.L. (2007) studied also a numerically natural convection heat transfer in a cubical enclosure with two active sectors on one vertical wall over a wide range of Rayleigh number. He described the flow patterns and temperature distribution and proposed an expression for overall heat transfer. In another study, Frederick R.L and Moraga S.G. (2007) investigated numerically three dimensional natural convection of air in a cubical enclosure with a fin on the hot wall. It was concluded that for $10^5 \leq Ra \leq 10^6$, a fin of partial width is more effective in promoting heat transfer than a fin of full width. Bocu Z and Altac Z (2011) studied numerically laminar natural convection heat transfer in 3-D rectangular air filled enclosures, with pins attached to the active wall. The Rayleigh numbers considered

in their study ranges from 10^5 to 10^7; they concluded that the mean Nusselt number increases with increasing Rayleigh number for a fixed case. Their investigation is an extension of the work already established by Belkadi *et al.* (2006) in which they treated similar cavity in two dimensional study. The most part of their simulation is to show the three dimensional effects and the influence of the hot wavy wall with partial partitions on the laminar natural convection.

In the present thesis, a finite element model has been developed to analyze the heat transfer enhancement of Cu-water nanofluid in differentially heated square cavity with a circular disk. The effect of magnetic field on the thermal properties or heat transfer enhancement of Cu-water nanofluid has also been addressed. The model has been validated against established results for natural convection of air and nanofluid in a differentially heated square cavity and cubical enclosure.

In the present study, natural convection flow of Cu-Water nanofluid inside a square cavity and cubical cavity has been investigated numerically at Ra = 10^3 to 10^6 One vertical wall of the cavity is hot, the opposite one is cold and the rest of the walls are adiabatic. Numerical results are obtained by using COMSOL Multiphysics software. The results in the form of streamlines and isotherms plots, average Nusselt number and local Nusselt number are presented for a wide range of Rayleigh numbers and different volume fraction of the nanoparticles .The effects of Rayleigh number on natural convection heat transfer of Cu-water based nanofluids inside square cavity and cubical enclosure are investigated numerically. For this purpose various combinations of Rayleigh number, Nusselt number, and volume fraction of the Cu solid nanoparticle are considered.

CHAPTER 3

Theoretical Description

3.1Mathematical Model

3.1.1 Mathematical Model of cubical cavity

The set of equations that governs the thermo-fluid flow is given as:

$$\frac{\partial u}{\partial x}+\frac{\partial v}{\partial y}+\frac{\partial w}{\partial z}=0 \tag{3.1}$$

$$u\frac{\partial u}{\partial x}+v\frac{\partial u}{\partial y}+w\frac{\partial u}{\partial z}=-\frac{1}{\rho_{nf}}\frac{\partial p}{\partial x}+\frac{\mu_{nf}}{\rho_{nf}}\left(\frac{\partial^2 u}{\partial x^2}+\frac{\partial^2 u}{\partial y^2}+\frac{\partial^2 u}{\partial z^2}\right) \tag{3.2}$$

$$u\frac{\partial v}{\partial x}+v\frac{\partial v}{\partial y}+w\frac{\partial v}{\partial z}=-\frac{1}{\rho_{nf}}\frac{\partial p}{\partial y}+\frac{\mu_{nf}}{\rho_{nf}\alpha_f}\left(\frac{\partial^2 v}{\partial x^2}+\frac{\partial^2 v}{\partial y^2}+\frac{\partial^2 v}{\partial z^2}\right)+\frac{(\rho\beta)_{nf}}{\beta_f}Ra\,\Pr\theta \tag{3.3}$$

$$u\frac{\partial w}{\partial x}+v\frac{\partial w}{\partial y}+w\frac{\partial w}{\partial z}=-\frac{1}{\rho_{nf}}\frac{\partial p}{\partial z}+\frac{\mu_{nf}}{\rho_{nf}}\left(\frac{\partial^2 w}{\partial x^2}+\frac{\partial^2 w}{\partial y^2}+\frac{\partial^2 w}{\partial z^2}\right) \tag{3.4}$$

$$u\frac{\partial T}{\partial x}+v\frac{\partial T}{\partial y}+w\frac{\partial T}{\partial z}=\alpha_{nf}\left(\frac{\partial^2 T}{\partial x^2}+\frac{\partial^2 T}{\partial y^2}+\frac{\partial^2 T}{\partial z^2}\right) \tag{3.5}$$

where u,v and w are the fluid velocity in x-direction , y-direction and z-direction respectively, p is the pressure and T is the temperature and ρ is the density, $(\rho Cp)_{nf}$ heat capacity, $(\rho\beta)_{nf}$ thermal expansion coefficient, and α_{nf} thermal diffusivity of the nanofluid are as following, respectively.

$$\rho_{nf}=(1-\varphi)\rho_f+\varphi\rho_s \tag{3.6}$$

$$(\rho C_p)_{nf}=(1-\varphi)(\rho C_p)_f+\varphi(\rho C_p)_s \tag{3.7}$$

$$(\rho\beta)_{nf}=(1-\varphi)(\rho\beta)_f+\varphi(\rho\beta)_s \tag{3.8}$$

$$\alpha_{nf} = \frac{k_{nf}}{\left(\rho C_p\right)_{nf}} \tag{3.9}$$

In the above equations, φ is the solid volume fraction, k_{nf} is the thermal conductivity of the nanofluid. The effective dynamic viscosity of the Cu-water nanofluid is calculated according to the Brinkman model (1952) as follows:

$$\mu_{nf} = \frac{\mu_f}{\left(1-\varphi\right)^{2.5}} \tag{3.10}$$

The effective thermal conductivity of the nanofluid is determined using the Maxwell model (1904) is as follows:

$$k_{nf} = k_f \frac{k_s + 2k_f - 2\phi\left(k_f - k_s\right)}{k_s + 2k_f + \phi\left(k_f - k_s\right)} \tag{3.11}$$

Governing equations of the convective heat transfer are non-dimensionalized with the following dimensionless parameters defined as:

$$\begin{aligned} &X = \frac{x}{h};\ Y = \frac{y}{h};\ Z = \frac{z}{h}; U = \frac{uh}{\alpha_f}; V = \frac{vh}{\alpha_f}; W = \frac{wh}{\alpha_f}; \\ &P = \frac{ph^2}{\rho_{nf}\alpha_f^2};\ \theta = \frac{T - T_c}{T_h - T_c} \end{aligned} \tag{3.12}$$

The dimensionless forms of the governing equations are:

$$\frac{\partial U}{\partial X} + \frac{\partial V}{\partial Y} + \frac{\partial W}{\partial Z} = 0 \tag{3.13}$$

$$U\frac{\partial U}{\partial X} + V\frac{\partial U}{\partial Y} + W\frac{\partial U}{\partial Z} = -\frac{\partial P}{\partial X} + \frac{\mu_{nf}}{\rho_{nf}\alpha_f}\left(\frac{\partial^2 U}{\partial X^2} + \frac{\partial^2 U}{\partial Y^2} + \frac{\partial^2 U}{\partial Z^2}\right) \tag{3.14}$$

$$U\frac{\partial V}{\partial X} + V\frac{\partial V}{\partial Y} + W\frac{\partial V}{\partial Z} = -\frac{\partial P}{\partial Y} + \frac{\mu_{nf}}{\rho_{nf}\alpha_f}\left(\frac{\partial^2 V}{\partial X^2} + \frac{\partial^2 V}{\partial Y^2} + \frac{\partial^2 V}{\partial Z^2}\right) + \frac{\left(\rho\beta\right)_{nf}}{\rho_{nf}\beta_f} Ra \Pr \theta \tag{3.15}$$

$$U\frac{\partial W}{\partial X}+V\frac{\partial W}{\partial Y}+W\frac{\partial W}{\partial Z}=-\frac{\partial P}{\partial Z}+\frac{\mu_{nf}}{\rho_{nf}\alpha_f}\left(\frac{\partial^2 W}{\partial X^2}+\frac{\partial^2 W}{\partial Y^2}+\frac{\partial^2 W}{\partial Z^2}\right) \tag{3.16}$$

$$U\frac{\partial \theta}{\partial X}+V\frac{\partial \theta}{\partial Y}+W\frac{\partial \theta}{\partial Z}=\frac{\alpha_{nf}}{\alpha_f}\left(\frac{\partial^2 \theta}{\partial X^2}+\frac{\partial^2 \theta}{\partial Y^2}+\frac{\partial^2 \theta}{\partial Z^2}\right) \tag{3.17}$$

Rayleigh number Ra and Prandtl number Pr are defined as

$$Ra=\frac{g\beta_f\left(T-T_c\right)h^3}{\alpha_f\upsilon_f};\ \Pr=\frac{\upsilon_f}{\alpha_f} \tag{3.18}$$

3.1.2 Mathematical model of square cavity

Natural convection is governed by the differential equations expressing conservation of mass, momentum and energy. The present flow is considered steady, laminar, incompressible and two-dimensional. The viscous dissipation term in the energy equation is neglected. The Boussinesq approximation is invoked for the nanofluid properties to relate density changes to temperature changes, and to couple in this way the temperature field to the flow field. It is taken that water and nanoparticles are in thermal equilibrium and no slip occurs between them. The density of the nanofluid is approximated by the Boussinesq model.

The governing equations for steady natural convection flow can be written as follows:

Mass Conservation Equation:

$$\frac{\partial u}{\partial x}+\frac{\partial v}{\partial y}=0 \tag{3.19}$$

Momentum Conservation Equations:

$$\rho_{nf}\left(u\frac{\partial u}{\partial x}+v\frac{\partial u}{\partial y}\right)=-\frac{\partial p}{\partial x}+\mu_{nf}\left(\frac{\partial^2 u}{\partial x^2}+\frac{\partial^2 u}{\partial y^2}\right) \tag{3.20}$$

$$\rho_{nf}\left(u\frac{\partial v}{\partial x}+v\frac{\partial v}{\partial y}\right)=-\frac{\partial p}{\partial y}+\mu_{nf}\left(\frac{\partial^2 v}{\partial x^2}+\frac{\partial^2 v}{\partial y^2}\right) \tag{3.21}$$

Energy Conservation Equation:

$$u\frac{\partial T}{\partial x}+v\frac{\partial T}{\partial y}=\alpha_{nf}\left(\frac{\partial^2 T}{\partial x^2}+\frac{\partial^2 T}{\partial y^2}\right) \tag{3.22}$$

3.1.3 Mathematical model of sqare cavity under magnetic field

The present flow is considered steady, laminar, incompressible and two-dimensional. The uniform magnetic field with a constant magnitude of B_o is considered in the horizontal direction. The cavity is filled with Cu-water (Pr = 6.2), and the physical properties of the fluid are assumed to be constant except for the density which is estimated by the Boussinesq's approximation. The governing equations for steady natural convection flow can be written as follows:

Mass Conservation Equation:

$$\frac{\partial u}{\partial x}+\frac{\partial v}{\partial y}=0 \tag{3.23}$$

Momentum Conservation Equations:

$$u\frac{\partial u}{\partial x}+v\frac{\partial u}{\partial y}=-\frac{1}{\rho_{nf}}\frac{\partial p}{\partial x}+\frac{\mu_{nf}}{\rho_{nf}}\left(\frac{\partial^2 u}{\partial x^2}+\frac{\partial^2 u}{\partial y^2}\right) \tag{3.24}$$

$$u\frac{\partial v}{\partial x}+v\frac{\partial v}{\partial y}=-\frac{1}{\rho_{nf}}\frac{\partial p}{\partial y}+\frac{\mu_{nf}}{\rho_{nf}}\left(\frac{\partial^2 v}{\partial x^2}+\frac{\partial^2 v}{\partial y^2}\right)+\frac{(\rho\beta)_{nf}}{\rho_{nf}}g\left(T-T_c\right)-\frac{\sigma_{nf}B_0^2 v}{\rho_{nf}} \tag{3.25}$$

Energy Conservation Equation:

$$u\frac{\partial T}{\partial x}+v\frac{\partial T}{\partial y}=\alpha_{nf}\left(\frac{\partial^2 T}{\partial x^2}+\frac{\partial^2 T}{\partial y^2}\right) \tag{3.26}$$

σ_{nf} is the electrical conductivity of the nanofluid, where

$$\sigma_{nf}=(1-\varphi)\sigma_f+\varphi\sigma_s$$

Governing equations of the convective heat transfer are non-dimensionalized with the following dimensionless parameters defined as:

$$X=\frac{x}{h};\ Y=\frac{y}{h};\ U=\frac{uh}{\alpha_f};V=\frac{vh}{\alpha_f};P=\frac{ph^2}{\rho_{nf}\alpha_f^2};\ \theta=\frac{T-T_c}{T_h-T_c};$$

The dimensionless forms of the governing equations are:

$$\frac{\partial U}{\partial X}+\frac{\partial V}{\partial Y}=0$$

$$U\frac{\partial U}{\partial X}+V\frac{\partial U}{\partial Y}=-\frac{\rho_f}{\rho_{nf}}\frac{\partial P}{\partial X}+\frac{\mu_{nf}}{\rho_{nf}\alpha_f}\left(\frac{\partial^2 U}{\partial X^2}+\frac{\partial^2 U}{\partial Y^2}\right)$$

$$U\frac{\partial V}{\partial X}+V\frac{\partial V}{\partial Y}=-\frac{\rho_f}{\rho_{nf}}\frac{\partial P}{\partial Y}+\frac{\mu_{nf}}{\rho_{nf}\alpha_f}\left(\frac{\partial^2 V}{\partial X^2}+\frac{\partial^2 V}{\partial Y^2}\right)+\frac{(\rho\beta)_{nf}}{\rho_{nf}\beta_f}Ra\,\Pr\theta-Ha^2\Pr V$$

$$U\frac{\partial \theta}{\partial X}+V\frac{\partial \theta}{\partial Y}=\frac{\alpha_{nf}}{\alpha_f}\left(\frac{\partial^2 \theta}{\partial X^2}+\frac{\partial^2 \theta}{\partial Y^2}\right)$$

where U and V fluid velocity in X-direction and Y-direction, respectively, P is pressure, B_0 is the magnetic field strength, θ is the temperature. Rayleigh number *Ra*, Prandtl number *Pr* and Hartman number *Ha* are defined as

$$Ra=\frac{g\beta_f\left(T-T_c\right)h^3}{\alpha_f\upsilon_f};\ \Pr=\frac{\upsilon_f}{\alpha_f};\ Ha=B_0h\sqrt{\frac{\sigma_{nf}}{\rho_{nf}\upsilon_f}}$$

In order to evaluate the heat transfer enhancement in the cavity, the local Nusselt number on the walls is defined as:

$$Nu_l=-\frac{k_{nf}}{k_f}\frac{\partial\theta}{\partial n}\bigg|_{wall}$$

where symbol n is the normal direction to the surface. Average Nusselt number along the hot walls of the cavity is considered to evaluate the overall heat transfer rate and is defined as:

$$Nu_{avg}=\int_0^1 Nu_l dY\Big|_{X=0}$$

3.1.4 Mathematical model of cubical cavity under magnetic field

Natural convection is governed by the differential equations expressing conservation of mass, momentum and energy. The present flow is considered steady, laminar, incompressible and three-dimensional. The uniform magnetic field with a constant magnitude of B_o is considered in the horizontal direction. The enclosure is filled with Cu-water nanofluid (Pr = 6.2) and the physical properties of the fluid are

assumed to be constant except for the density which is estimated by the Boussinesq's approximation. The viscous dissipation term in the energy equation is neglected. The Boussinesq's approximation is invoked for the nanofluid properties to relate density changes to temperature changes and to couple in this way the temperature field to the flow field. It is taken that water and nanoparticles are in thermal equilibrium and no slip occurs between them. The density of the nanofluid is approximated by the Boussinesq model. The governing equations for steady natural convection flow can be written as follows:

Mass Conservation Equation:

$$\frac{\partial u}{\partial x}+\frac{\partial v}{\partial y}+\frac{\partial w}{\partial z}=0$$

Momentum Conservation Equations:

$$u\frac{\partial u}{\partial x}+v\frac{\partial u}{\partial y}+w\frac{\partial u}{\partial z}=-\frac{1}{\rho_{nf}}\frac{\partial p}{\partial x}+\frac{\mu_{nf}}{\rho_{nf}}\left(\frac{\partial^2 u}{\partial x^2}+\frac{\partial^2 u}{\partial y^2}+\frac{\partial^2 u}{\partial z^2}\right)$$

$$u\frac{\partial v}{\partial x}+v\frac{\partial v}{\partial y}+w\frac{\partial v}{\partial z}=-\frac{1}{\rho_{nf}}\frac{\partial p}{\partial y}+\frac{\mu_{nf}}{\rho_{nf}}\left(\frac{\partial^2 v}{\partial x^2}+\frac{\partial^2 v}{\partial y^2}+\frac{\partial^2 v}{\partial z^2}\right)$$
$$+\frac{(\rho\beta)_{nf}}{\rho_{nf}}g\left(T-T_c\right)-\frac{\sigma_{nf}B_0^2 v}{\rho_{nf}}$$

$$u\frac{\partial w}{\partial x}+v\frac{\partial w}{\partial y}+w\frac{\partial w}{\partial z}=-\frac{1}{\rho_{nf}}\frac{\partial p}{\partial z}+\frac{\mu_{nf}}{\rho_{nf}}\left(\frac{\partial^2 w}{\partial x^2}+\frac{\partial^2 w}{\partial y^2}+\frac{\partial^2 w}{\partial z^2}\right)$$

Energy Conservation Equation:

$$u\frac{\partial T}{\partial x}+v\frac{\partial T}{\partial y}+w\frac{\partial T}{\partial z}=\alpha_{nf}\left(\frac{\partial^2 T}{\partial x^2}+\frac{\partial^2 T}{\partial y^2}+\frac{\partial^2 T}{\partial z^2}\right)$$

The dimensionless forms of the governing equations are:

$$\frac{\partial U}{\partial X}+\frac{\partial V}{\partial Y}+\frac{\partial W}{\partial Z}=0$$

$$U\frac{\partial U}{\partial X}+V\frac{\partial U}{\partial Y}+W\frac{\partial U}{\partial Z}=-\frac{\rho_f}{\rho_{nf}}\frac{\partial P}{\partial X}+\frac{\mu_{nf}}{\rho_{nf}\alpha_f}\left(\frac{\partial^2 U}{\partial X^2}+\frac{\partial^2 U}{\partial Y^2}+\frac{\partial^2 U}{\partial Z^2}\right)$$

$$U\frac{\partial V}{\partial X}+V\frac{\partial V}{\partial Y}+W\frac{\partial V}{\partial Z}=-\frac{\rho_f}{\rho_{nf}}\frac{\partial P}{\partial Y}+\frac{\mu_{nf}}{\rho_{nf}\alpha_f}\left(\frac{\partial^2 V}{\partial X^2}+\frac{\partial^2 V}{\partial Y^2}+\frac{\partial^2 V}{\partial Z^2}\right)$$
$$+\frac{(\rho\beta)_{nf}}{\rho_{nf}\beta_f}Ra\,\Pr\theta-Ha^2\Pr V$$

$$U\frac{\partial\theta}{\partial X}+V\frac{\partial\theta}{\partial Y}+W\frac{\partial\theta}{\partial Z}=\frac{\alpha_{nf}}{\alpha_f}\left(\frac{\partial^2\theta}{\partial X^2}+\frac{\partial^2\theta}{\partial Y^2}+\frac{\partial^2\theta}{\partial Z^2}\right)$$

where U, V and W fluid velocity in X-direction, Y-direction and Z-direction respectively, P is pressure, B_0 is the magnetic field strength, θ is the temperature. Rayleigh number *Ra*, Prandtl number *Pr* and Hartman number *Ha* are defined as

$$Ra=\frac{g\beta_f\left(T-T_c\right)h^3}{\alpha_f\upsilon_f};\ \Pr=\frac{\upsilon_f}{\alpha_f};\ Ha=B_0h\sqrt{\frac{\sigma_{nf}}{\rho_{nf}\upsilon_f}}$$

In order to evaluate the heat transfer enhancement in the cavity, the local Nusselt number on the walls is defined as:

$$Nu_l=-\frac{k_{nf}}{k_f}\frac{\partial\theta}{\partial n}\bigg|_{wall}$$

where symbol n is the normal direction to the surface. Average Nusselt number along the hot walls of the cavity is considered to evaluate the overall heat transfer rate and is defined as:

$$Nu_{avg}=\int_0^1\int_0^1 Nu_l\,dY\,dZ\Big|_{X=0}$$

3.2 Algorithm

In the iterative Newton-Raphson algorithm, the discrete forms of the continuity, momentum and energy equations are solved to find out the value of the velocity and the temperature. It is essential to guess the initial values of the variables. Then the numerical solutions of the variables are obtained while the convergent criterion is fulfilled.

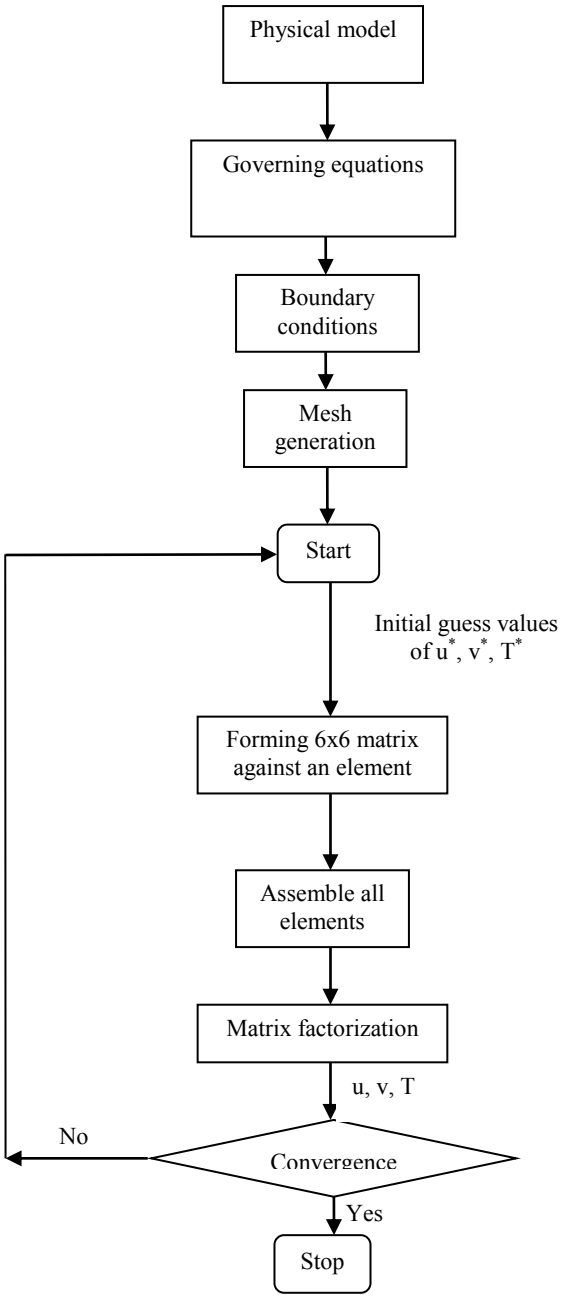

3.3 Solution of system of equations

A system of linear algebraic equations has been solved by the UMFPACK. UMFPACK is a set of routines for solving asymmetric sparse linear systems Ax = b, using the Asymmetric Multi Frontal method and direct sparse LU factorization. Five primary UMFPACK routines are required to factorize Ax = b:

1. Pre-orders the columns of A to reduce fill-in and performs a symbolic analysis.
2. Numerically scales and then factorizes a sparse matrix.
3. Solves a sparse linear system using the numeric factorization.
4. Frees the Symbolic object.
5. Frees the Numeric object.

Additional routines are:

1. Passing a different column ordering
2. Changing default parameters
3. Manipulating sparse matrices
4. Getting LU factors
5. Solving the LU factors
6. Computing determinant

UMFPACK factorizes PAQ, PRAQ, or $PR^{-1}AQ$ into the product LU, where L and U are lower and upper triangular, respectively, P and Q are permutation matrices, and R is a diagonal matrix of row scaling factors (or R = I if row-scaling is not used). Both P and Q are chosen to reduce fill-in (new non zeros in L and U that are not present in A). The permutation P has the dual role of reducing fill-in and maintaining numerical accuracy (via relaxed partial pivoting and row interchanges). The sparse matrix A can be square or rectangular, singular or non-singular, and real or complex (or any combination). Only square matrices A can be used to solve Ax = b or related systems. Rectangular matrices can only be factorized. UMFPACK first finds a column pre-ordering that reduces fill-in, without regard to numerical values. It scales and analyzes the matrix, and then automatically selects one of three strategies for pre-ordering the rows and columns: asymmetric, 2-by-2, and symmetric. These strategies are described below.

One notable attribute of the UMFPACK is that whenever a matrix is factored, the factorization is stored as a part of the original matrix so that further operations on the

matrix can use this factorization. Whenever a factorization or decomposition is calculated, it is preserved as a list (element) in the factor slot of the original object. In this way a sequence of operations, such as determining the condition number of a matrix and then solving a linear system based on the matrix, do not require multiple factorizations of the intermediate results.

Conceptually, the simplest representation of a sparse matrix is as a triplet of an integer vector i giving the row numbers, an integer vector j giving the column numbers, and a numeric vector x giving the non-zero values in the matrix. The triplet representation is row-oriented if elements in the same row were adjacent and column-oriented if elements in the same column were adjacent. The compressed sparse row (csr) or compressed sparse column (csc) representation is similar to row-oriented triplet or column-oriented triplet respectively. These compressed representations remove the redundant row or column in indices and provide faster access to a given location in the matrix.

3. 4 Thermo physical properties

Thermo physical properties of the Cu-water nanofluid are determined following

Table 3.1.Thermo-physical properties of water and Cu nanoparticle

Physical properties	Water	Cu
c_p (J/kg K)	4179	385
ρ (kg/m^3)	997.1	8933
k (W/m- K)	0.613	400
(K^{-1})	21x 10^{-5}	1.67 x 10^{-5}
α(m^2 s^{-1})	1.471 x 10^{-7}	-

CHAPTER 4

Natural Convection of Cu-water Nanofluid in Square Cavity

4.1 Physical Model of Square Cavity

Natural convection is governed by the differential equations expressing conservation of mass, momentum and energy. The flow model is based on the assumptions that the fluid is Newtonian and that the properties are constant with the exception of the density in the body force term of the momentum equation. The Boussinesq approximation is invoked for the fluid properties to relate density changes to temperature changes and so to couple in this way the temperature field to the flow field.The viscous dissipation term in the energy equation is neglected. It is taken that water and nanoparticles are in thermal equilibrium and no slip occurs between them. The density of the nanofluid is approximated by the Boussinesq model. The governing equations for natural convection flows using conservation of mass, momentum and energy can be written as with the physical dimensional as shown in fig.4.1. The bottom and the upper wall of the cavity are adiabatic. The left vertical wall is maintained at hot temperature and the right wall is cold.

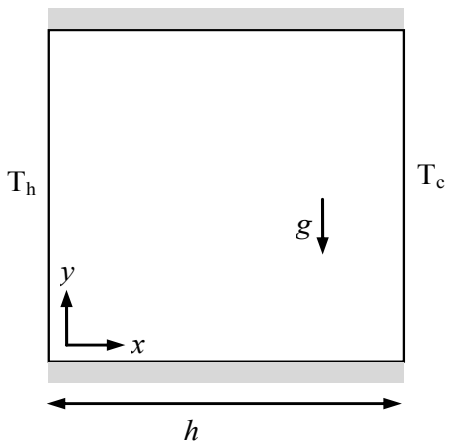

Fig.4.1 Schematic diagram of the physical system.

4.2 Model Validation

4.1.1 Natural convection of air filled in square cavity

The model is solved by using commercial finite element package COMSOL Multiphysics. It has been validated against benchmark solutions obtained in the literature as shown in the

Table 4.1. Natural convection of air inside a square cavity whose two sides are set to differential temperatures while keeping the top and bottom surfaces at adiabatic condition is a classic case for validation. Average Nusselt number for the hot wall calculated from the present model is compared with the data available in the literature and found very accurate for various high Rayleigh numbers.

Table 4.1. Average Nusselt number for the hot wall of the air filled square cavity obtained by various studies are shown and compared with present study for different Rayleigh numbers

Rayleigh number (Ra)	Present study	Vahl Davis (1983)	Fusegi et al. (1991)	Comini et al. (1995)	Khanafer et al. (2003)	Bilgen (2005)
10^4	2.2448	2.243	2.302	-	2.245	2.245
10^5	4.5216	4.519	4.646	4.503	4.522	4.521
10^6	8.8262	8.799	9.012	8.825	8.826	8.800
10^7	16.5301	-	16.543	16.533	-	16.629

4.1.2 Natural convection of Cu-water nanofluid in square cavity

A second degree of validation has been done for Cu-water nanofluid. Calculated average Nusselt number of the present study was compared against that of a Cu-water nanofluid filled square cavity for various Grashof number and found satisfactory.

Table 4.2. Comparison of average Nusselt number calculated on hot wall in Cu-water nanofluid filled square cavity with Khanafer et al. (2003)

Grashof number (Gr)	Present study	Khanefer et al (2003)
10^3	2.5662	2.835
10^4	5.4050	5.895
10^5	10.6669	11.245

4.1.3 Natural Convection of air in Square Cavity

Table 4.3. Comparison of average Nusselt number obtained with the computer code and those of Fusegi et al. (1991) and Frederick et al. (2000) for air (Pr = 0.71)

Rayleigh number (Ra)	Present study	Fusegi *et al.* (1991)	Frederick *et al.* (2000)
10^3	1.072	1.085	1.071
10^4	2.075	2.100	2.057
10^5	4.375	4.361	4.353
10^6	8.755	8.770	8.740

4.2 Natural Convection of Cu-Water Nanofluid in Square Cavity

In the present study, steady and laminar natural convection of Cu -water nanofluids in a square enclosure with differentially heated vertical walls have been studied by numerical means. The effects of the Rayleigh number, solid volume fraction on the heat and momentum transport characteristics in Cu-water nanofluid have been investigated systematically.

In the present investigation, the influences of Rayleigh number Ra and solid volume fraction of nanoparticles φ on the streamlines and isotherms patterns are assumed while Prandtl number is kept constant at Pr = 6.2. The values of Rayleigh numbers and solid volume fraction of nanoparticles considered are $Ra = 10^3, 10^4, 10^5, 10^6$ and $\varphi = 0, 0.05, 0.1, 0.15, 0.2$. Fig. 4.2 demonstrates the effects of Rayleigh number Ra and solid volume fraction φ upon streamlines patterns in the square cavity filled with Cu-water nanofluid. The figure demonstrates that circulation cells are formed in the clockwise direction for lower values of Rayleigh numbers. It is clear that the flow strengths are influenced by the presence of nanoparticle. Two primary vortices are found in the left and right side of the circular disk at Ra = 10^5 .The shapes of these vortices change from circular to triangular with the increasing of φ. This happens as a result of getting higher buoyancy force. Fig.4.2 shows the temperature distribution in the square cavity for different Ra and φ. As can be seen from the isotherms in Fig. 4.3, at $Ra = 10^3, 10^4, 10^5, 10^6$ parallel isotherms with the walls of the cavity exist for all range of the solid volume fraction of the nanofluid which is characteristic of

conduction heat transfer. At *Ra* for all range of the solid volume fraction of the nanofluid, distinct thermal boundary layers are formed adjacent to the vertical isothermal walls of the cavity which states convective heat transfer.

Fig. 4.7.shows variation of the average Nusselt number Nu_{avg} of the hot walls of the square cavity with solid volume fraction φ of the nanofluid and the Rayleigh number *Ra* for the square cavity. Moreover it is found that at $Ra = 10^3$-10^4, the average Nusselt number does not change significantly. However, as the Rayleigh number increases, the effect of the convection dominates the heat transfer. In addition, the addition of nanoparticles to the pure water increases the thermal conductivity. As a result, the heat transfer effect of nanofluid is higher than that of pure water and the effect of nanoparticle addition in the base fluid on the heat transfer performance is better at low Rayleigh numbers than at high Rayleigh numbers. Fig.4.7. represents the effect of average Nusselt number Nu_{avg} due to the various Rayleigh numbers *Ra* as well as solid volume fraction φ for the square cavity. It is seen from figures that Nu_{avg} enhances sharply up to $Ra=10^4$ and beyond this region they raise gradually.Finally it is seen that the heat transfer decreases or increases depending on the value of the base-fluid Rayleigh number. It is true that the addition of Cu nanoparticles in water increases its thermal conductivity, therefore improves the conductive heat transfer in the nanofluid compared to conductive heat transfer in the base fluid. But on the other hand, just after the onset of convection adding nanoparticles enhances the heat transfer only for a given values of the temperature difference.

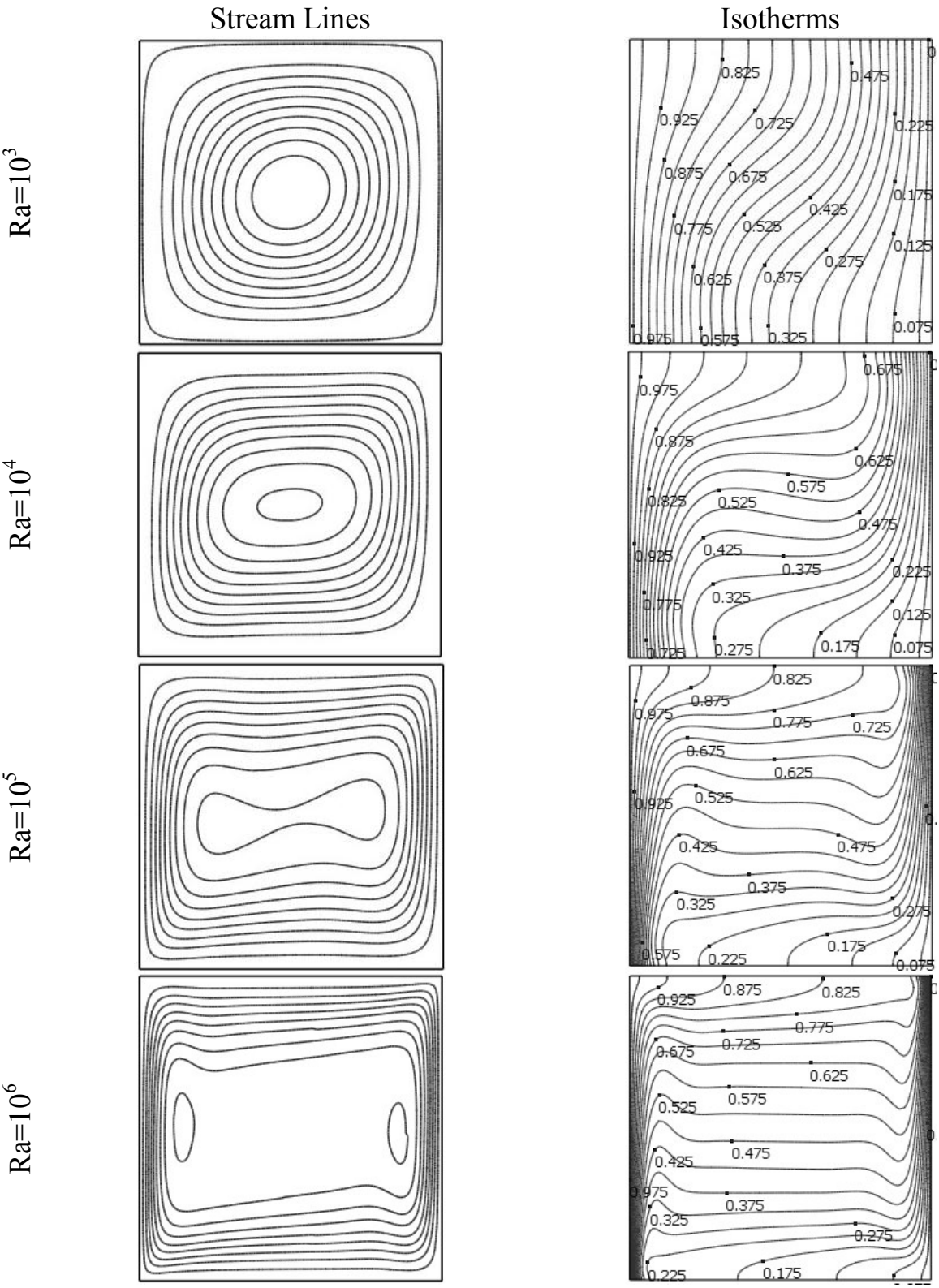

Figure 4.2: Streamlines and Isotherm patterns for φ=0 at different Rayleigh numbers.

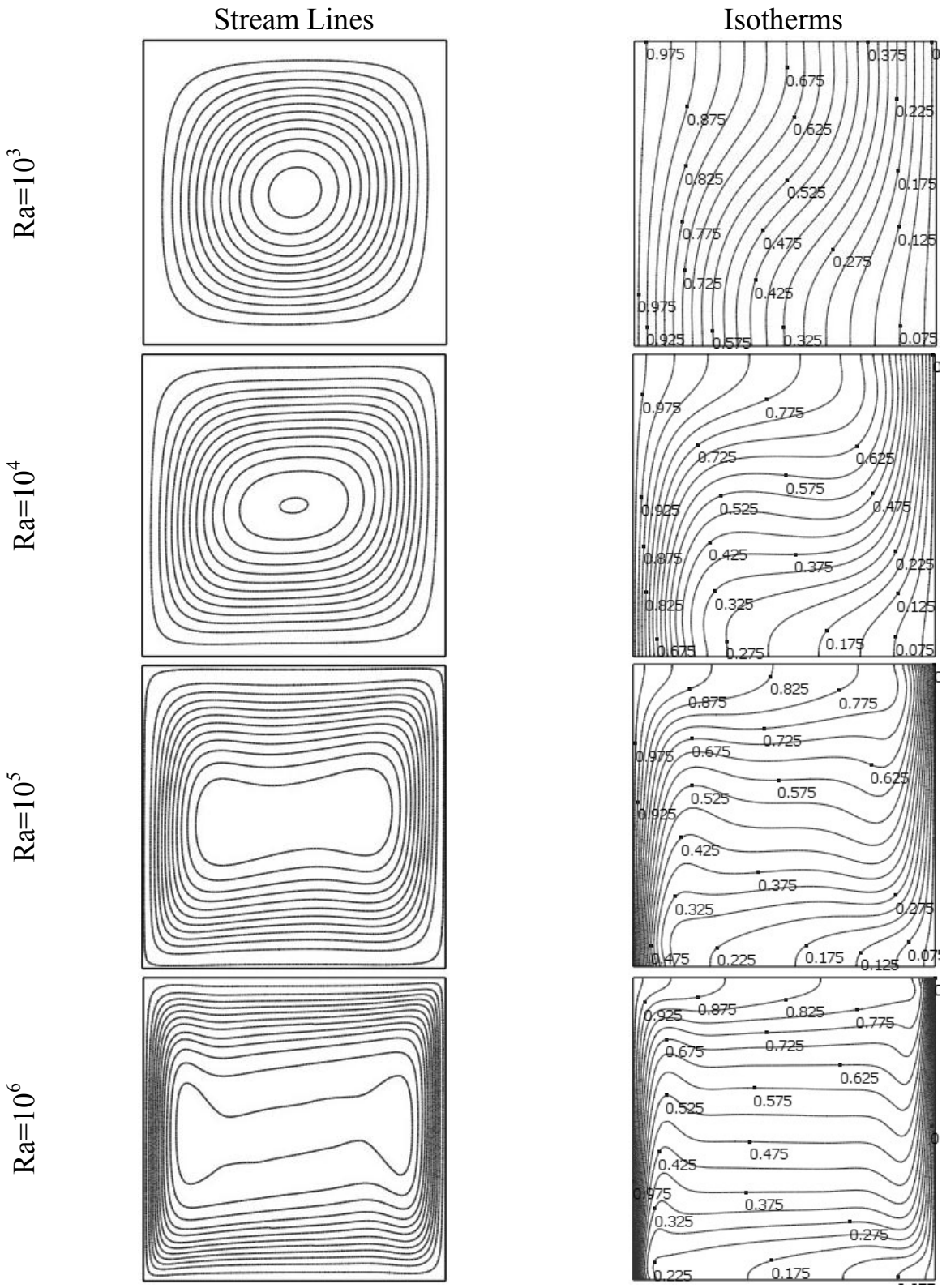

Figure 4.3: Streamlines and Isotherm patterns for φ=0.05 at different Rayleigh numbers.

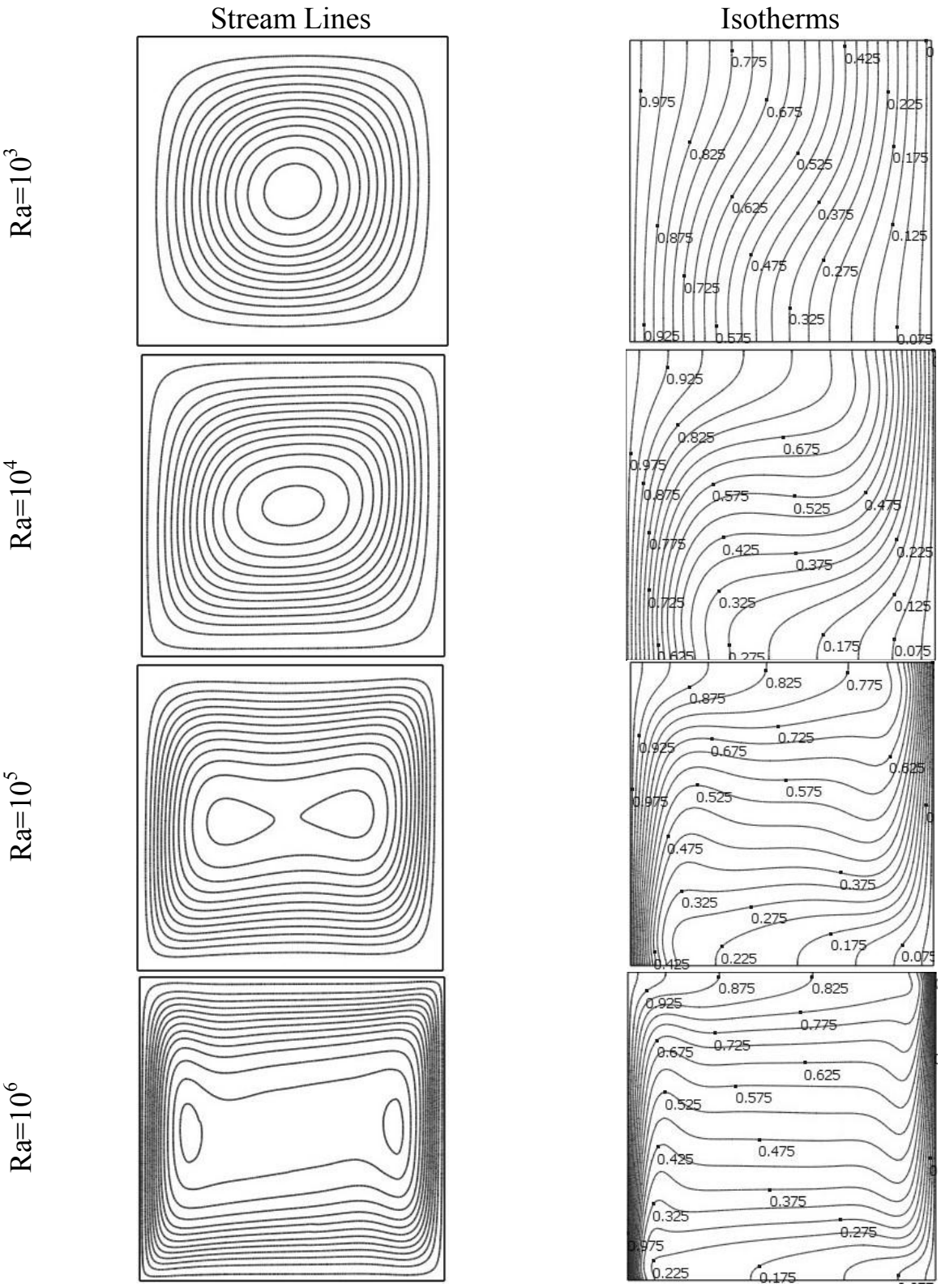

Figure 4.4: Streamlines and Isotherm patterns for φ=0.1 at different Rayleigh numbers.

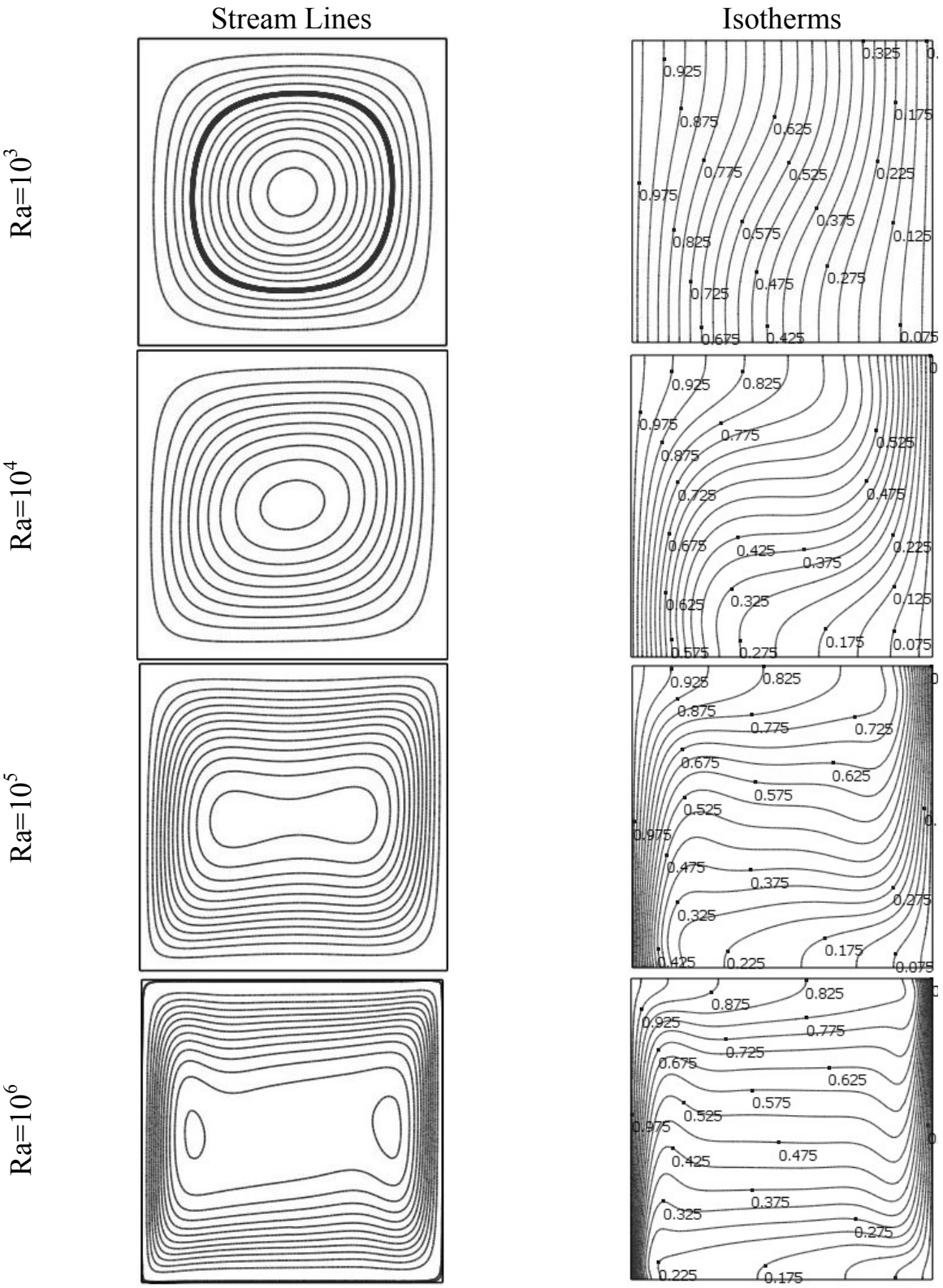

Figure 4.5: Streamlines and Isotherm patterns for φ=0.15 at different Rayleigh numbers.

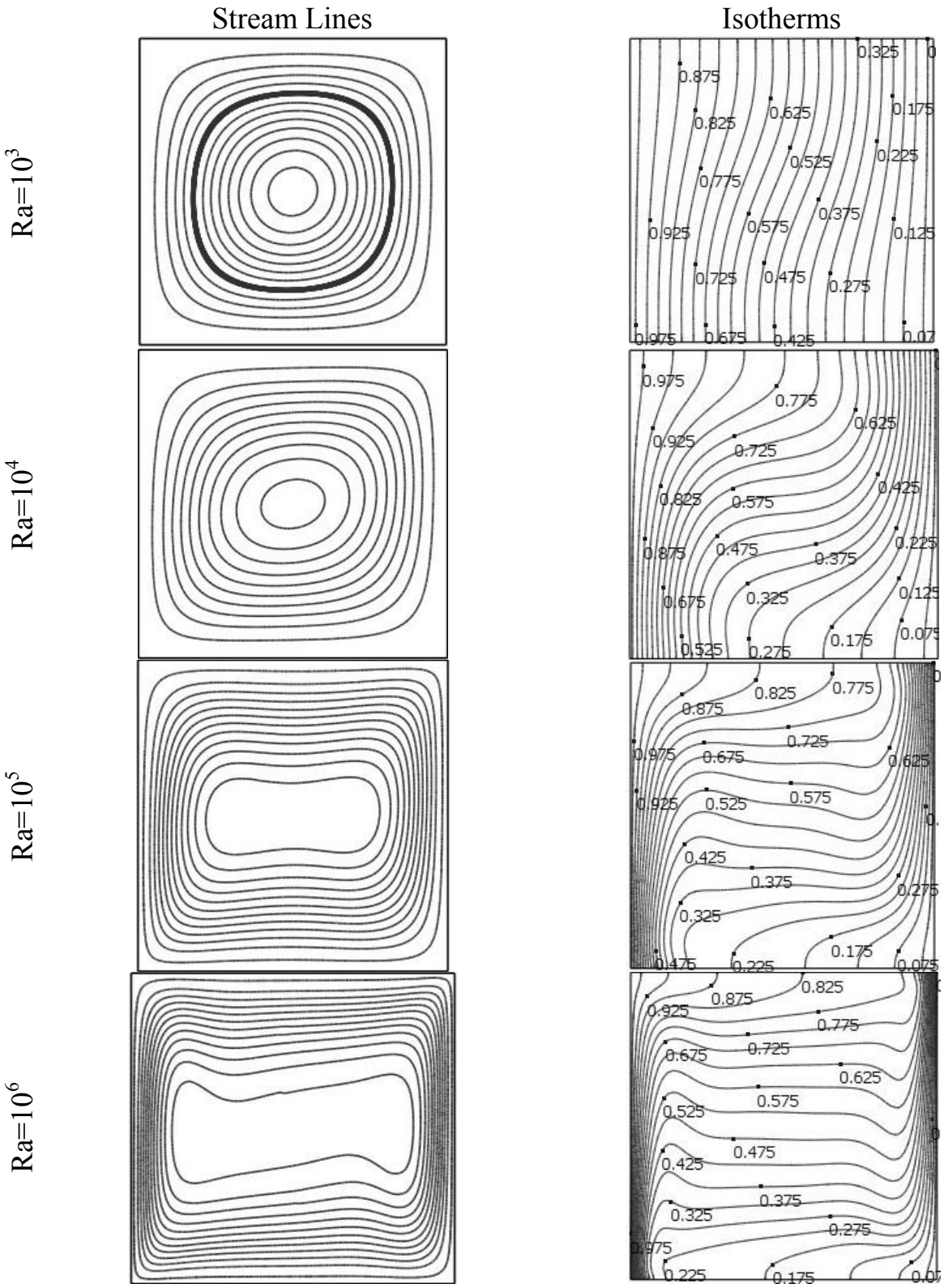

Figure 4.6: Streamlines and Isotherm patterns for φ=0.2 at different Rayleigh numbers.

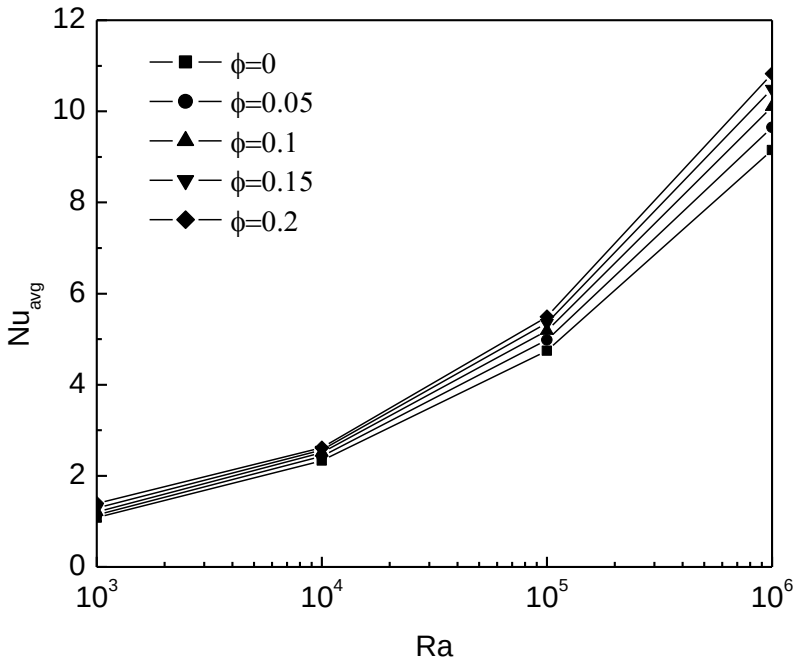

Figure 4.7: Variation of average Nusselt number with different Rayleigh numbers for different volume fractions

4.3 Natural convection of Cu-water nanofluid in square cavity with a circular disk.

A schematic view of a square cavity with a circular disk considered in the present study is shown in Fig. 4.8. side of the square cavity and diameter of the circular disk are denoted by h and d respectively. The problem is formulated in two-dimensional Cartesian coordinate system. The cavity is filled with Cu-water nanofluid which is considered to be Newtonian, laminar and incompressible.

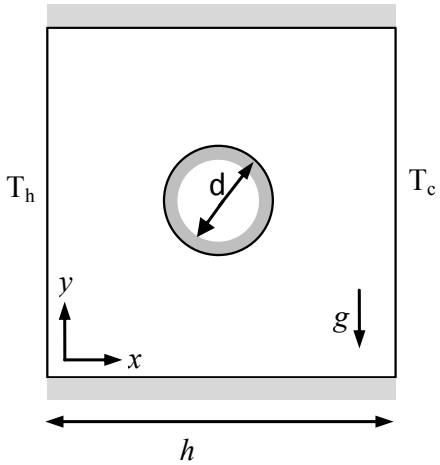

Fig.4.8. Schematic view of a square cavity with a circular disk

4.3 .1 Adiabatic circular disk

The first problem is defined as differentially heated square cavity with an adiabatic circular disk at the centre of the cavity. The ratio of diameter of the disk (d) to sides of the square cavity (h) is taken as $\lambda = d / h = 0.2$ Thermal boundary conditions are taken as $T = T_h$ for the hot left wall, $T = T_c$ for the cold right wall and adiabatic condition $\partial T/\partial n = 0$ for the top, bottom and disk walls. No-slip condition is imposed on all surfaces.

No-slip condition is imposed for all velocities on the wall. Thermal boundary conditions are

$T = T_h$ for the hot walls $T = T_c$ for the cold walls and $\frac{\partial T}{\partial n} = 0$ for the adiabatic walls, where n is normal direction to the walls, that using the dimensionless parameters the following boundary conditions are used for the equations (3.19) to (3.22):

On the hot walls : $U = V = 0; \theta = 1$

On the cold walls : $U = V = 0; \theta = 0$

On the adiabatic walls : $U = V = 0$; $\frac{\partial \theta}{\partial n} = 0$

In the present investigation, the influences of Rayleigh number Ra and solid volume fraction of nanoparticles φ on the streamlines and isotherms patterns were assumed while Prandtl number is kept constant at $(Pr = 6.2)$. The values of Rayleigh numbers and solid volume fraction of nanoparticles considered are $Ra = 10^3, 10^4, 10^5, 10^6$ and φ = 0, 0.05, 0.1, 0.2. Fig 4.9 demonstrates the effects of Rayleigh number Ra and solid volume fraction φ upon streamlines patterns in the square cavity with adiabatic circular disk filled with Cu-water nanofluid. The figure demonstrates that circulation cells are formed in the clockwise direction for lower values of Rayleigh numbers. It is clear that the flow strengths are influenced by the presence of nanoparticle. The behavior is similar to the trend encountered at lower Rayleigh number. Two primary vortices are found in the left and right side of the circular disk at $Ra = 10^5$ .The shapes of these vortices change from circular to triangular with the increasing of Ra. This happens as a result of getting higher buoyancy force.

Fig.4.10 shows the temperature distribution in the square cavity with adiabatic circular disk for Ra and φ . As can be seen from the isotherms in Fig. 4.3, at $Ra = 10^3 - 10^6$, parallel isotherms with the walls of the cavity exist for all range of the solid volume fraction of the nanofluid which is characteristic of conduction heat transfer. At 10^6, for all range of the solid volume fraction of the nanofluid, distinct thermal boundary layers are formed adjacent to the vertical isothermal walls of the cavity which states convective heat transfer.

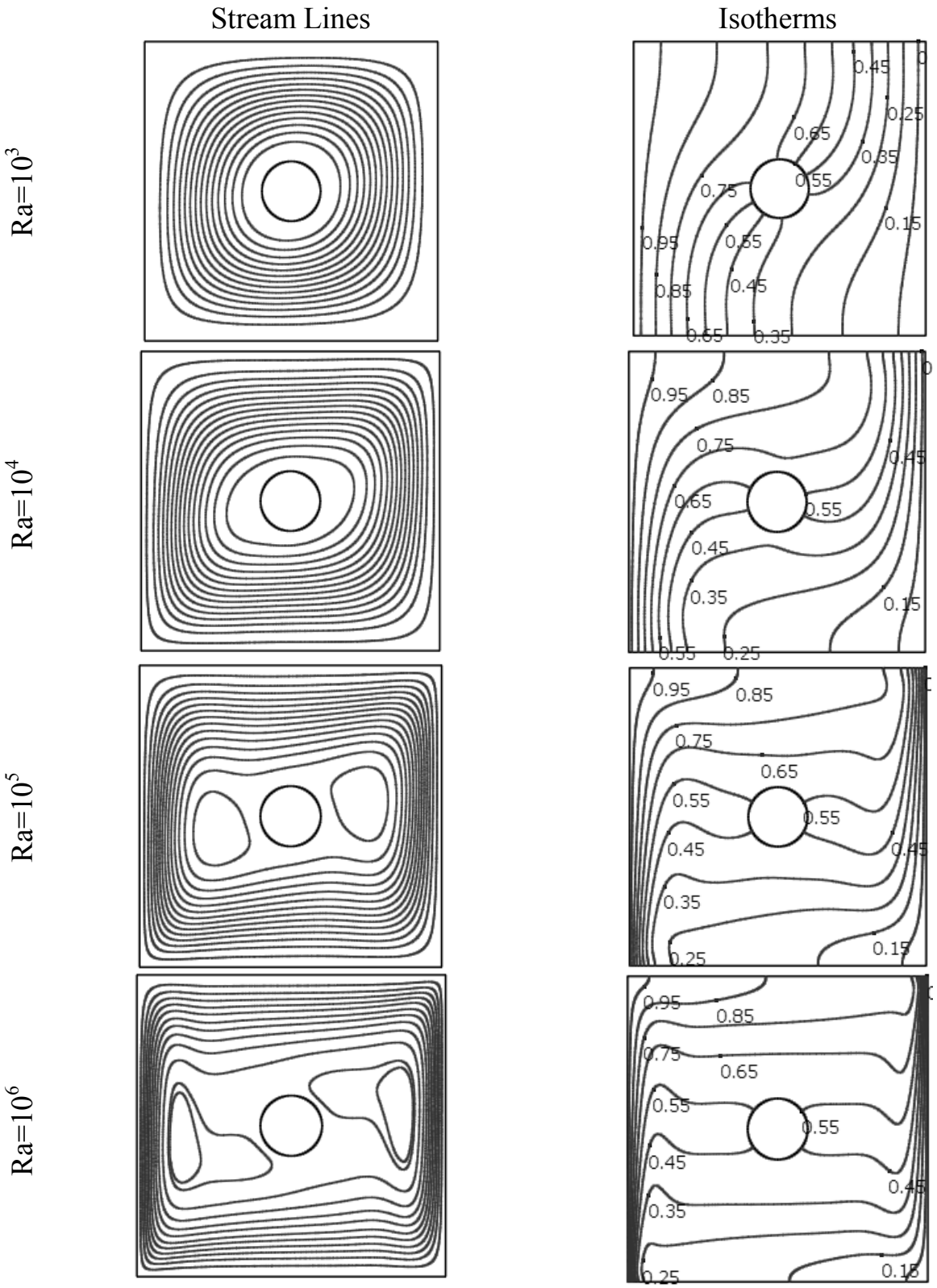

Fig 4.9: Streamlines and Isotherm patterns for pure water for φ=0 at different Rayleigh numbers.

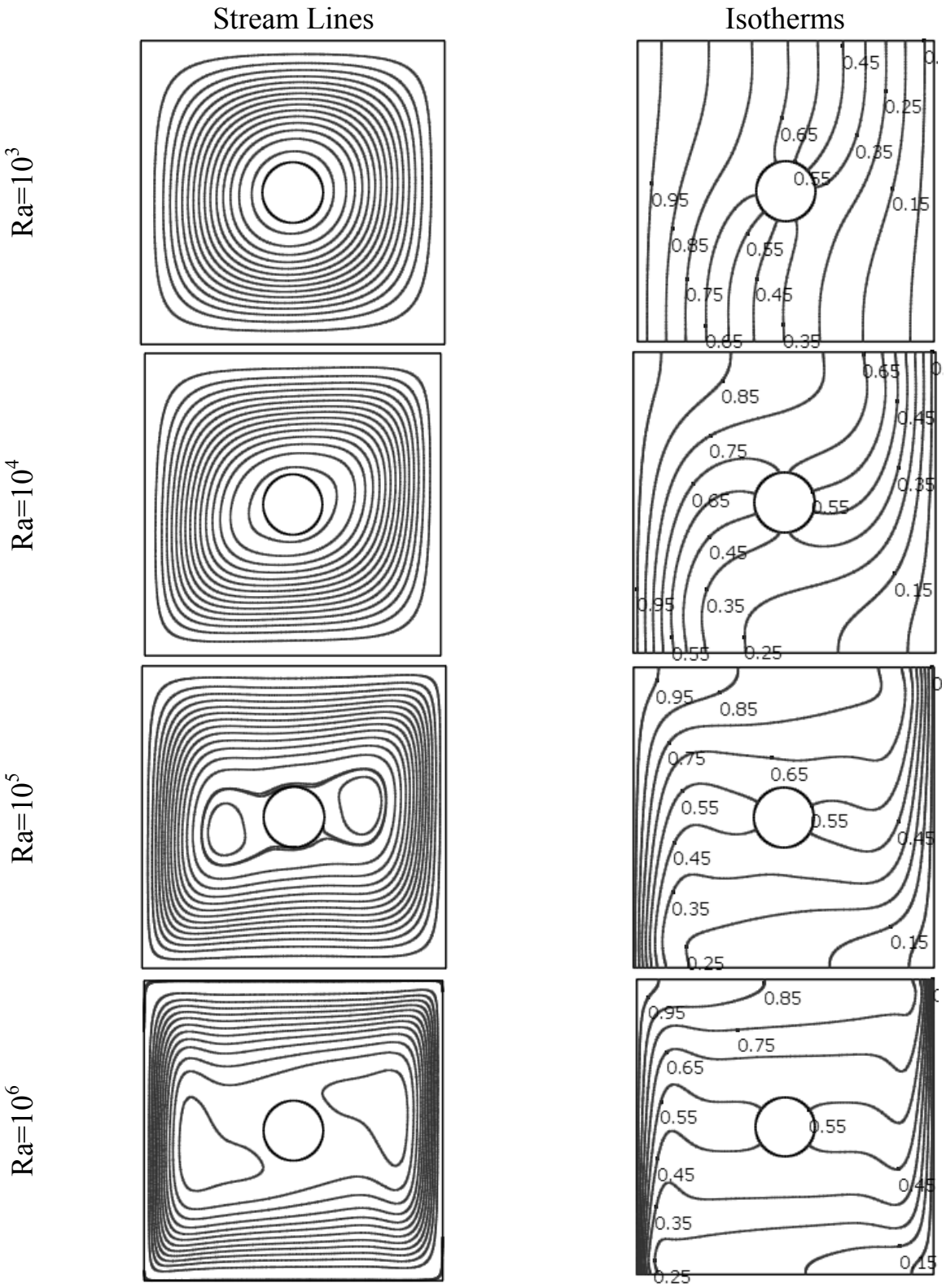

Fig.4.10: Streamlines and Isotherm patterns of Cu-water nanofluid for φ=0.05 at different Rayleigh numbers.

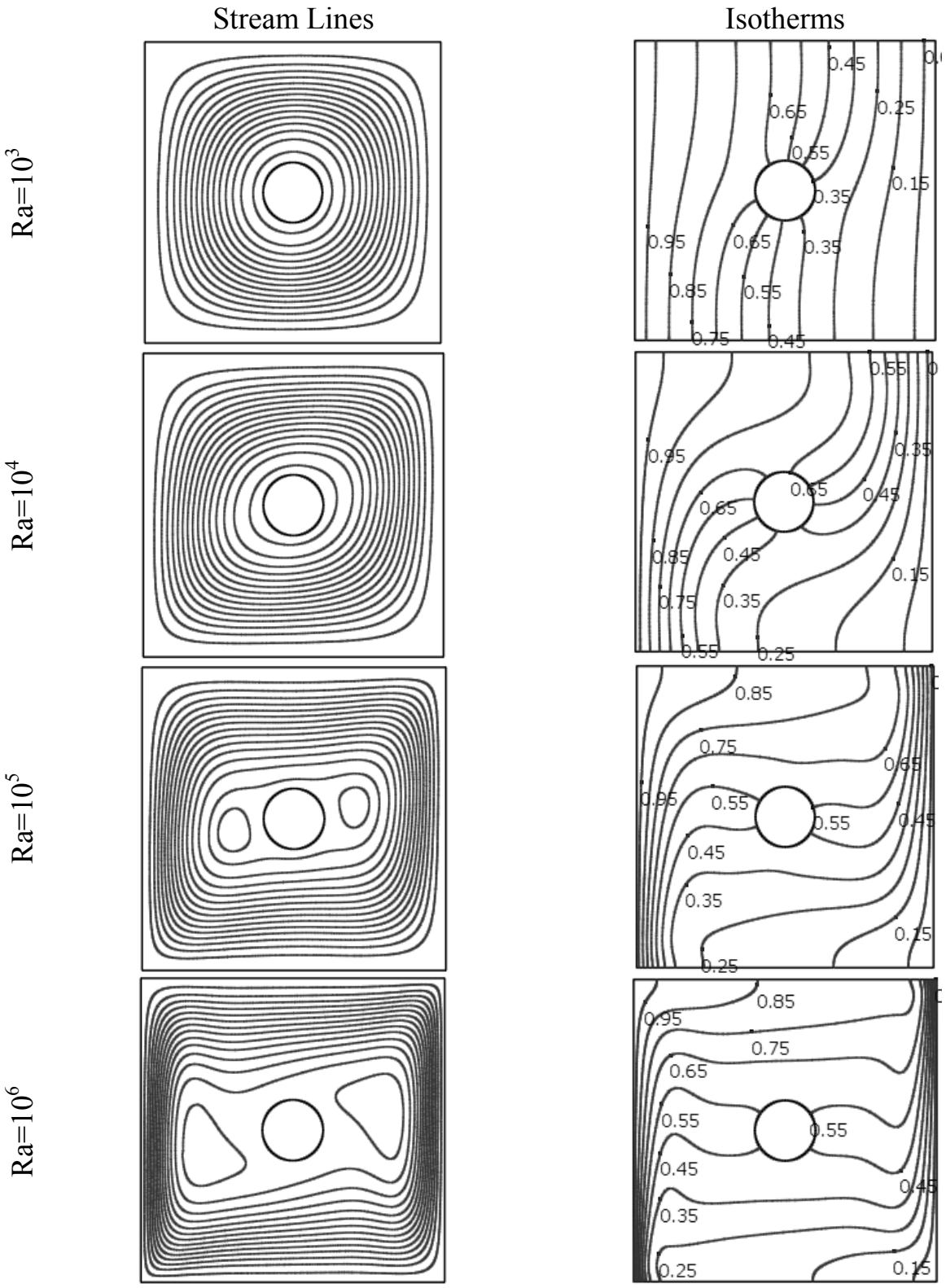

Fig.4.11: Streamlines and Isotherm patterns of Cu–water nanofluid for φ=0.1 at different Rayleigh numbers.

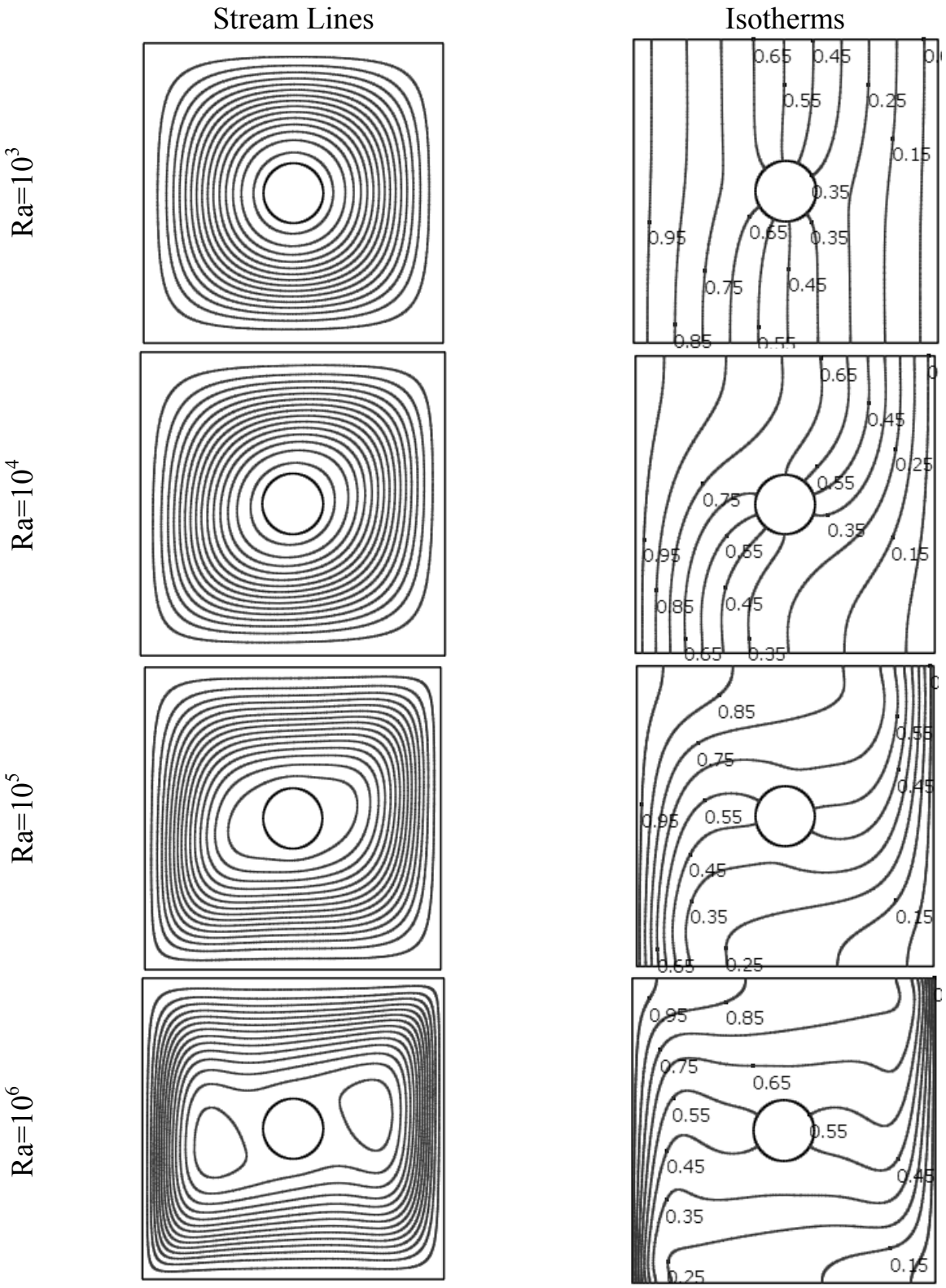

Fig.4.12: Streamlines and Isotherm patterns of Cu–water nanofluid for φ=0.15 at different Rayleigh numbers.

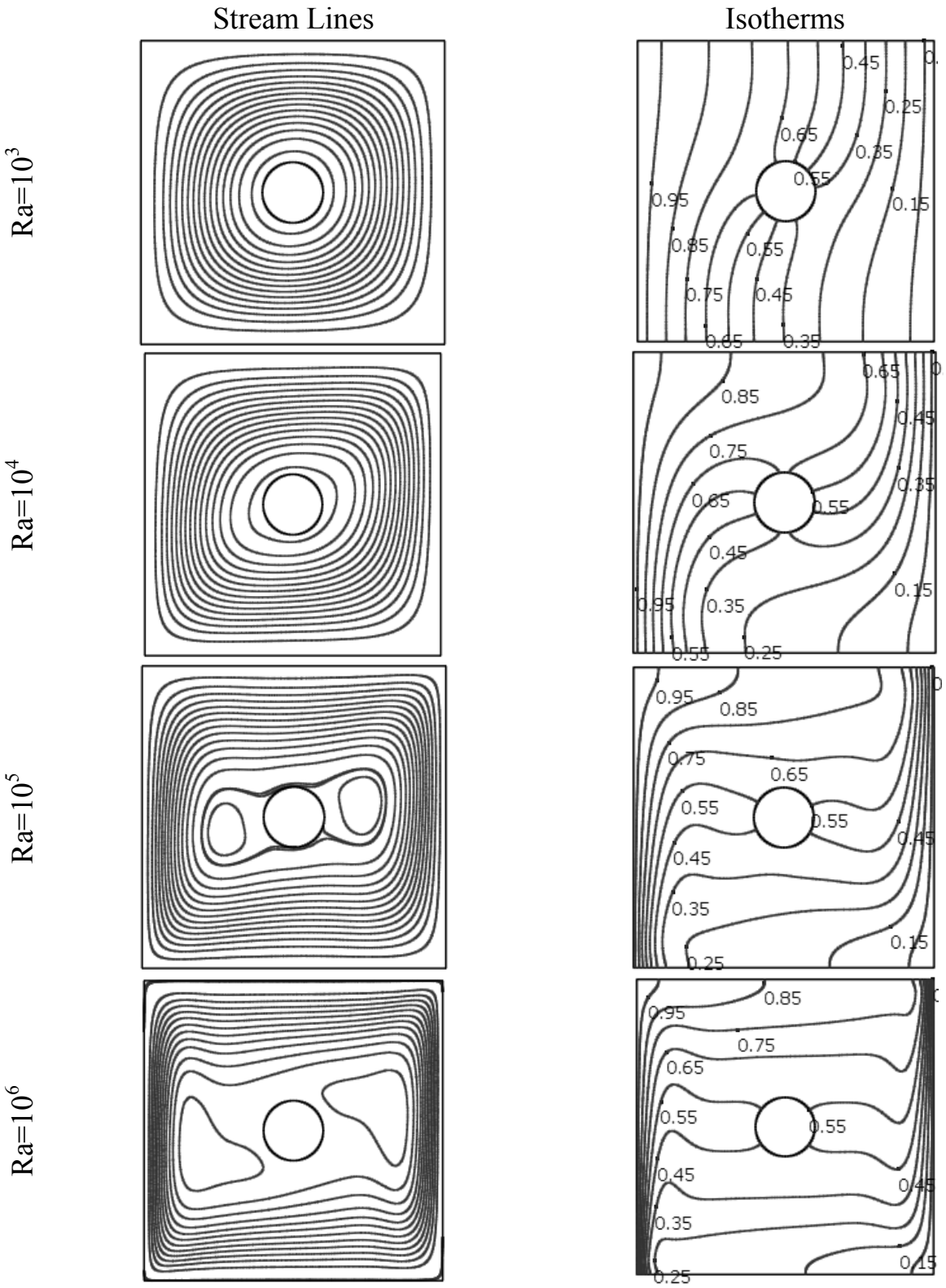

Fig.4.13: Streamlines and Isotherm patterns of Cu–water nanofluid for φ=0.2 at different Rayleigh numbers.

4.3.2 Cold circular disk

In eqs. (3.19) to (3.22) the following boundary conditions are obtained for cold circular disk.

On the disk wall: $U = V = 0; \quad \theta = 0$

On the left and right walls: $U = V = 0; \quad \theta = 1$

On the top and bottom walls: $U = V = 0; \quad {\partial\theta}/{\partial n} = 0$

In Fig.4.14 to Fig.4.18. the results are presented in terms of streamlines and isotherms for different choice of solid volume fractions φ and different Rayleigh numbers Ra in the square cavity containing cold circular disk. Two symmetric flow circulation patterns are observed within the cavity and flow patterns are qualitatively similar for water and nanofluids. The shape of streamlines changes slightly with the increasing of the solid volume fraction φ because of higher concentration of nanoparticles. As the volume fraction of nanoparticle enhances from 0 to 0.2, the isotherm contours tend to get affected considerably.

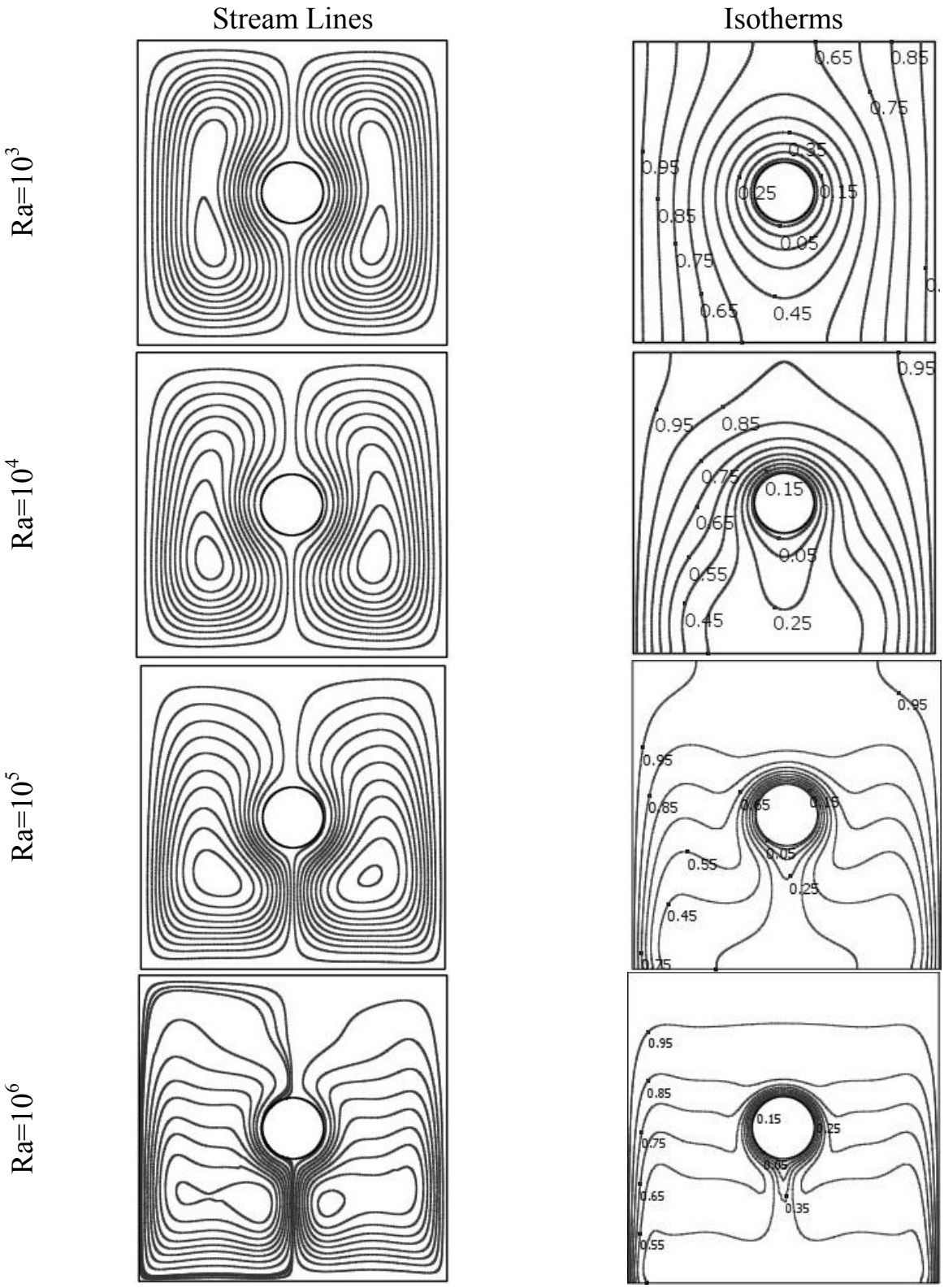

Fig.4.14: Streamlines and Isotherm patterns of pure water nanofluid for φ=0 at different Rayleigh numbers.

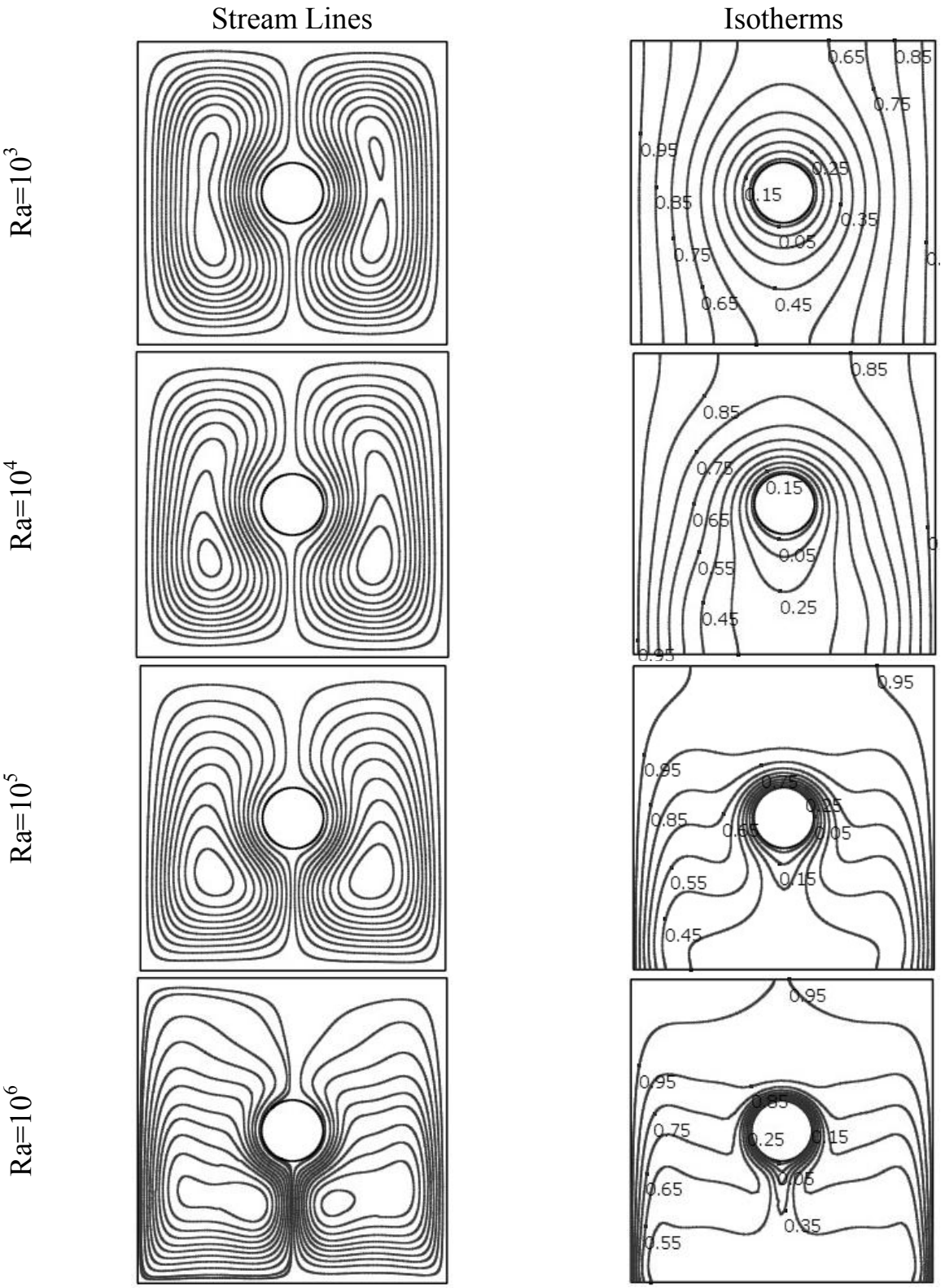

Fig 4.15: Streamlines and Isotherm patterns for Cu–water nanofluid in square cavity with cold circular disk for φ=0.05 at different Rayleigh numbers.

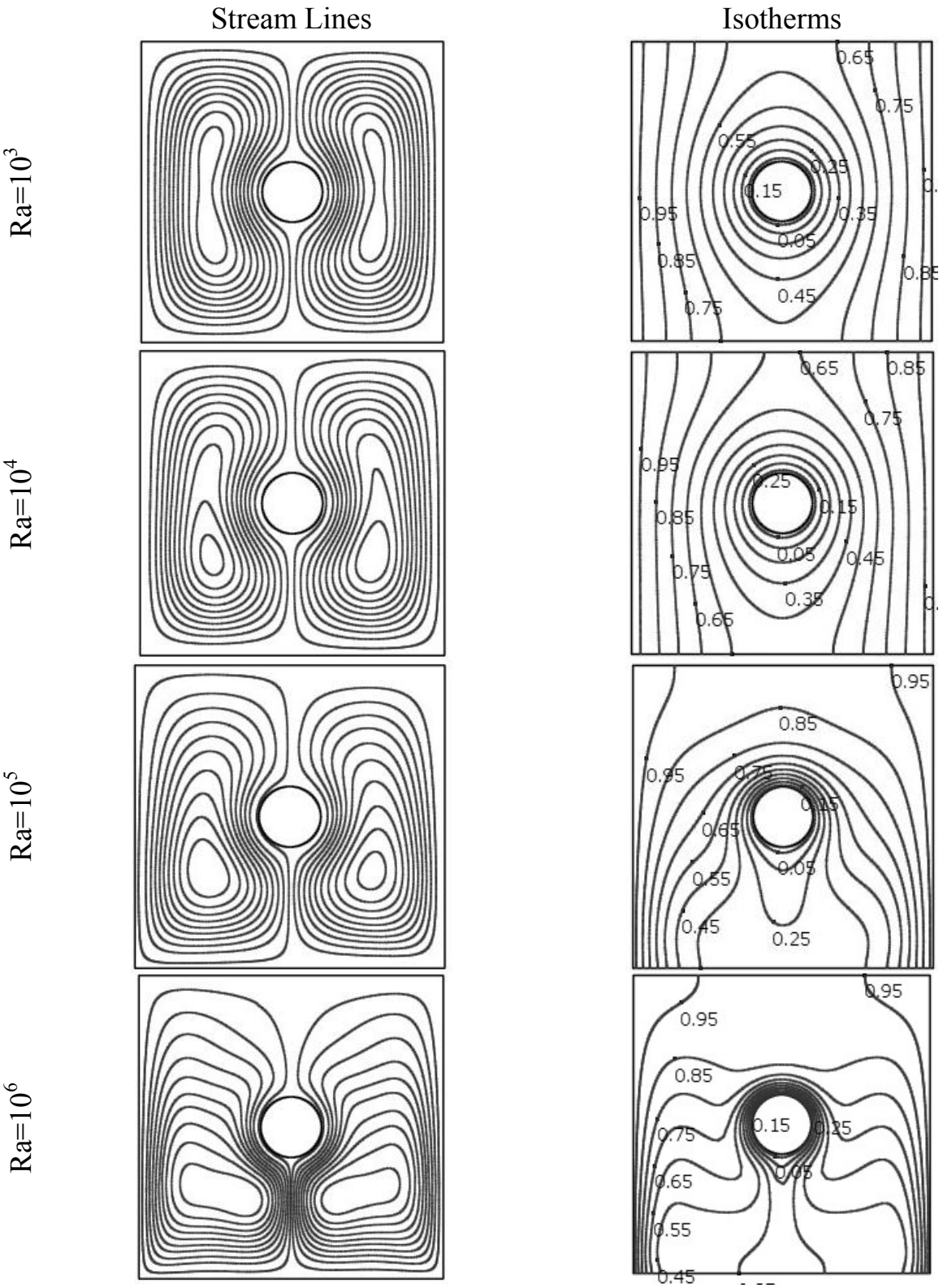

Fig 4.16: Streamlines and Isotherm patterns for Cu–water nanofluid in square cavity with cold circular disk for φ=0.1 at different Rayleigh numbers.

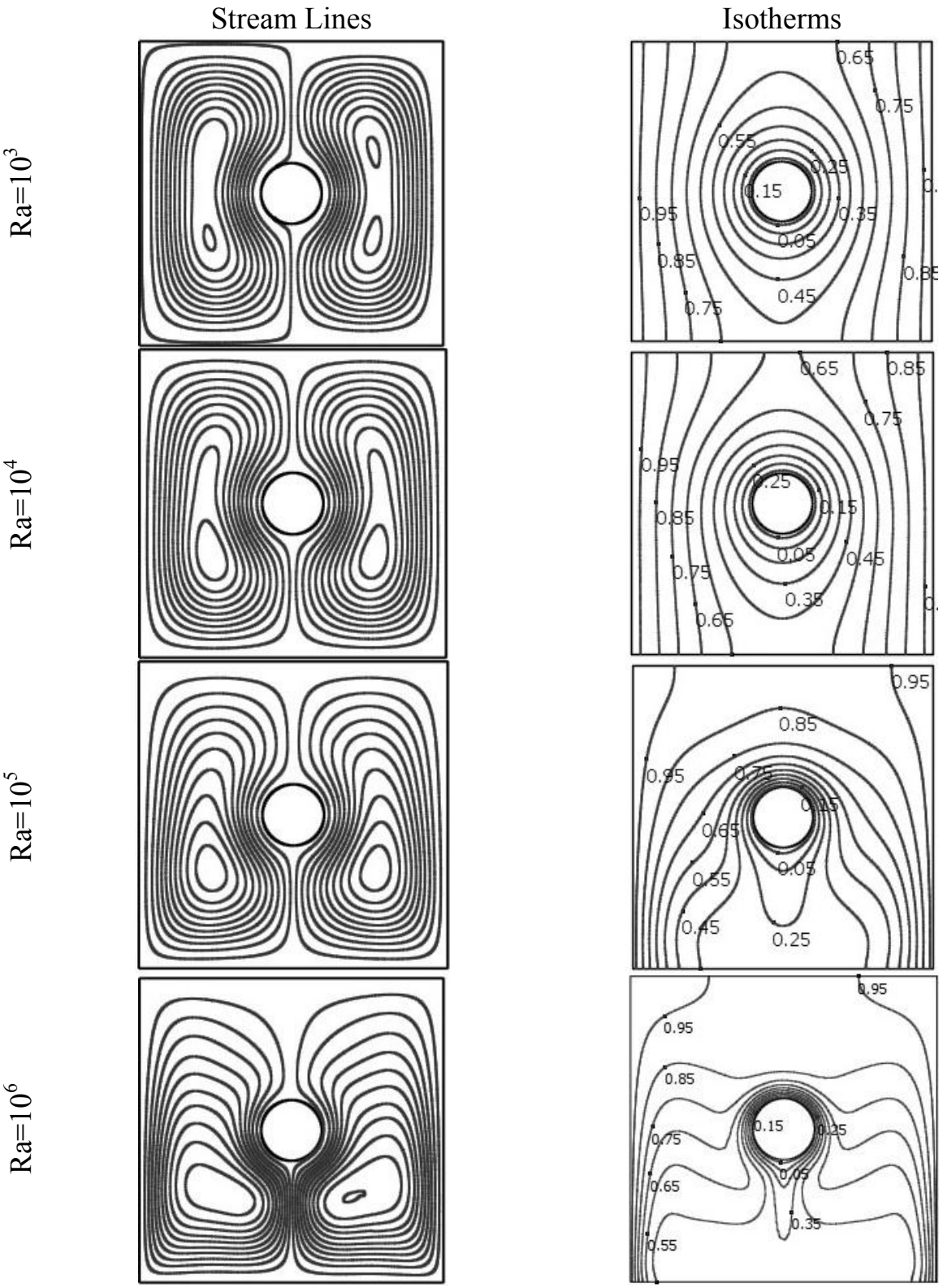

Fig 4.17: Streamlines and Isotherm patterns for Cu–water nanofluid in square cavity with cold circular disk for φ=0.15 at different Rayleigh numbers.

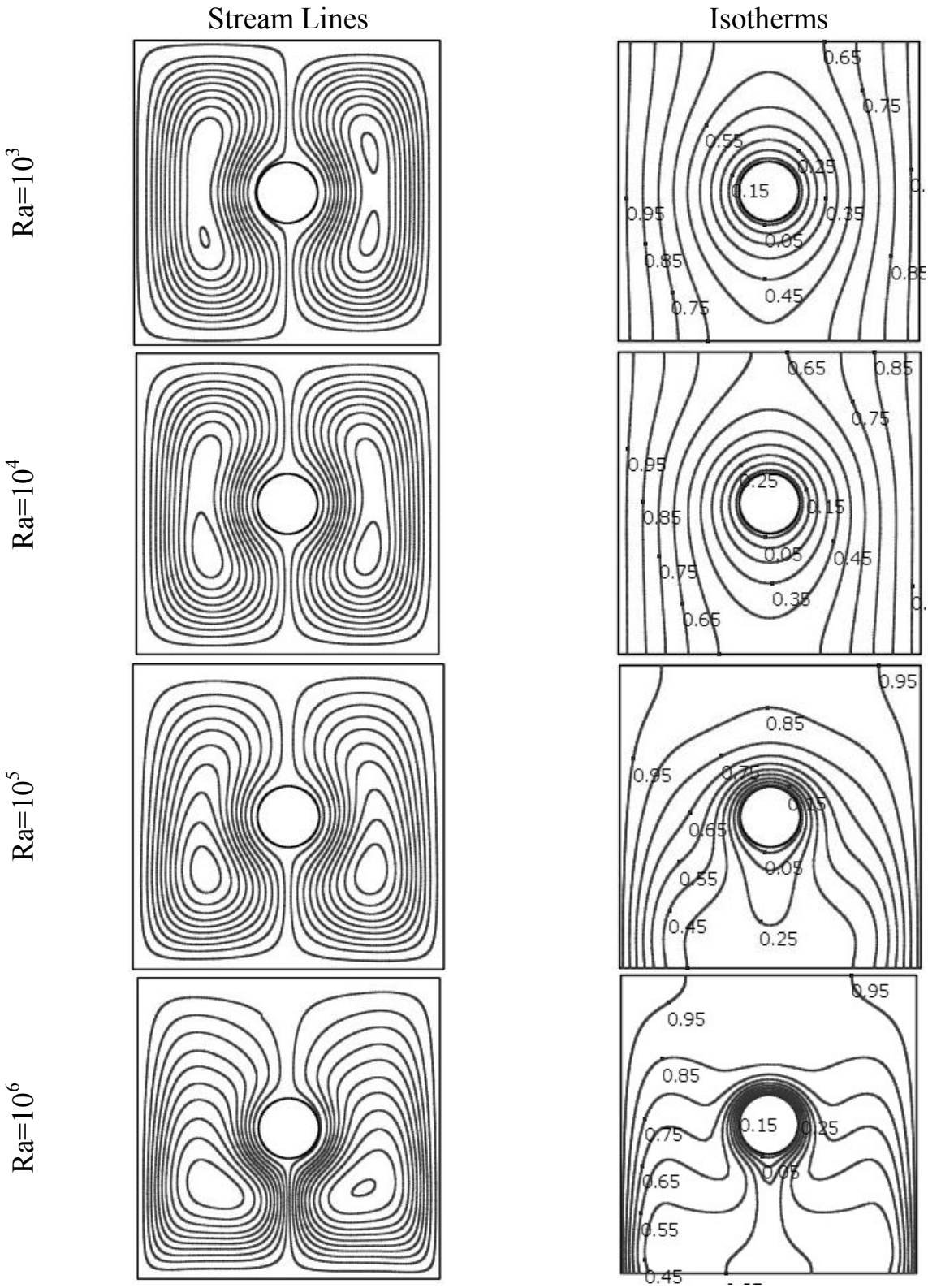

Fig 4.18: Streamlines and Isotherm patterns for Cu–water nanofluid in square cavity with cold circular disk for φ=0.2 at different Rayleigh numbers.

4.3.3 Heated circular disk

In eqs. (3.19) to (3.22) the following boundary conditions are obtained for heated circular disk. On the disk wall: $U = V = 0; \quad \theta = 1$

On the left and right walls: $U = V = 0; \quad \theta = 0$

On the top and bottom walls: $U = V = 0; \quad {}^{\partial\theta}/_{\partial n} = 0$

In Fig.4.19 to Fig.4.23. the results are presented in terms of streamlines and isotherms for different choice of solid volume fractions φ and different Rayleigh numbers Ra in the square cavity containing heated circular disk. The flow rate exists with maximum value in the centre of the circulation. As the parameter Ra increases, the flow rates at the centers of circulation increase. In Fig.4.20 for increment of Ra, the isothermal lines become more condensed near the heated disk. This figure shows that from the middle portion of the bottom wall fluid rise up around the circular disk along two vertical walls using symmetric rolls inside the cavity. Moreover, it is observed that raising the Rayleigh numbers causes the higher depth of the thermal boundary layer near the heated surface that point towards a steep temperature gradient and consequently, an enhancement on the whole heat transfer inside the cavity. It is seen that, pure water moves more rapidly than the solid concentrated nanofluids and raising of φ shows a deformation at the isothermal lines near the upper part of the top portion of the heated circular disk.

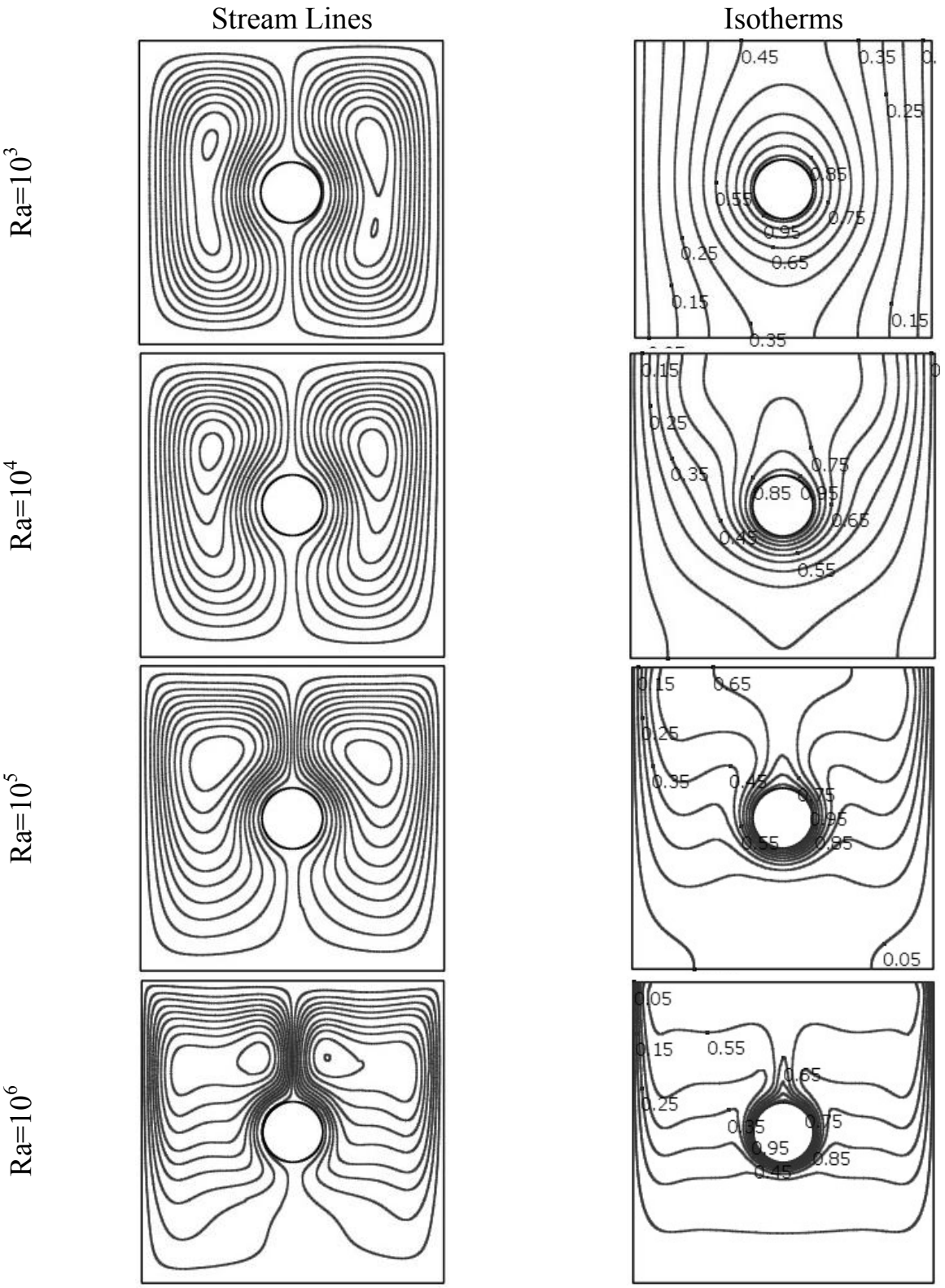

Fig.4.19: Streamlines and Isotherm patterns for base fluid for φ=0 at different Rayleigh numbers.

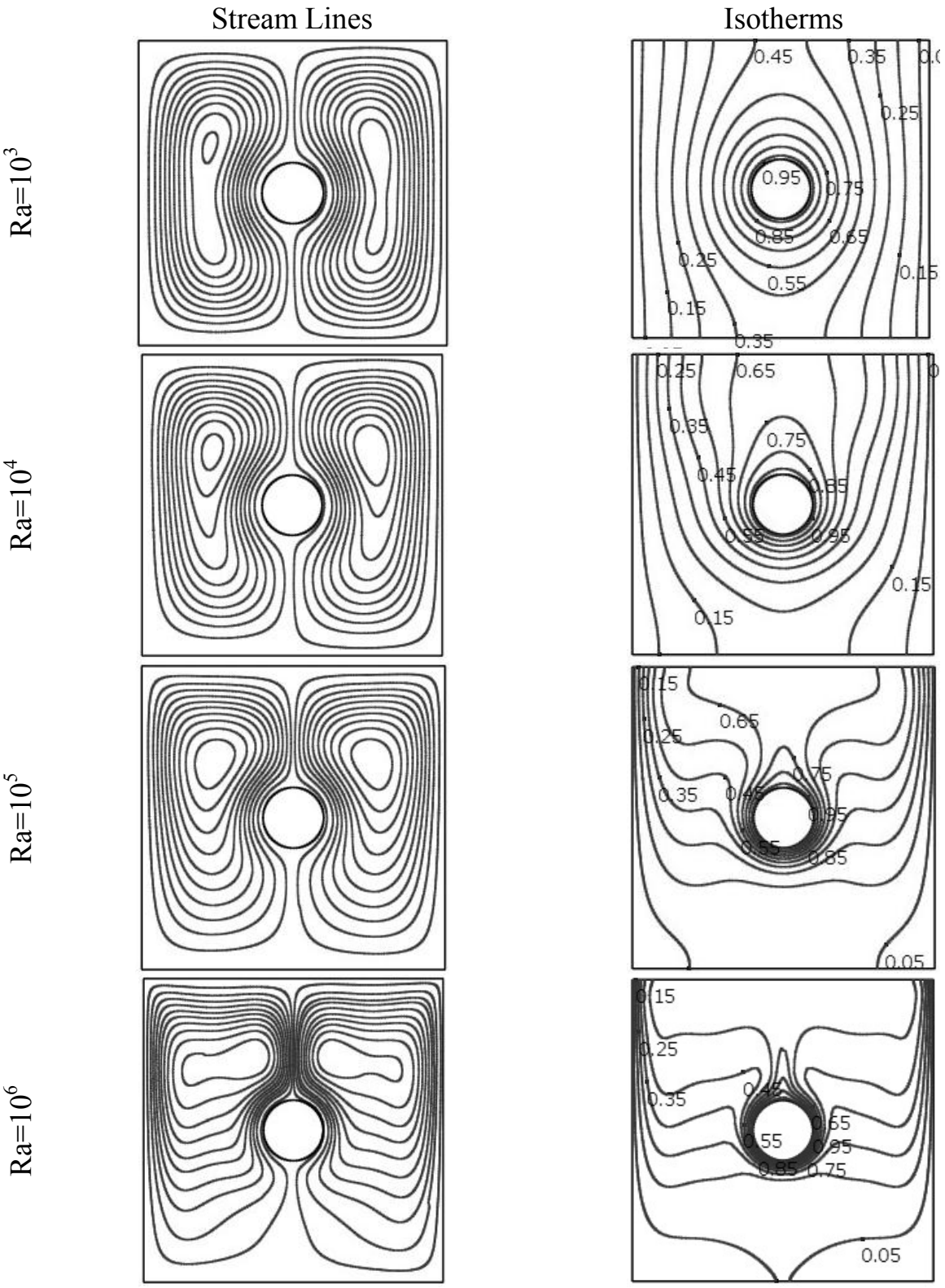

Fig 4.20: Streamlines and Isotherm patterns for Cu–water nanofluid for φ=0.05 at different Rayleigh numbers.

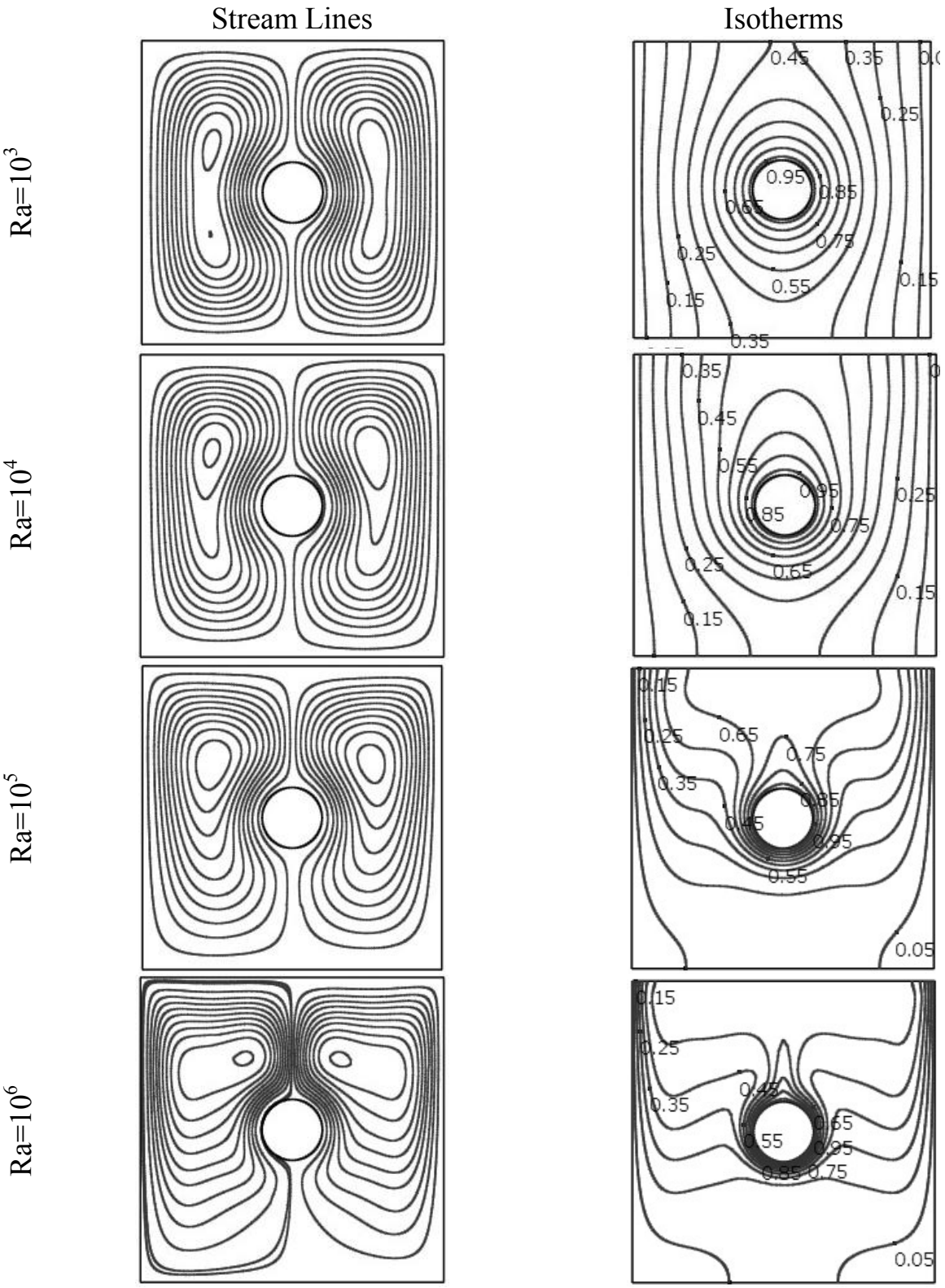

Fig 4.21: Streamlines and Isotherm patterns for Cu–water nanofluid for φ=0.1 at different Rayleigh numbers.

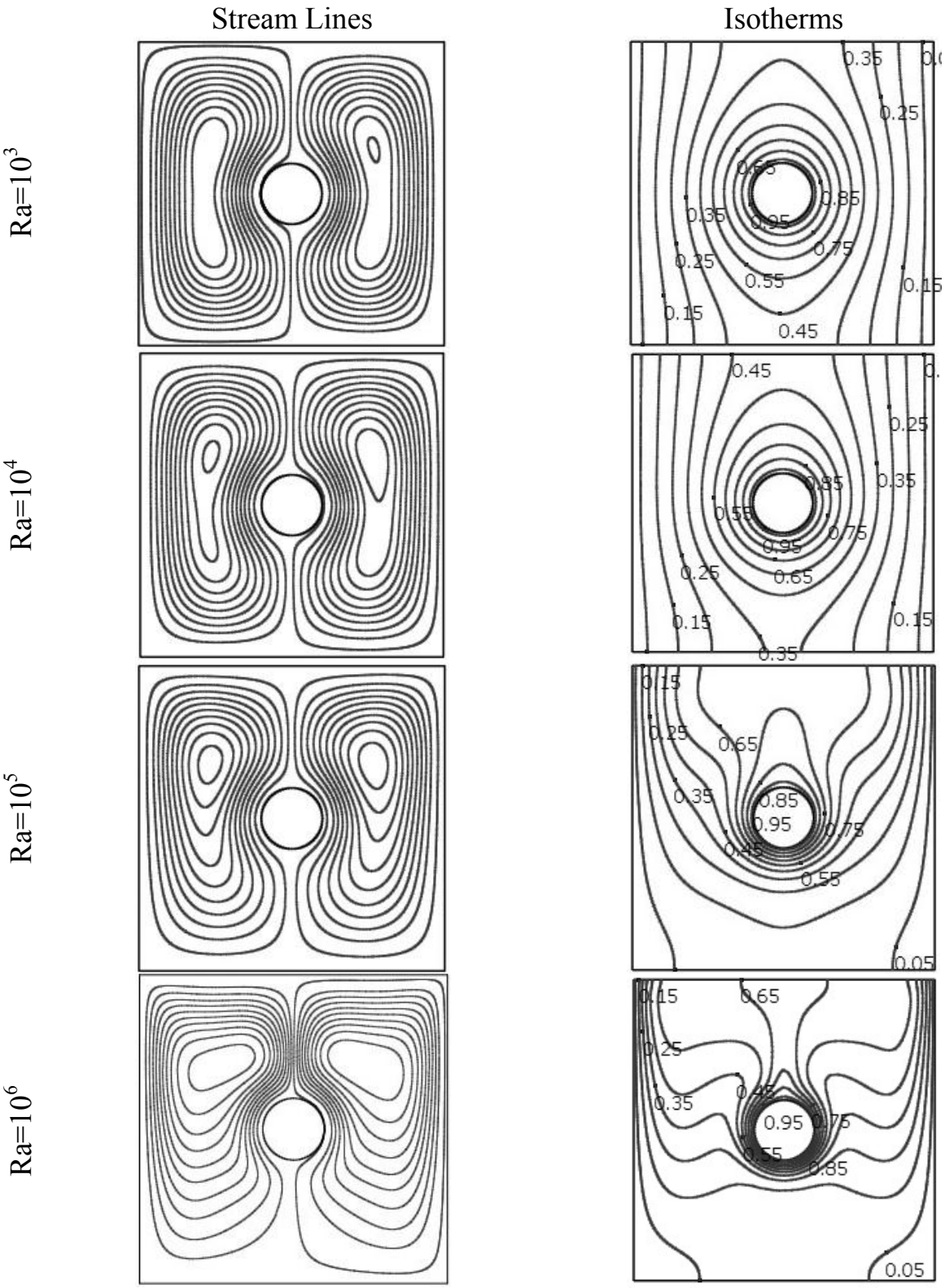

Fig 4.22: Streamlines and Isotherm patterns for Cu–water nanofluid for φ=0.15 at different Rayleigh numbers.

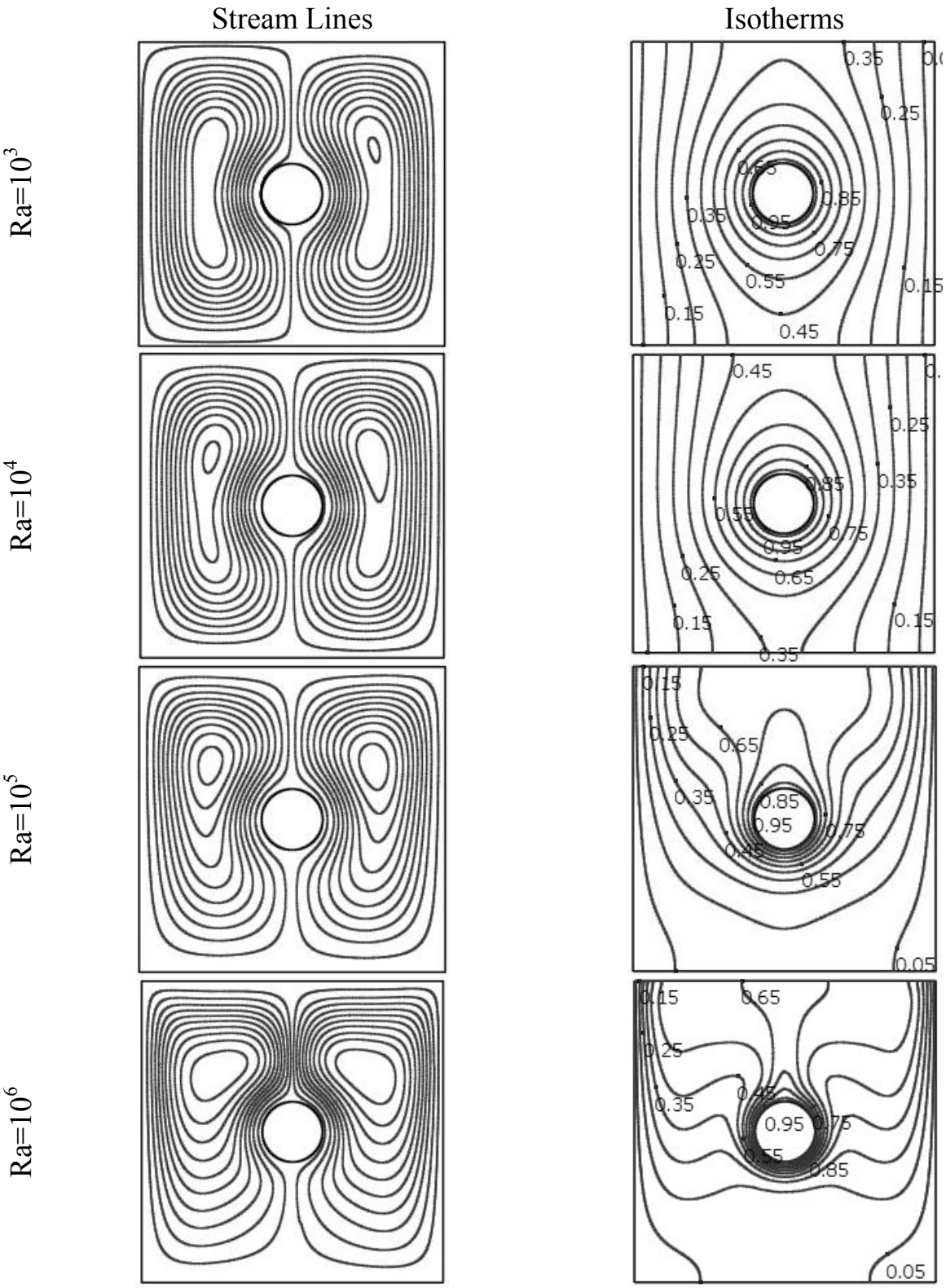

Fig 4.23: Streamlines and Isotherm patterns for Cu–water nanofluid for φ=0.2 at different Rayleigh numbers.

Fig.4.24(a) shows variation of the average Nusselt number $\mathrm{Nu_{avg}}$ of the hot walls of the square cavity with solid volume fraction φ of the nanofluid and the Rayleigh number Ra for the square cavity with the adiabatic circular disk. It is evident from the figure that the average Nusselt number increases with increase in the solid volume fraction of the nanofluid for all range of the Rayleigh number considered. Moreover it is found that at $Ra = 10^3 - 10^6$ the average Nusselt number does not change significantly. However, as the Rayleigh number increases, the effect of the convection dominates the heat transfer. Consequently, a high value of average Nusselt number is obtained. Moreover, the addition of nanoparticles to the pure water increases the thermal conductivity. As a result, the heat transfer effect of nanofluid is higher than that of pure water and the effect of nanoparticle addition in the base fluid on the heat transfer performance is better at low Rayleigh numbers than at high Rayleigh numbers.

Fig. 4.24(b) presents the variation of average Nusselt number Nu_{avg} the volume fraction φ using different values of Rayleigh number Ra for the square cavity with the cold circular disk. The figure shows that the heat transfer increases almost monotonically with increasing the volume fraction for all Rayleigh numbers.

Fig. 4.24(c) displays the effect of average Nusselt number Nu_{avg} due to the various Rayleigh numbers Ra as well as solid volume fraction φ for the square cavity with the cold circular disk. It is seen from figures that Nuavg enhances sharply upto $Ra = 10^4$ and beyond this region they rise gradually.

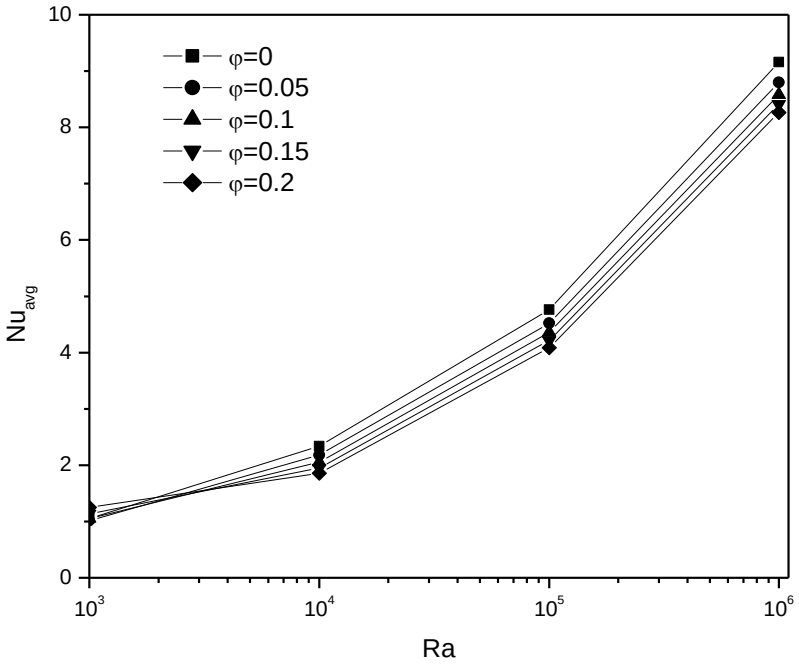

Fig.4.24 (a) Average Nusselt number for different volume fraction of adiabatic circular disk.

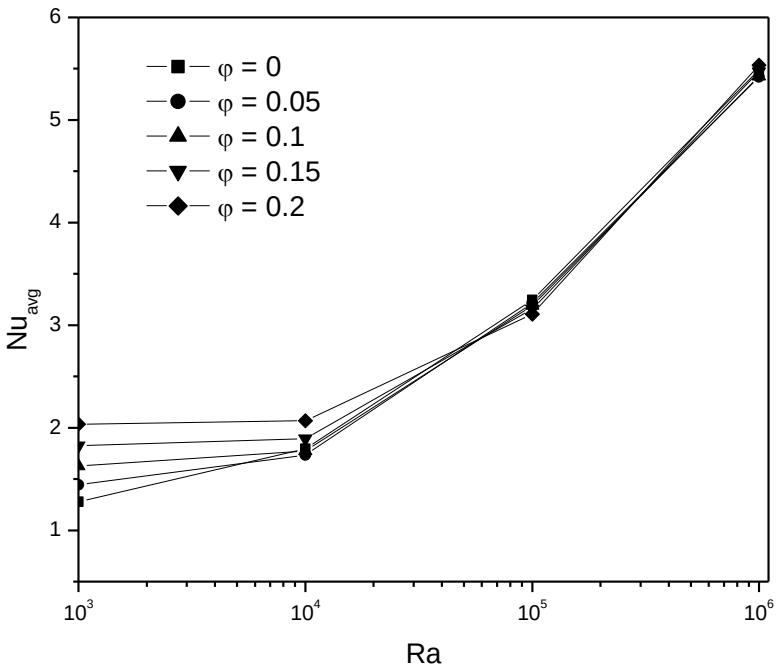

Fig 4.24 (b) Average Nusselt number for different volume fraction of cold circular disk.

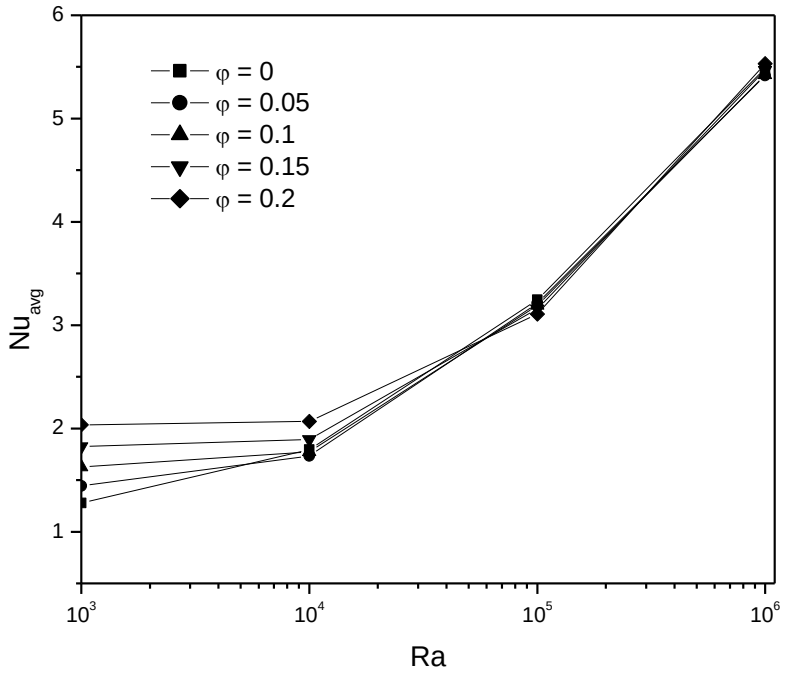

Fig.4.24(c): Average Nusselt number for different volume fraction of heated circular disk.

4.4 Natural convection of Cu-water nanofluid in square cavity with a circular disk under a magnetic field

A schematic view of a square cavity with circular disk considered in the present study is shown in Fig. 4.25. side walls are the heated surfaces (hot and cold walls). Top, bottom walls of the cavity and the circumference of circular disk are assumed to be adiabatic. Arm length of the cavity and radius of the circular disk are denoted by h and a, respectively. The problem is considered two-dimensional. A uniform magnetic field strength of B_0 is considered in the horizontal direction. The cavity is filled with Cu-water ($\mathrm{Pr} = 6.2$) and the thermophysical properties of Cu nanoparticles and water as base fluid are listed in Table 1. The nanofluid is considered to be Newtonian, and the nanofluid flow is assumed to be laminar and incompressible. It is assumed that nanoparticles and base fluid are in thermal equilibrium and there is no slip between them.

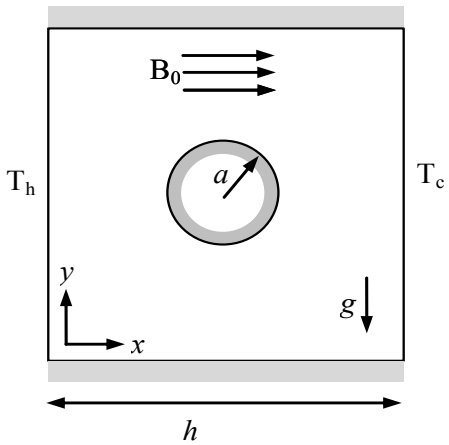

Fig.4.25. Schematic view of the square cavity with a circular disk

No-slip condition is imposed on all surfaces. Thermal boundary conditions are $\mathrm{T} = \mathrm{T_h}$ for the left hot wall, $\mathrm{T} = \mathrm{T_c}$ for the right cold wall and $\partial \mathrm{T}/\partial \mathrm{n} = 0$ for the top, bottom and disk adiabatic walls. Using the dimensionless parameters in Eq. (3.19) to (3.22) the following boundary conditions are obtained.

On the hot wall: $\mathrm{U} = \mathrm{V} = 0; \quad \theta = 1$

On the cold wall: $U = V = 0; \quad \theta = 0$

On the adiabatic walls $U = V = 0; \quad {\partial\theta}/{\partial n} = 0$

Analysis of heat transfer enhancement of Cu-water nanofluid is conducted in a square cavity with a circular disk at the centre of the cavity. The ratio of disk radius (a) to length of the cavity (h) is defined as $\lambda = a/h$ and its value is taken as 0.1. Other variables considered for the parametric study are Rayleigh number,$Ra = 10^3, 10^4, 10^5, 10^6$, Hartmann number, $Ha = 0,10, 30,50,100$, solid volume fraction of nanoparticles $\varphi = 0, 0.05, 0.1, 0.15, 0.2$.

In this chapter, natural convection heat transfer in square cavity with a circular disk in the presence of a magnetic field is investigated numerically using Finite Element Method. Calculations are made for various values of the Hartmann number, Ha = 0, 10, 30, 50,100, and Rayleigh number, Ra = 10^3, 10^4, 10^5,10^6. Fig. 4.25 shows the isotherms and streamlines for different values of Rayleigh number and Hartmann number. At Ra = 10^3, the isotherms are parallel to each other and take the shape of the enclosure which are the main characteristics of conduction heat transfer mechanism. At Ra = 10^4, the circulation of the flow shows that the main eddy is divided into two eddies around the circular disk. Also, as Rayleigh number increases, the isotherms become more distorted which is due to the domination of convective heat transfer mechanism at higher Rayleigh numbers. At this Rayleigh number, a thermal plume appears over the hot surface. At Ra = 10^5, circular disk appears between two clockwise eddies. It is worthwhile mentioning that the effect of magnetic field is to decrease the value of the velocity magnitude throughout the enclosure because the presence of magnetic field introduces a force called the Lorentz force, which acts against the flow if the magnetic field is applied in the normal direction. This type of resisting force slows down the fluid velocity. Increasing Hartmann number has no significant effect on isotherms and streamlines at low Rayleigh number. At Ra = 10^4, as Hartmann number increases, secondary eddies disappear and the core of vorticity moves upward. At Ra = 10^5,

increasing Hartmann number up to Ha = 10, two other counter clockwise eddies appear. But in higher values of Hartmann number, it can be seen that all secondary eddies become smaller. Also, it can be seen that in the presence of magnetic field, thermal plumes disappear. Effects of the Rayleigh number and Hartmann number on local Nusselt number are shown in Figure 4.25 to 4.26 At Ra = 10^3, the local Nusselt number profiles are symmetric, which indicates the domination of conduction heat transfer mechanism. For higher Rayleigh number, local Nusselt number profiles are not symmetric and have extremums because of the presence of thermal plumes. In the absence of magnetic field, for Ha=0, the local Nusselt number profile has three local minima but as Hartmann number increases, these extrema disappear because of domination of conduction mechanism. Figures 5.2 to 5.4 show the effects of the Rayleigh number and Hartmann number. As Rayleigh number increases, buoyancy force increases so that both thermal and velocity boundary layer thicknesses decrease. Increasing Rayleigh number leads to increase in averageNusselt number. When the magnetic field is imposed on the enclosure, the velocity field is suppressed owing to the retarding effect of the Lorentz force. As Hartmann number increases boundary layer thicknesses increase, and in turn the average Nusselt number decreases.

Fig.4.25 illustrates the streamlines and isotherms for $\varphi = 0.1$and $\mathrm{Ha} = 10$ for different Rayleigh numbers. For $\mathrm{Ra} = 10^3$ the heat transfer due to convection is very small and only one circulation around the circular disk at the centre is visible. However, as Rayleigh number increases flow tends to move towards the wall and at $\mathrm{Ra} = 10^5$ two distinct eddies at both sides of the adiabatic disk are observed. Isotherms of the Fig.4.25 shows that both sides of the disk attain temperature equilibrium as the Rayleigh number increases. For higher Rayleigh numbers heated nanofluid tends to move upward near the hot wall and goes downward very close to the cold wall. Fig.4.25 shows very significant patterns of streamlines and isotherms for different Rayleigh numbers.

Fig.4.29(a) shows the variation of average Nusselt number with Hartman number for a square cavity with a circular disk at $\mathrm{Ra} = 10^5$. It confirms that the heat transfer is reduced with increasing Hartman number for all volume fractions. Higher volume fraction shows a small higher average Nusselt number.

Fig.4.29(b) shows the change in average Nusselt number with Hartmann number at different values of the Rayleigh number at volume fraction $\varphi = 0.2$. Results show that, the general behavior of solid particles addition is to mitigate the velocity field within the enclosure. Results also show the increase in the Hartmann number also leads to higher suppression of flow field. The magnetic field does not have a considerable effect at low Rayleigh number. In this case the average Nusselt number remains unchanged when the Hartmann number changes. The heat transfer rate increases due to convection for Cu-water naofluid at higher Rayleigh numbers. It increases with an increase of the Rayleigh number but it decreases with an increase of the Hartmann number. Moreover the increment of the nanofluid volume fraction leads to enhancement or deterioration of the heat transfer performance depending on the value of Hartmann and Rayleigh numbers.

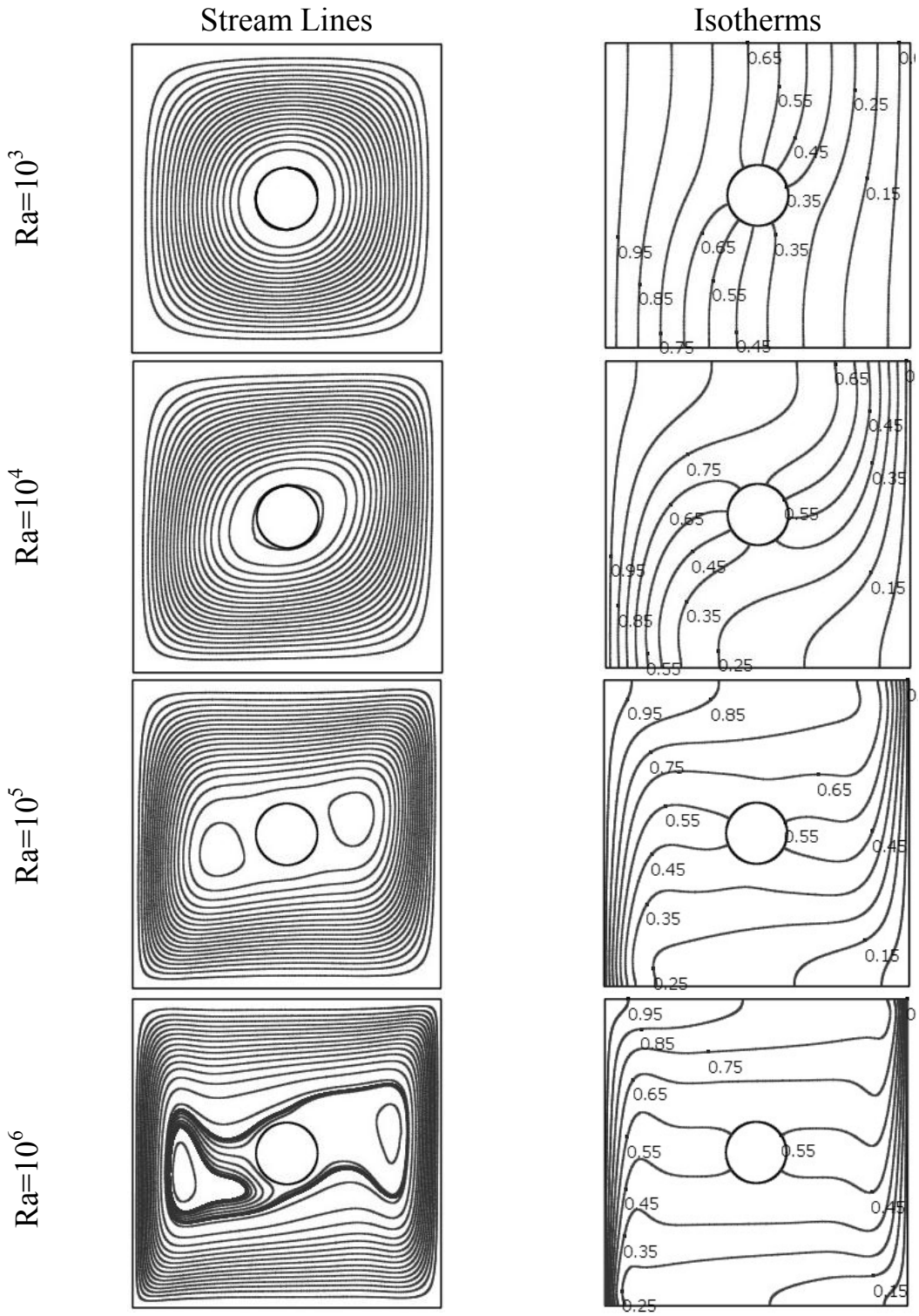

Fig.4.26: Streamlines and isotherms patterns for Cu-water nanofluid for $Ha = 10$ and $\varphi = 0.1$ for $Ra = 10^3, 10^4, 10^5, 10^6$.

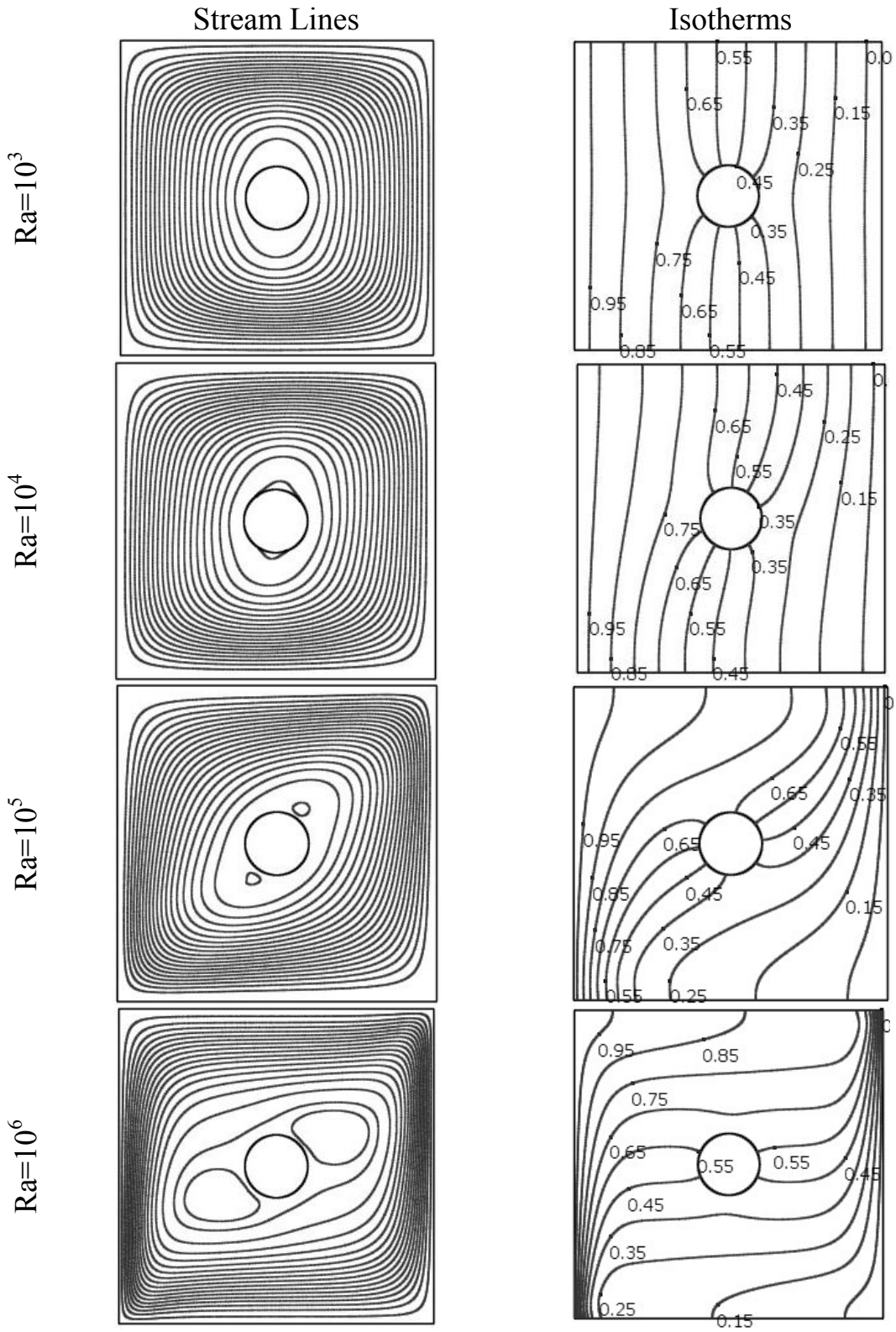

Fig.4.27: Streamlines and isotherms patterns for Cu-water nanofluid for $Ha = 50$ and $\varphi = 0.1$ for $Ra = 10^3, 10^4, 10^5, 10^6$.

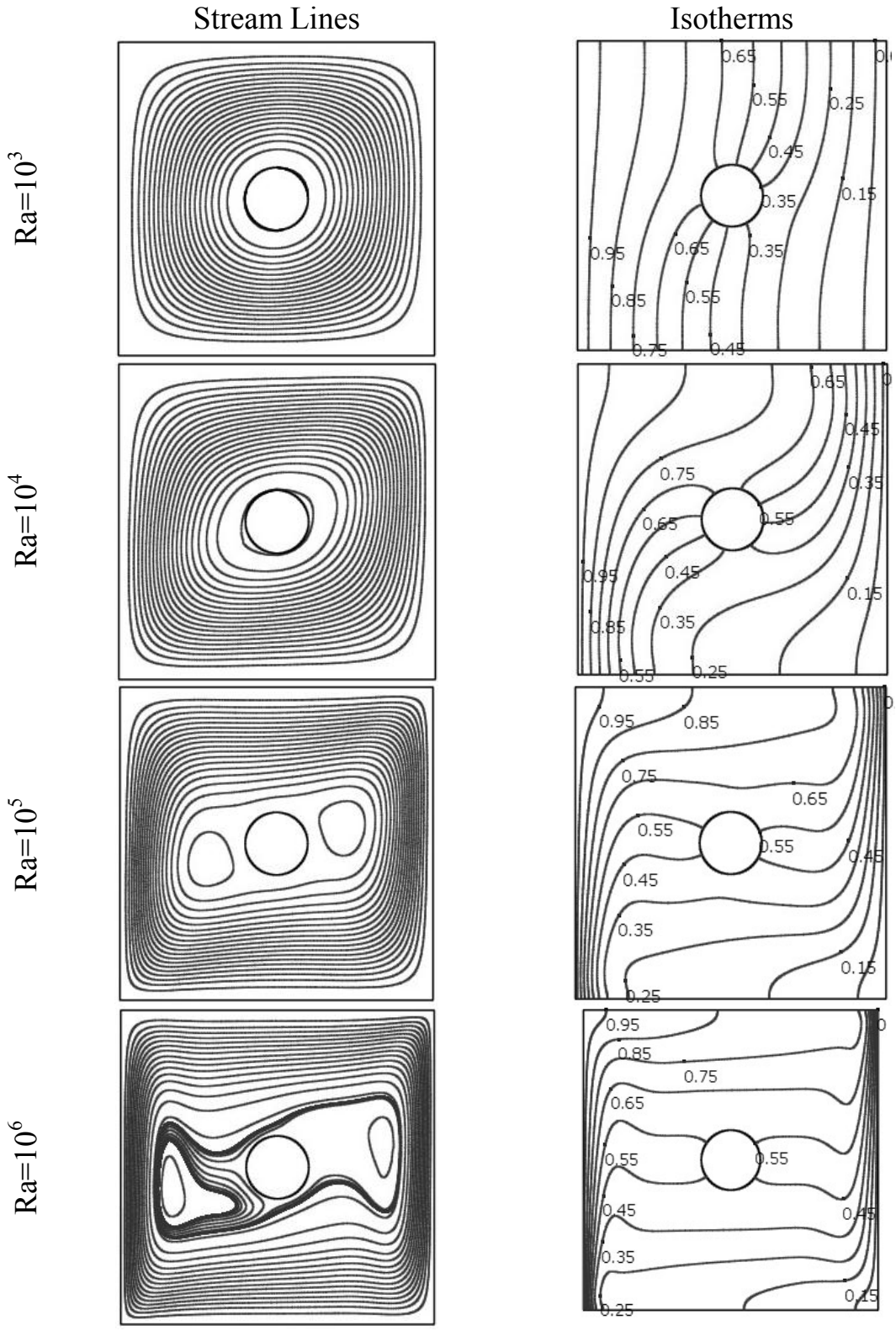

Fig.4.28: Streamlines and isotherms patterns for Cu-water nanofluid for $Ha = 100$ and $\varphi = 0.1$ for $Ra = 10^3, 10^4, 10^5, 10^6$.

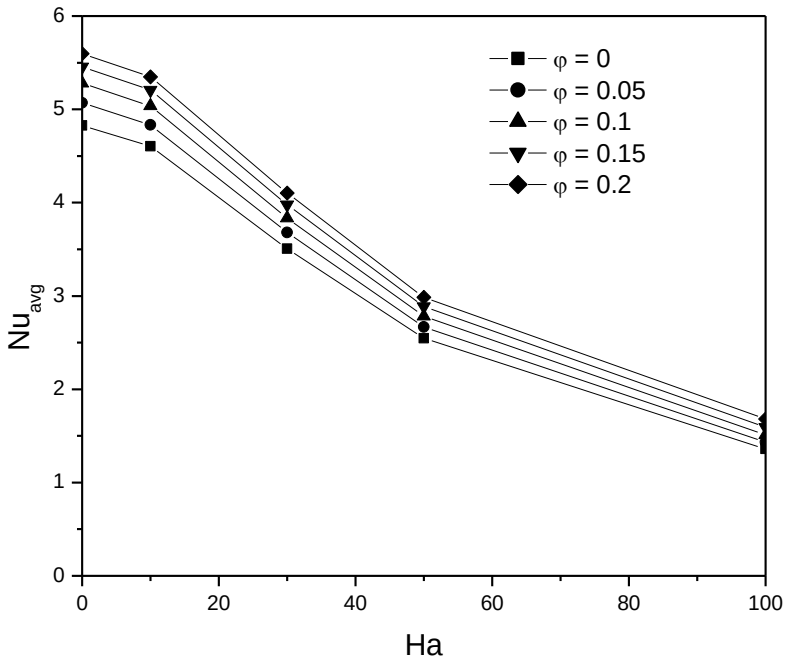

(a)

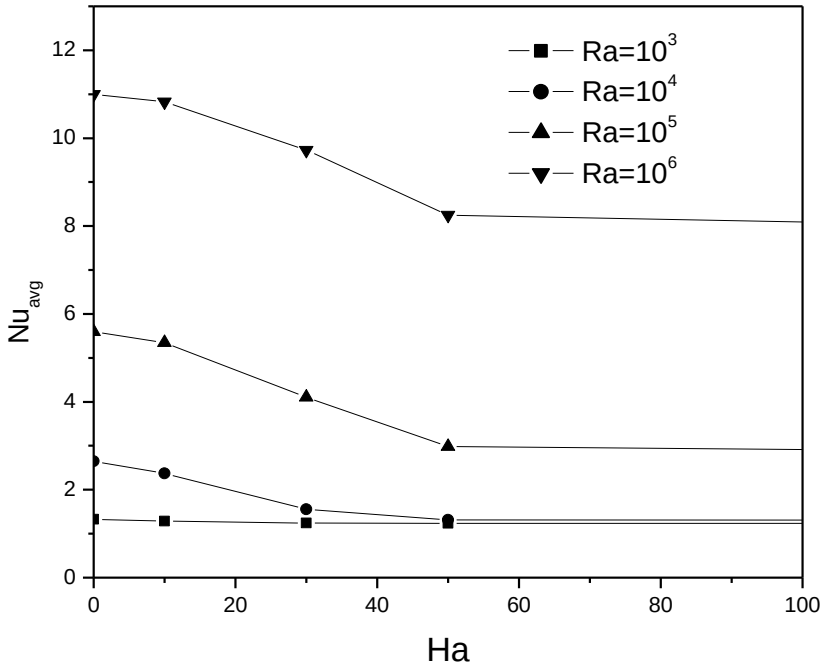

(b)

Fig.4.29. Variation of the average Nusselt numbers with Hartman numbers for (a) different volume fractions $\varphi = 0, 0.05, 0.1, 0.15, 0.2$ (b) different Rayleigh numbers $\mathrm{Ra} = 10^3, 10^4, 10^5, 10^6$ for $\varphi = 0.2$

CHAPTER 5

Natural Convection of Cu-water Nanofluid in Cubical Cavity

5.1Introduction

A schematic view of a cubical enclosure considered in the present study is shown in Fig.5.1. side of the cubical enclosure is denoted by Th and Tc. The problem is formulated in three-dimensional Cartesian coordinate system. The enclosure is filled with Cu-water nanofluid which is considered to be Newtonian, laminar and incompressible. Nanoparticle and base fluid are in thermal equilibrium and there is no slip between them.

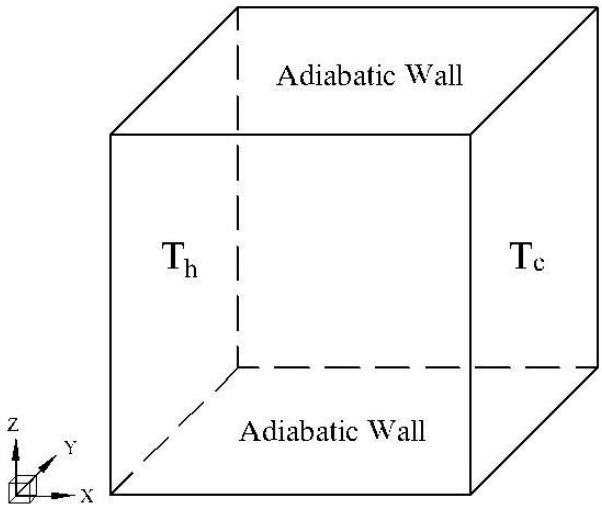

Fig.5.1: Schematic diagram of Cubical cavity

No-slip condition is imposed for all velocities on the wall. Thermal boundary conditions are $T = T_h$ for the hot walls, $T = T_c$ for the cold walls and $\frac{\partial T}{\partial n} = 0$ for the adiabatic walls, where n is normal direction to the surface. Using the dimensionless parameters the following boundary conditions are used for the equations (6.12) to (6.16):

on the hot walls : $U = V = W = 0; \theta = 1$

on the cold walls : $U = V = W = 0; \theta = 0$

on the adiabatic walls : $U = V = W = 0; \frac{\partial \theta}{\partial n} = 0$

The local Nusselt number of the heat source is expressed as

$$Nu_l = \frac{hH}{k_f}$$

\where the heat transfer coefficient is

$$h = \frac{q_w}{T_h - T_c}$$

Nusselt number can be written as

$$Nu = -\frac{k_{nf}}{k_f}\frac{\partial\theta}{\partial n}\bigg|_{X=0}$$

The average Nusselt number of the hot wall is obtained by integrating the local Nusselt number along the hot wall as follows

$$Nu_{avg} = \int_0^1\int_0^1 NudYdZ\bigg|_{X=0}$$

In this problem, the hydrodynamic and thermal characteristics of Cu–water nanofluid, filling a differentially heated cubic enclosure are numerically investigated. The global field characteristics are examined by viewing comprehensive three-dimensional contours of the temperature and flow fields. Results of Cu-water nanofluid in cubical enclosure for four Rayleigh numbers Ra = 10^3,10^4, 10^5 and 10^6 are inspected in detail for the various solid volume fractions of nanoparticle. At each Rayleigh number, the converged solution for a lower Rayleigh number is used as the initial guess. In actual computations, transient calculations are conducted by an implicit method to generate steady-state solutions. The former cast exemplifies a flow field in which the relative importance of convection is generally less significant. However, the later has been validated after comparison between the obtained results and experimental and numerical ones already found in the literature. To make clear the effect of main parameters such as the Rayleigh number, the nanoparticle volume fraction, and average Nusselt number, the convection phenomenon is reported by means of streamlines, temperature iso-surfaces and temperature profiles.

A special attention is paid to the Nusselt number evolution. Compared to a 2-D investigation, and when the convection mode dominates, taking into account the third direction leads to significant modifications on the nanofluid motion and heat transfer as well as the conductive regime dominates, the use of a 2-D configuration is found to be valid to predict the studied phenomenon.

In fig.5.2, it is illustrated that comparisons of three dimensional isotherms plots in the symmetry plane (Z = 0.5) with the two dimensional isotherms. These will test the validity of two dimensional assumptions, which has been routinely invoked for numerical studies. In general the change are very small at Ra= 10^6.

Fig. 5.2 represents the profiles of the average Nusselt numbers along the z-direction at each Rayleigh number studied. For the Rayleigh numbers smaller than 10^5 the average Nusselt number increases as the symmetry plane is approached. The overall three dimensional Nusselt numbers are found to be appreciably smaller than for the two dimensional results. At Ra = 10^6 the difference is considerably small compared with the cases of lower Rayleigh numbers. This can be explained by noting that overall Nusselt number is almost uniform along z-direction.

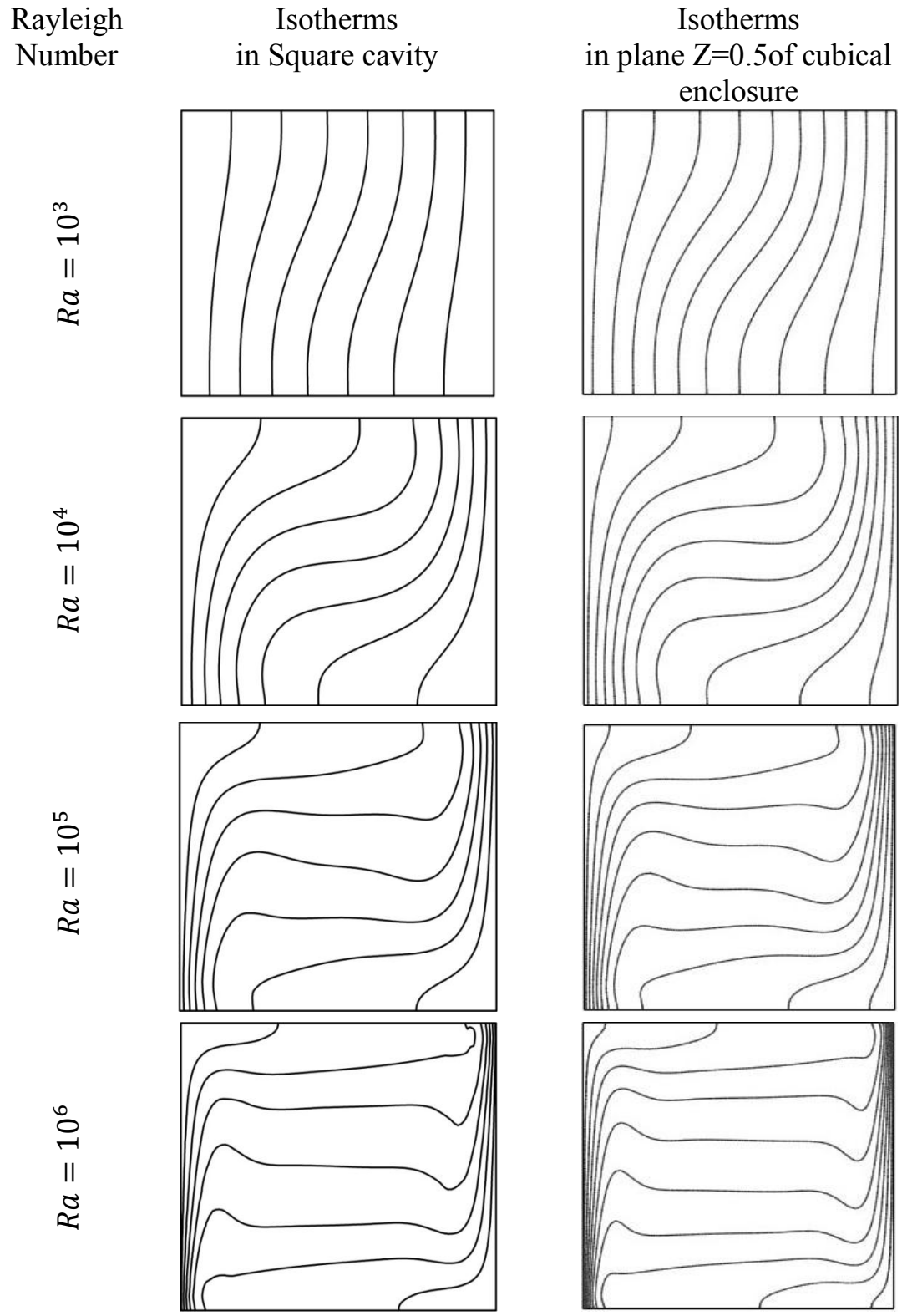

Fig.5.2. Contour plot of Cu-water Nanofluid of φ = 0.1 in 3D enclosure at Z=0.5 and square cavity for different Rayleigh Numbers.

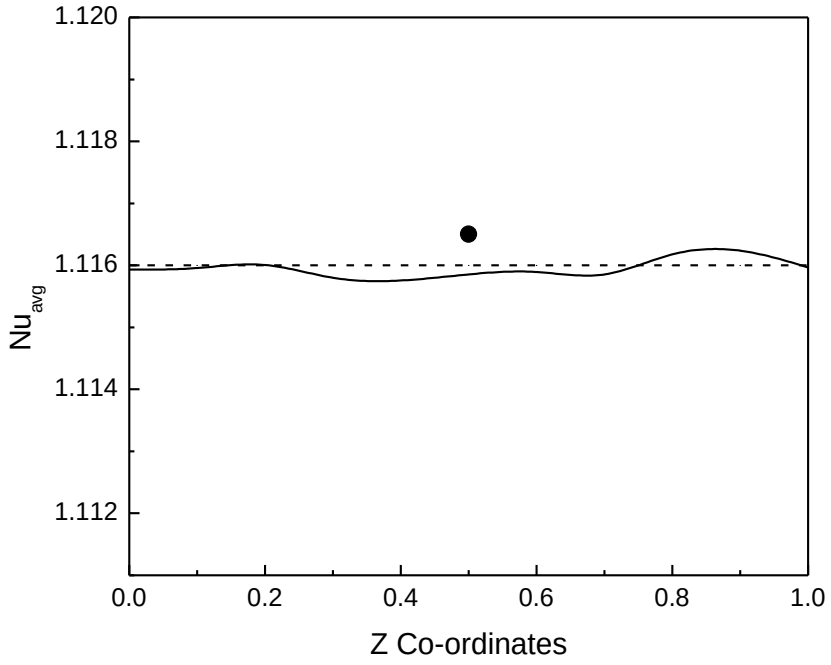
1.120
1.118
1.116
1.114
1.112
Nu_avg
0.0
0.2
0.4
0.6
0.8
1.0
Z Co-ordinates

Ra=10^3

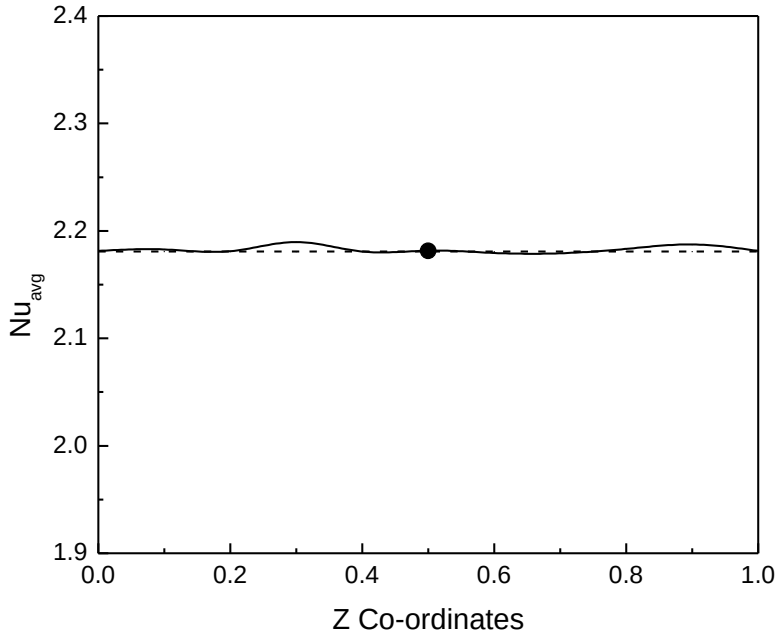
2.4
2.3
2.2
2.1
2.0
1.9
Nu_avg
0.0
0.2
0.4
0.6
0.8
1.0
Z Co-ordinates

Ra=10^4

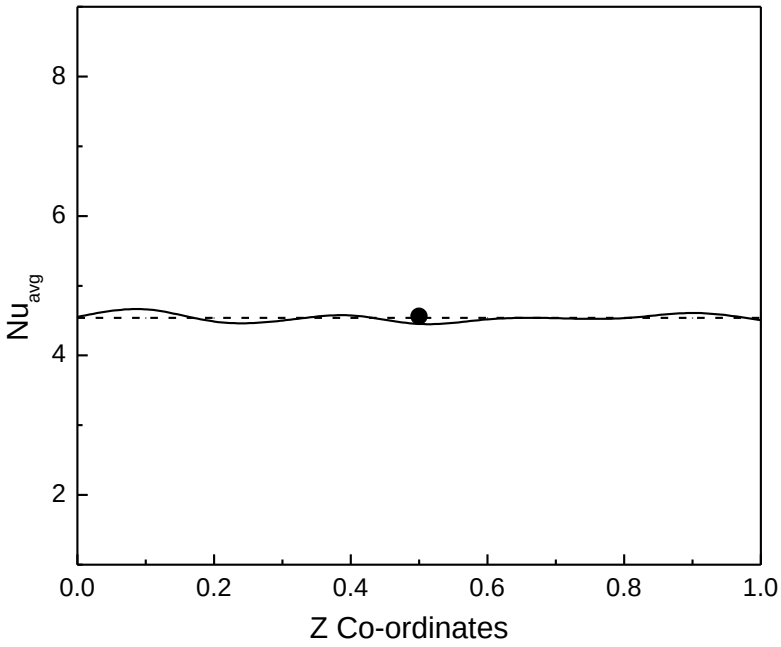

Ra=10^5

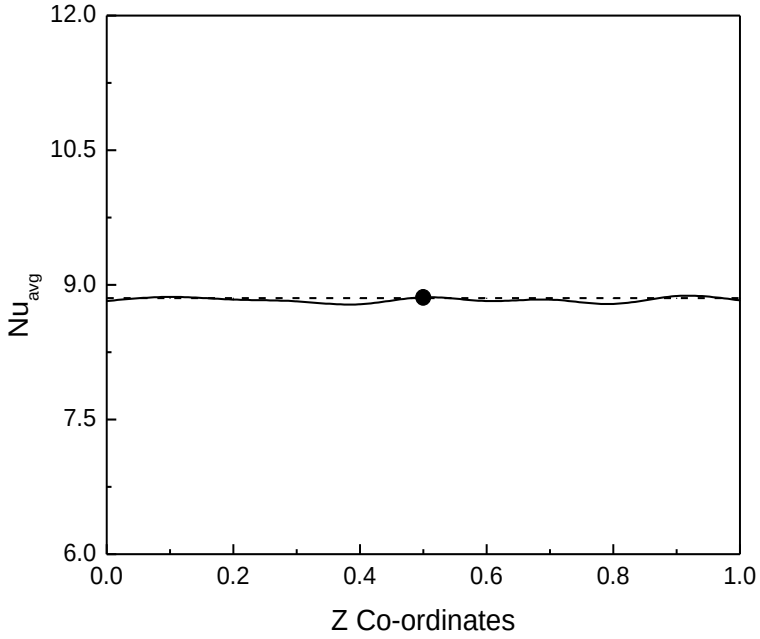

Ra=10^6

Fig. 5.3: Distribution of average Nusselt number in the z- direction (---)Nu_{avg} (z) and (——) $Nu_{overall}$ (three dimensional); ●,Nu_{avg} (z) (two dimensional);(a) Ra=10^3; (b) Ra=10^4;(c) Ra=10^5; (d) Ra=10^6;

Rayleigh Number | Slice Plot

$Ra=10^3$

$Ra=10^4$

$Ra=10^5$

$Ra=10^6$

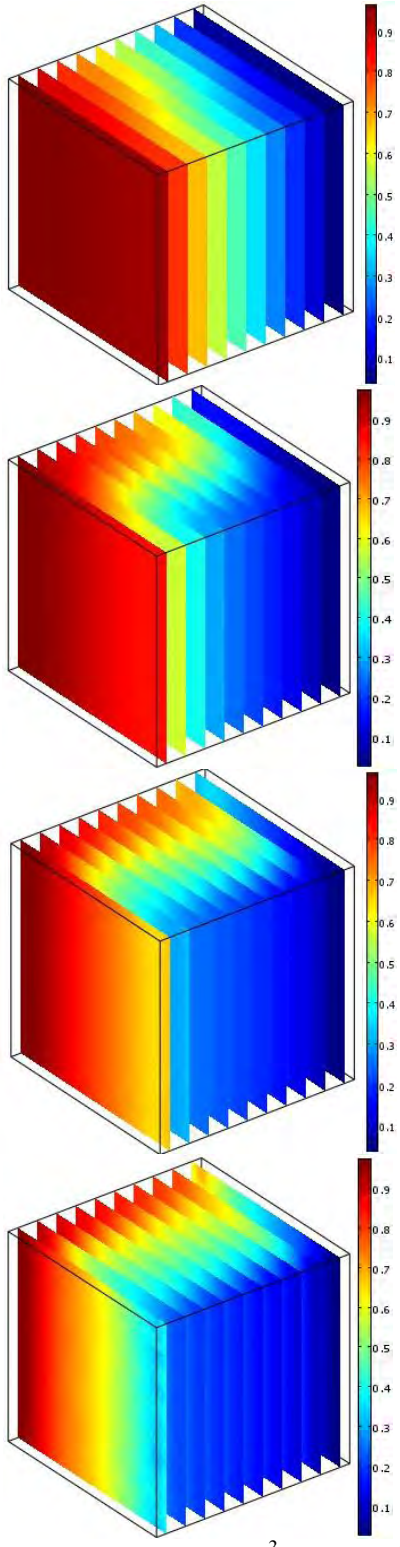

Fig.5.4.: Slice Plot of Cu-water nanofluid for Ra = 10^3 - Ra= 10^6 at φ=0.02

Rayleigh Number | Iso surface Plot

$Ra=10^3$

$Ra=10^4$

$Ra=10^5$

$Ra=10^6$

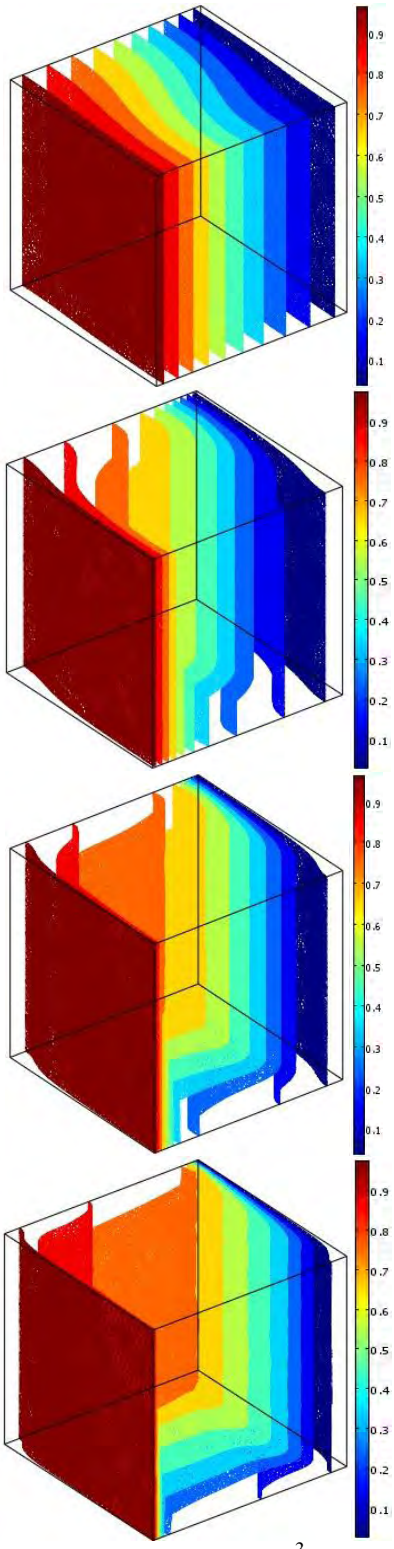

Fig.5.5.: Iso surface Plot of Cu-water nanofluid for Ra = 10^3 - Ra= 10^6 at φ=0.02

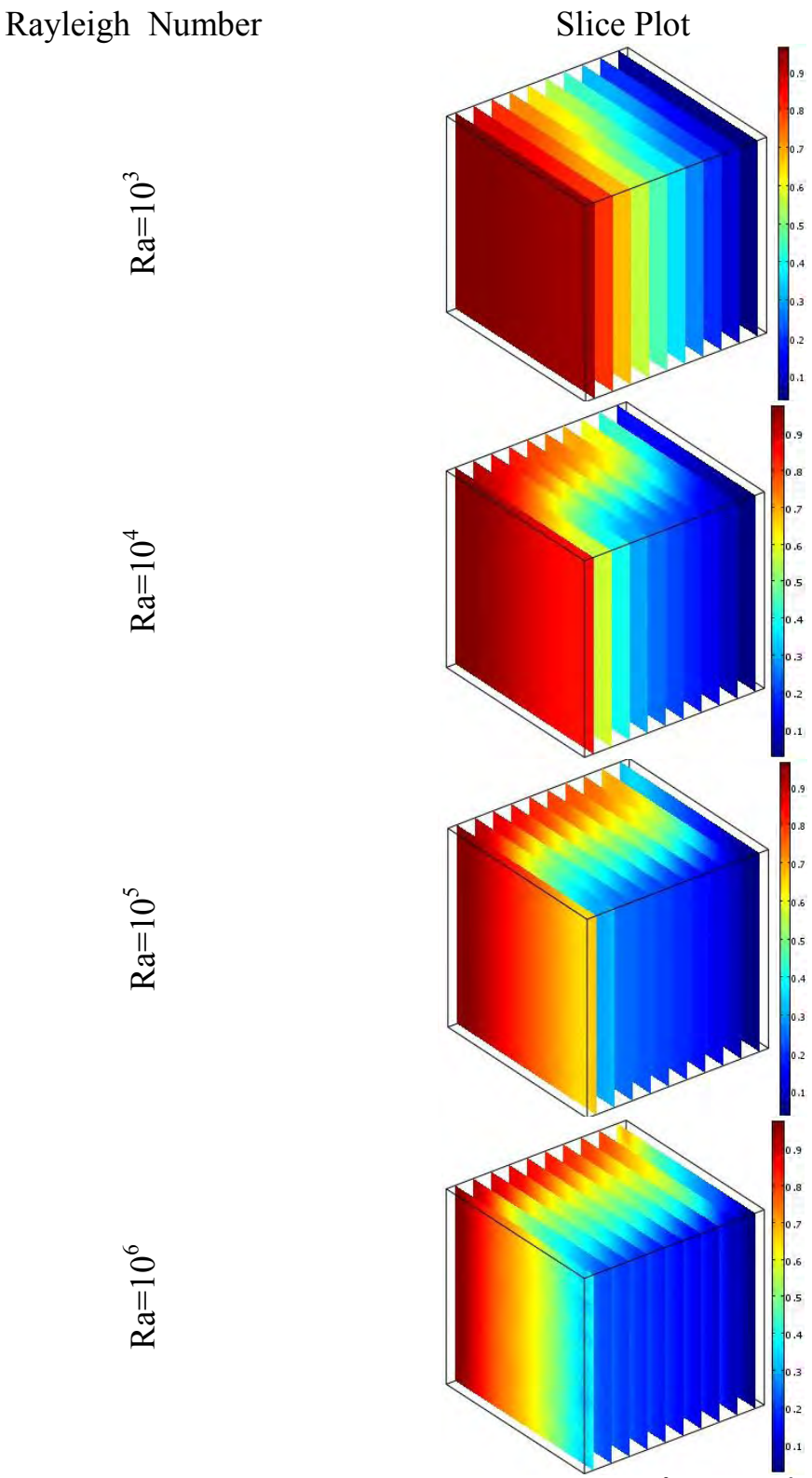

Fig.5.6.: Slice Plot of Cu-water nanofluid for Ra = 10^3 - Ra= 10^6 for φ=0.05

Rayleigh Number | Iso surface Plot

$Ra=10^3$

$Ra=10^4$

$Ra=10^5$

$Ra=10^6$

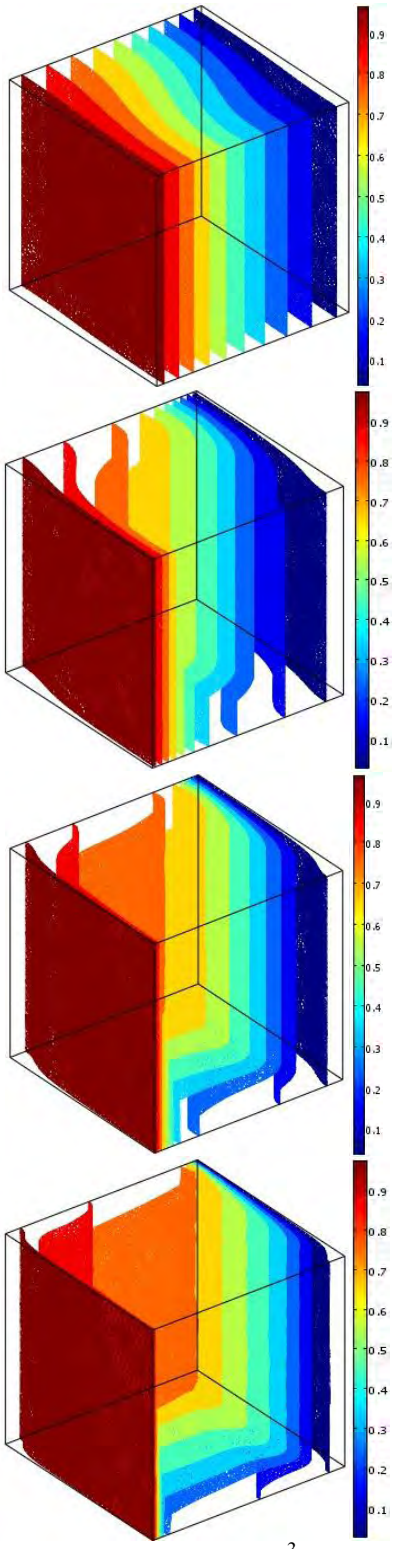

Fig.5.7: Iso surface Plot of Cu-water nanofluid for Ra = 10^3 - Ra= 10^6 at φ=0.05

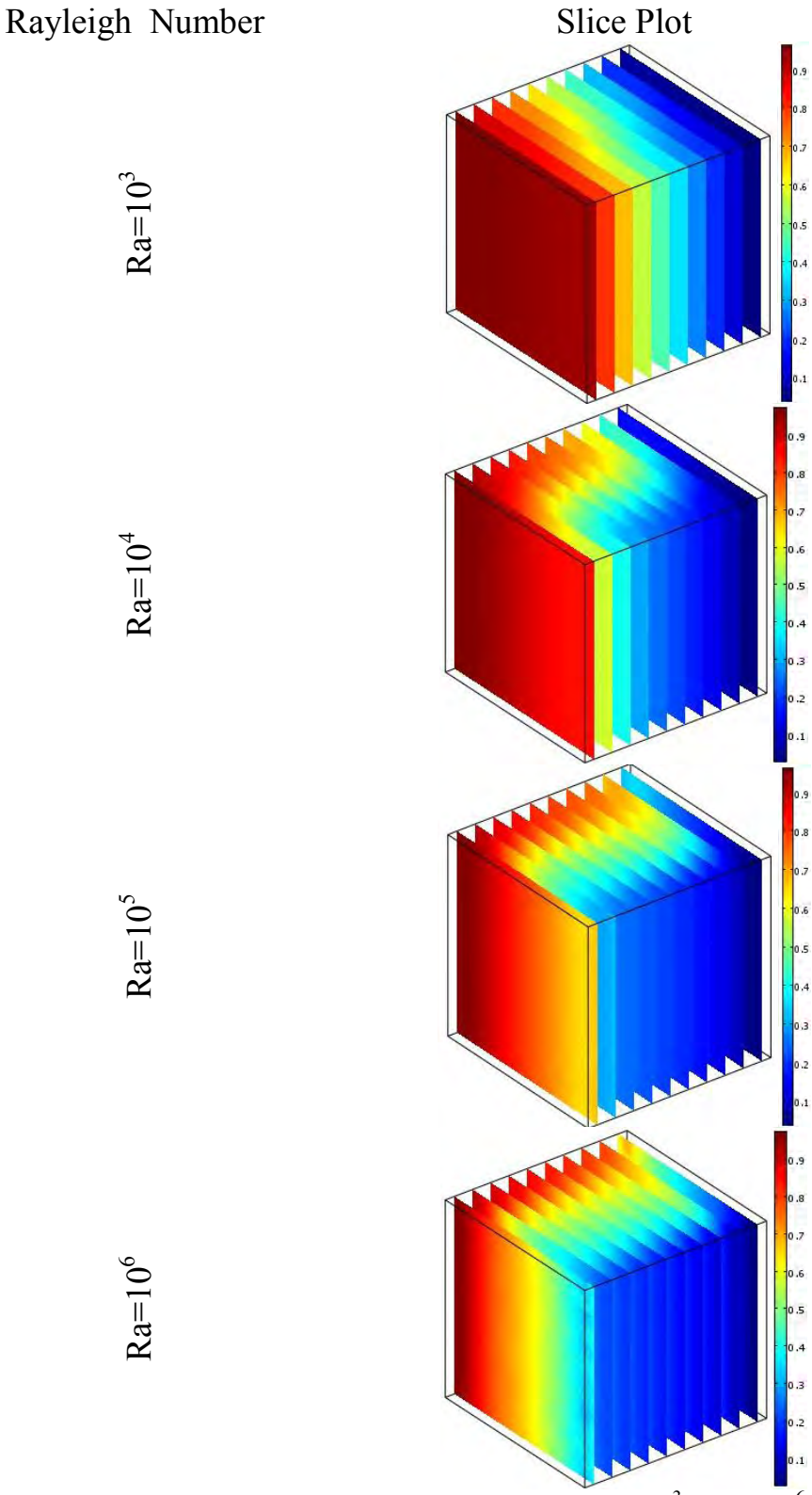

Fig.5.8: Slice Plot of Cu-water nanofluid for Ra = 10^3 - Ra= 10^6 for φ=0.1

Rayleigh Number | Iso surface Plot

$Ra=10^3$

$Ra=10^4$

$Ra=10^5$

$Ra=10^6$

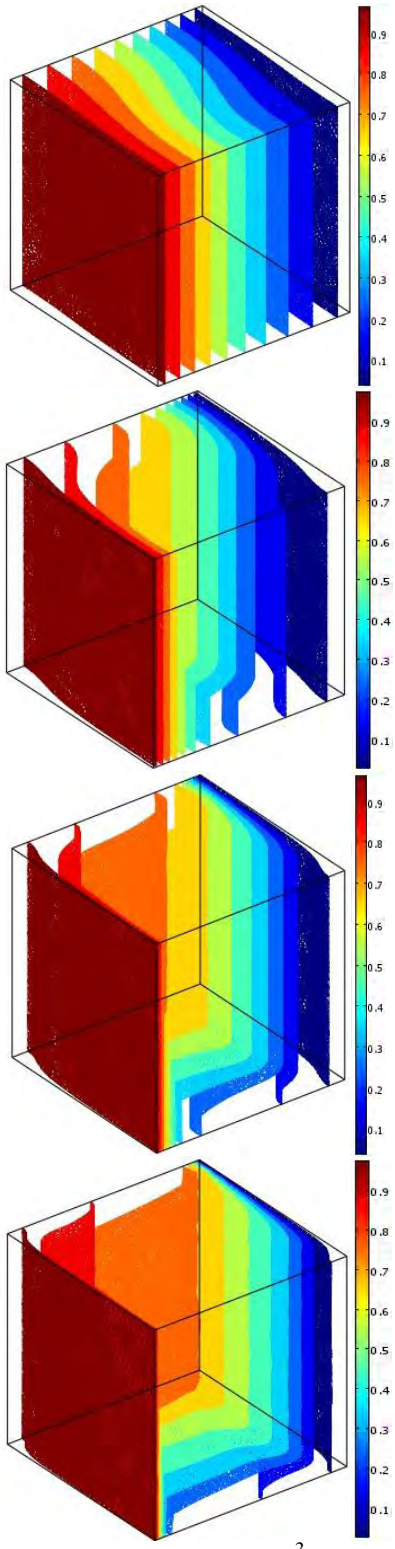

Fig.5.9: Iso surface Plot of Cu-water nanofluid for Ra = 10^3 - Ra= 10^6 at φ=0.1

In the present report a numerical investigation concerning the effects of average Nusselt number Nu_{avg} with solid volume fraction φ of nanoparticle using different values of Rayleigh number Ra on velocity and temperature field around an adiabatic, cold and heated circular disk placed in the square cavity is accounted. The focal point of the present investigation is to calculate the average heat transfer rate in the square cavity with different conditions of the circular disk filled by Cu-water nanofluid with Rayleigh number $Ra = 10^4$ while Pr is fixed at 6.2. The subsequent findings can be seen from the current numerical analysis:

- Ra and φ significantly affect the configuration of the streamlines and isotherms within the square cavity containing adiabatic, cold and heated circular disk.
- It is clear from the figures that the presence of the nanoparticle plays a significant role to increase the heat transfer.
- The results indicate that the Nusselt number increases as the volume fraction increases.
- The presence of the nanoparticle in the fluid changes the characteristics of the base fluid.

CHAPTER 6

Natural convection of Cu-water nanofluid in cubical enclosure with circular cylinder

6.1 Introduction

An adiabatic cylinder is inserted into a cubical enclosure with four adiabatic walls. Front wall is heated and back wall is cold. All walls have no-slip boundary condition applied for velocity. The heat is transferred from the heated wall to the fluid around the cylinder causing density changes that result in buoyancy forces. As natural convection develops fluid rises around the cylinder and transports heat towards the cold walls. The heat flux depends on nanofluids in this work, the shape of the cylinder and the orientation of the enclosure with respect to gravity. The centre of the cylinder is located at the centre of the enclosure. The shape of the base of the cylinder is a circle. The temperature of the heated wall is constant Th and the temperature of the cold walls is also constant Tc shown in the following figure.6.1.

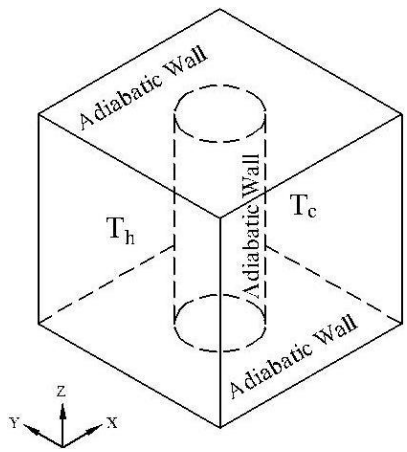

Figure.6.1: Schematic diagram of Cubical cavity with adiabatic cylinder

6.2 Results and discussion

6.2.1 Cubical enclosure with adiabatic circular cylinder

The results show highest heat transfer enhancement in the conduction dominated flow regime, where the enhanced thermal properties of nanofluid play an important

role. When convection is the dominant heat transfer mechanism, use of nanofluid yields a smaller increase in heat transfer efficiency.

Since the cylinder is adiabatic, the heat is transferred from heated wall to cylinder into the fluid. Hot fluid around the cylinder exhibits buoyancy forces against gravity. As it reaches the top wall, it turns towards the side walls creating two vortices one on each side of the enclosure. Slice Plot and Isosurfaces for the case of $\varphi = 0$ of Cu-water nanofluid are shown in Fig. 6.2. and Fig.6.3.

At Ra = 10^4 the temperature field is symmetrical. As the temperature difference between the cylinder and the walls is small in this case, the flow field exhibits top to bottom symmetry as well as left and right symmetry. As the temperature difference is increased we observe a break-up of top–bottom symmetry. Hot fluid close to the cylinder rises upwards and flows downwards along the vertical wall.

A break in symmetry is observed in the 3-D structure of the flow field as Rayleigh number is increased. At low Rayleigh number the flow is symmetrical above and around the cylinder. This symmetry is lost when the Rayleigh number is increased. At Ra =10^5 stronger motion in the direction along the cylinder is observed above the cylinder. As a smaller portion of heat is transferred from the top of the cylinder this 3-D nature of the flow has a small impact on the overall heat transfer.

From Fig.6.2. to Fig.6.7. represent slice plot and isosurfaces for different Rayleigh numbers Ra=10^3,10^4,10^5,10^6 for various solid volume fractions of nanoparticles φ = 0, 0.02, 0.05, 0.08, 0.1.

Fig.6.8. shows that average Nusselt number increases with increases of solid volume fractions of nanoparticles φ .

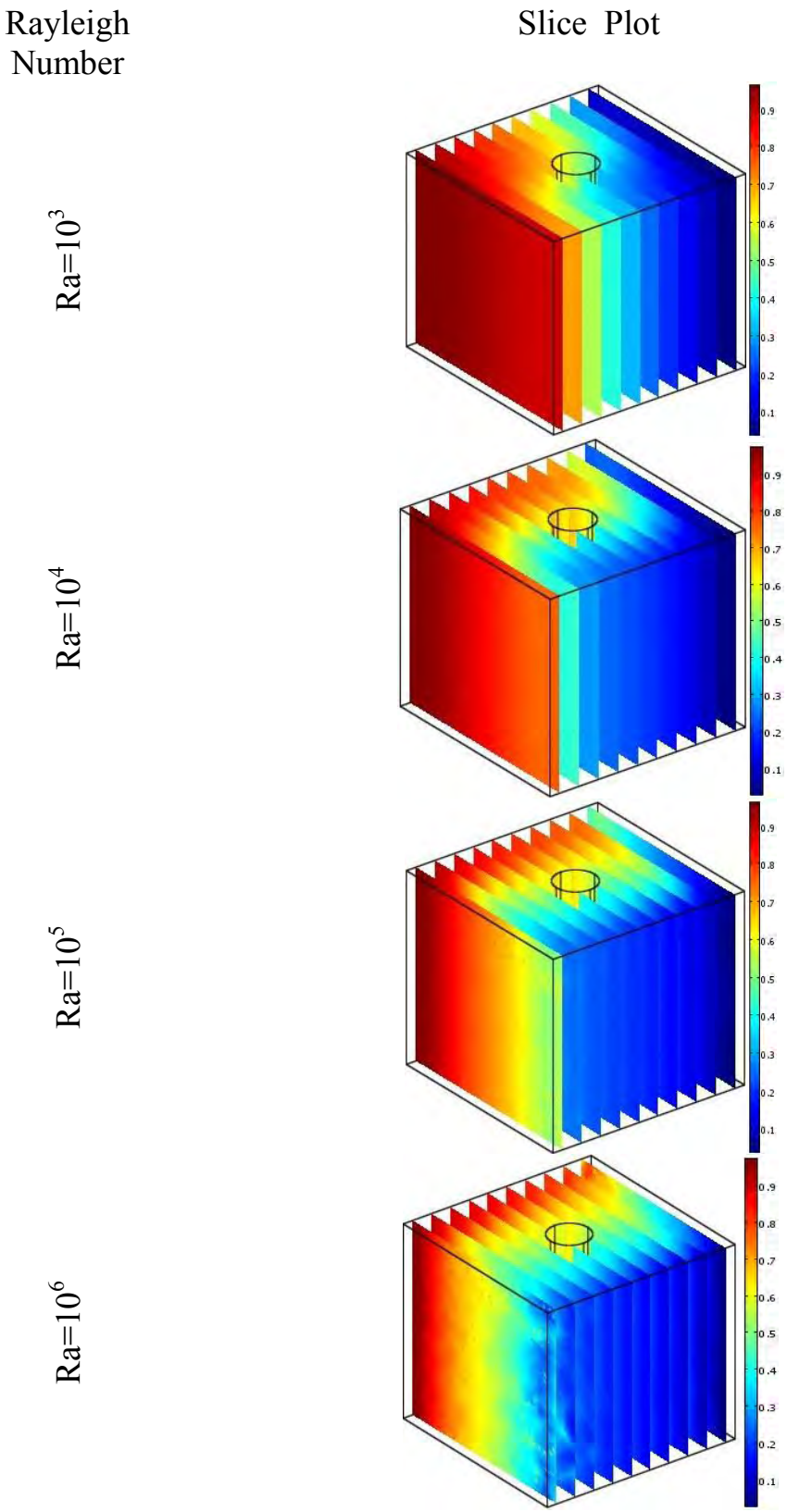

Fig. 6.2: Slice Plot of pure water for Ra = 10^3 - Ra= 10^6 at φ=0

Rayleigh Number

Iso surface Plot

$Ra=10^3$

$Ra=10^4$

$Ra=10^5$

$Ra=10^6$

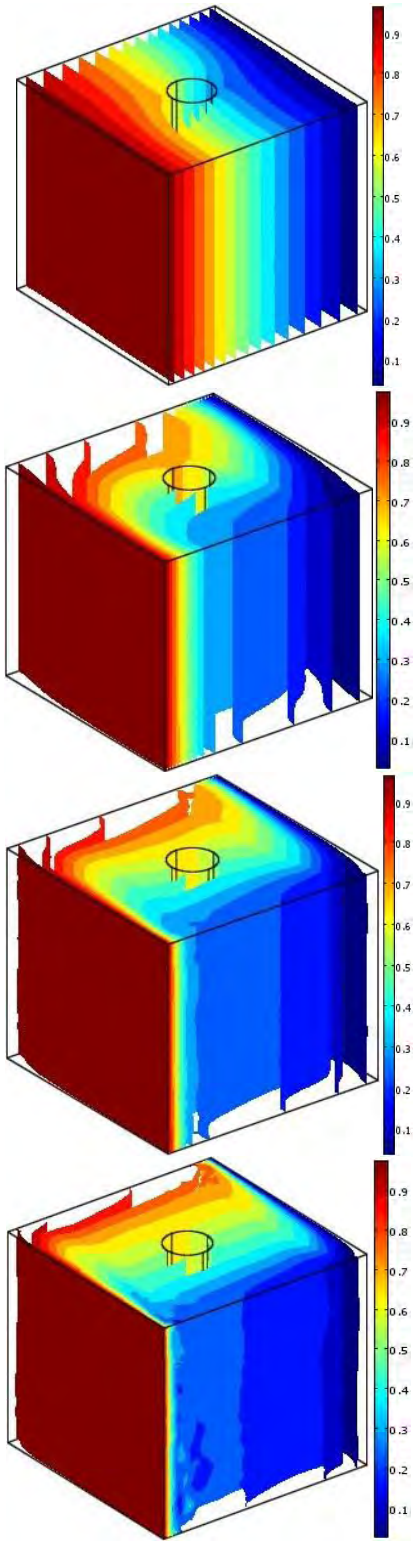

Fig.6.3: Iso surface Plot of pure water for Ra = 10^3 - Ra= 10^6 at φ=0

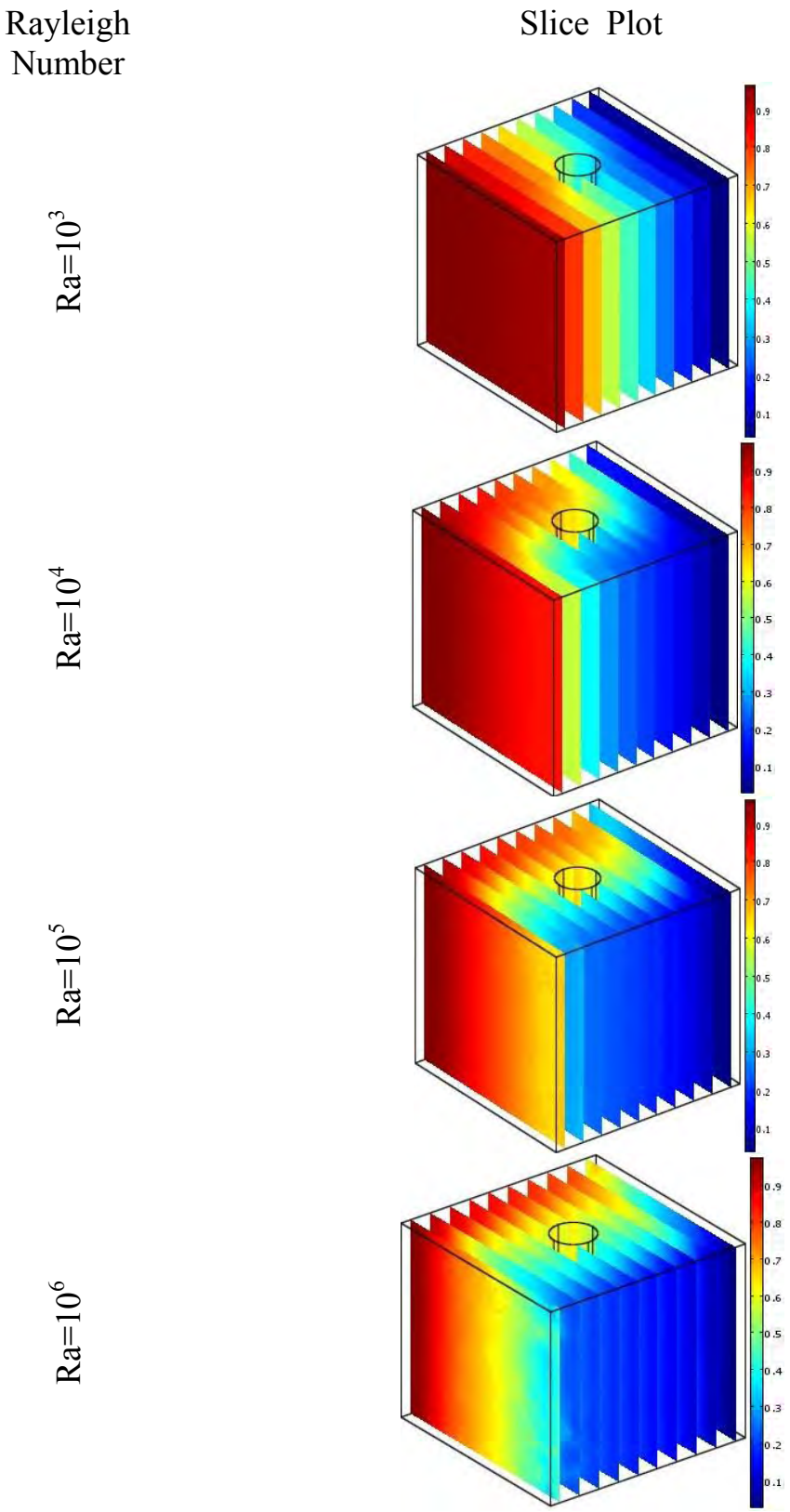

Fig.6.4: Slice Plot of Cu-water nanofluid for Ra = 10^3 - Ra= 10^6 at φ=0.05

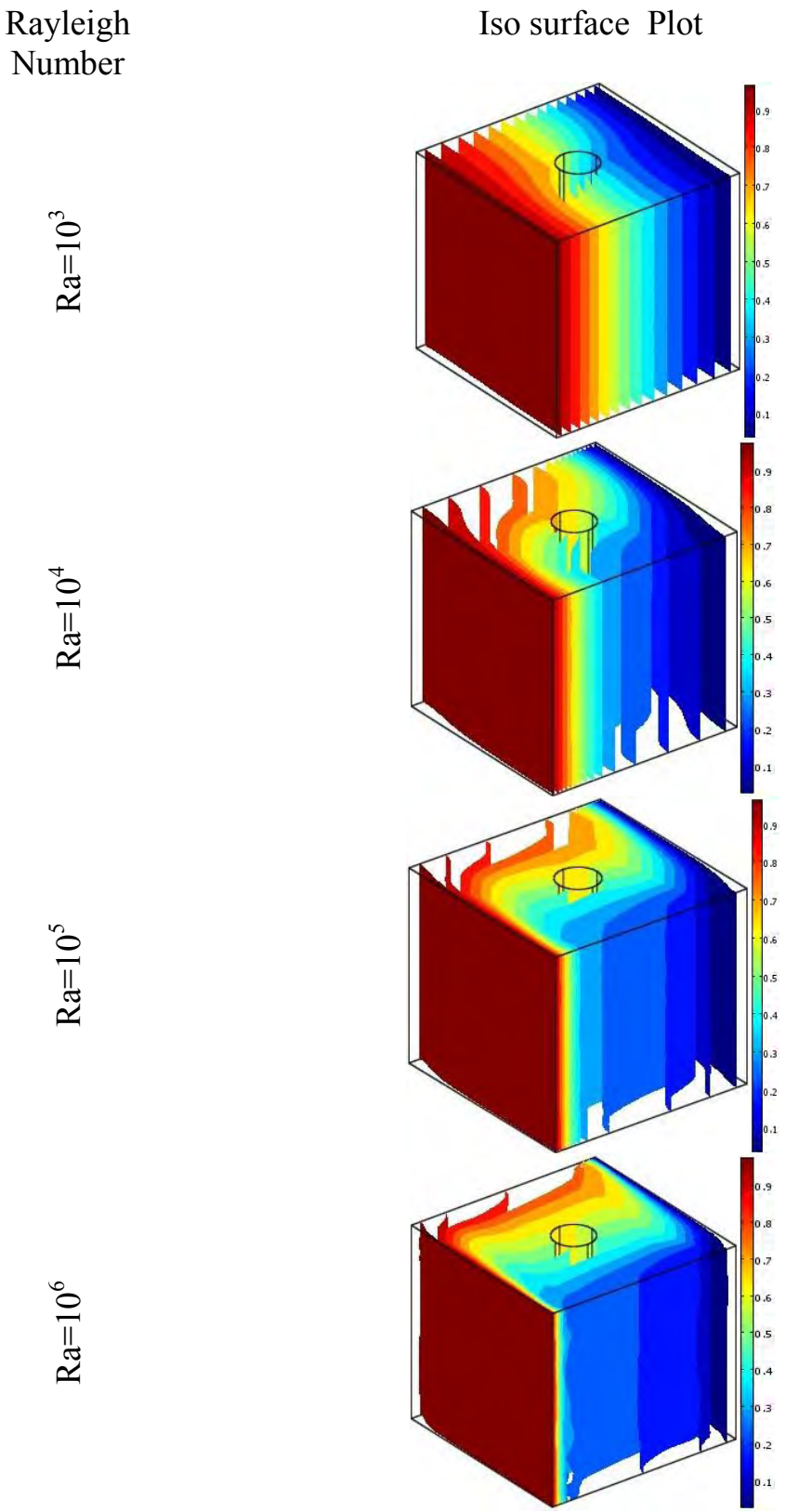

Fig. 6.5: Iso surface Plot of Cu-water nanofluid for Ra = 10^3 - Ra= 10^6 at φ=0.05

Rayleigh Number

Slice Plot

$Ra=10^3$

$Ra=10^4$

$Ra=10^5$

$Ra=10^6$

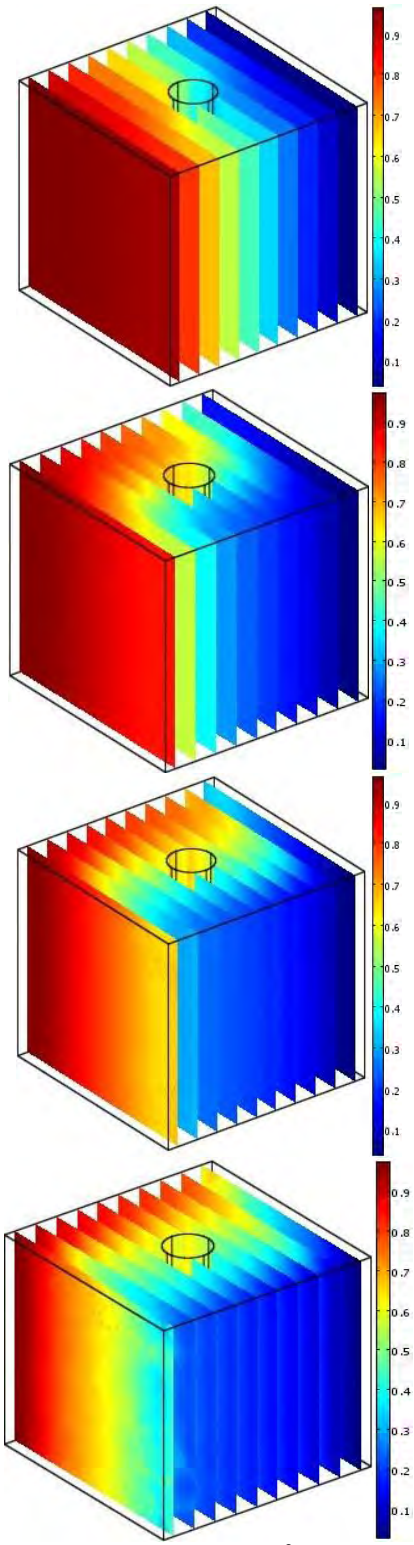

Fig. 6.6: Slice Plot of Cu-water nanofluid for Ra = 10^3 - Ra= 10^6 at φ=0.1

Rayleigh Number

Iso surface Plot

$Ra=10^3$

$Ra=10^4$

$Ra=10^5$

$Ra=10^6$

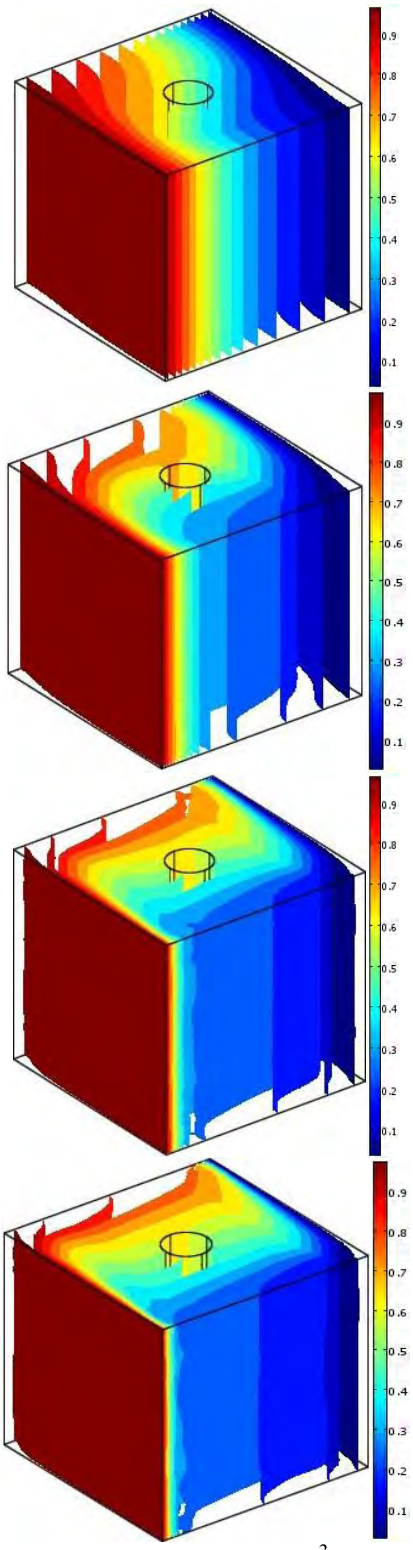

Fig. 6.7: Iso surface Plot of Cu-water nanofluid for Ra = 10^3 - Ra= 10^6 at φ=0.1

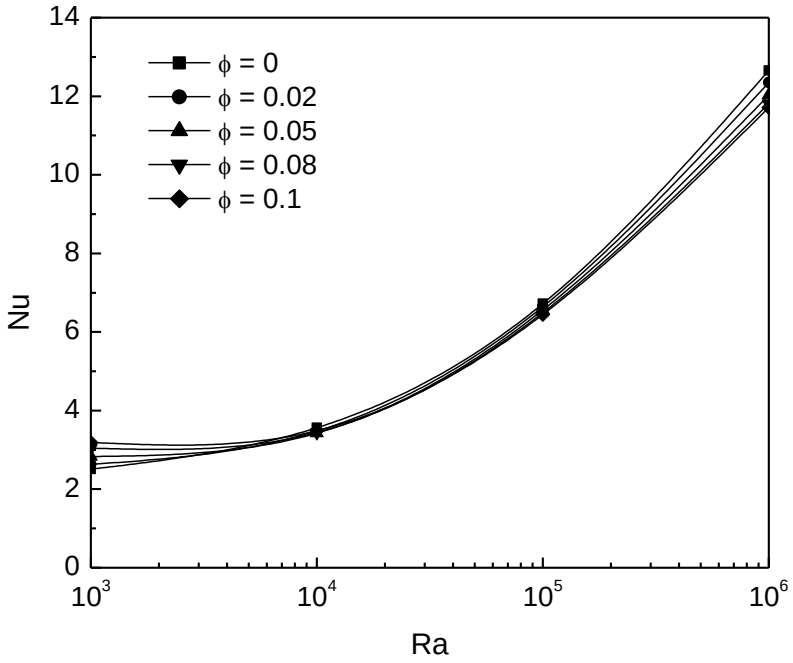

Fig.6.8. Variation of average Nusselt number for different volume fractions φ = 0, 0.02, 0.05, 0.08, 0.1 with different Rayleigh numbers Ra = 10^3, 10^4, 10^5, 10^6.

6.2 .2 Cubical enclosure with heated circular cylinder

Since the cylinder is heated so the heat is transferred from the cylinder into the fluid. Hot fluid around the cylinder exhibits buoyancy forces and starts to rise against gravity. As it reaches the top wall, it turns towards the side walls creating two vortices one on each side of the enclosure. Streamlines at xy plane for the case of φ=0.1 Cu-water nanofluids are shown in Fig. 6.15. At Ra =10^4 the flow field is symmetrical and features four vortices in the top left, top right, bottom left and bottom right corners. As the temperature difference between the cylinder and the walls is small in this case, the flow field exhibits top to bottom symmetry as well as left–right symmetry. As the temperature difference is increased, we observe a break-up of top–bottom symmetry. Hot fluid close to the cylinder rises upwards and flows downwards along the vertical wall. The velocity magnitude is highest close to the cylinder.In this case most of the heat is transferred via conduction and flow has a very small impact on temperature distribution. At higher Rayleigh number values, the differences are more visible, especially at the top of the cylinder. There, in the case of pure water, the contours are narrower than in the case of the nanofluid.

It is observed that in the heated circular cylinder case in Fig.6.9 and Fig6.10, the highest heat flux is located at the bottom of the cylinder.Considering the changes in heat flux along the z axis, at Ra $= 10^3$ the heat transfer is dominated by conduction and thus temperature contours keep the oval shape around the cylinder. Streamlines reveal a symmetrical flow field with a vortex on both sides of the cylinder. Vortex centres are located approximately on a diagonal line going through the enclosure from the top-left corner to the bottom-right corner.

At Ra=10^4 the heat transfer is dominated by convection mode and the differences are more visible, especially at the top of the cylinder.

Fig.6.15. Illustrates that the streamlines and isotherms at xy plane for Z =0.5 around the cylinder. Streamlines reveal a symmetrical flow field with a vortex on both sides of the cylinder. For higher Rayleigh numbers Ra = 10^5,10^6 most of the heat is transferred by convection and thus the heat conductivity of the working fluid is not very important. Then it is observed an increase in heat transfer, it is relatively smaller than the increase in the conduction dominated flow regime.

Comparing the results of the 2-D and 3-D simulations, it is observed no major differences in heat transfer enhancement. The 3-D simulation consistently shows slightly smaller heat transfer rates.

Fig.6.16. shows that the mean Nusselt number is found to be an increasing function of the nanoparticles volume fraction with respect to the Rayleigh number, especially in the convective regime.

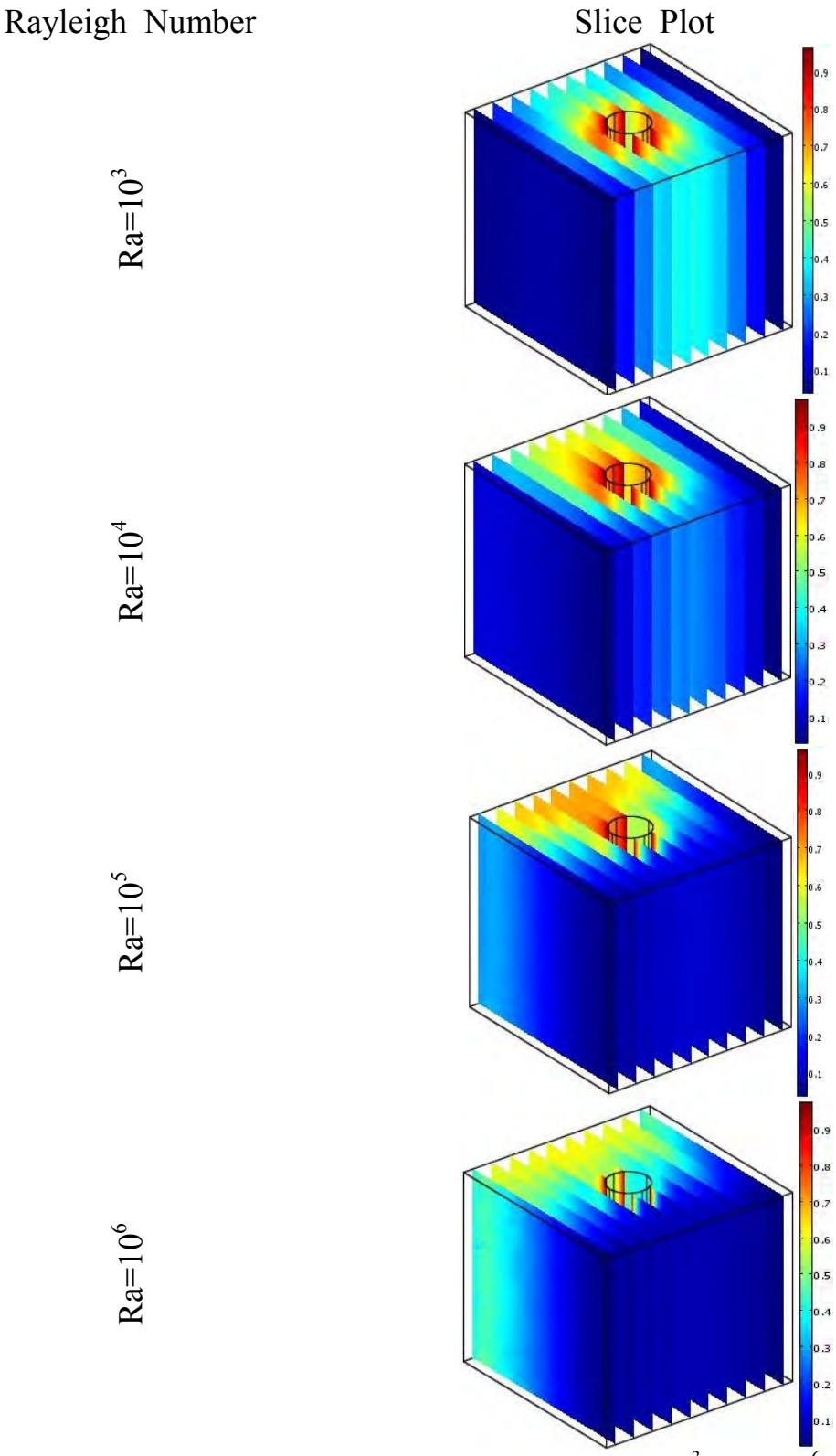

Fig. 6.9: Slice Plot of Cu-water nanofluid for Ra = 10^3 - Ra= 10^6 at φ=0.1

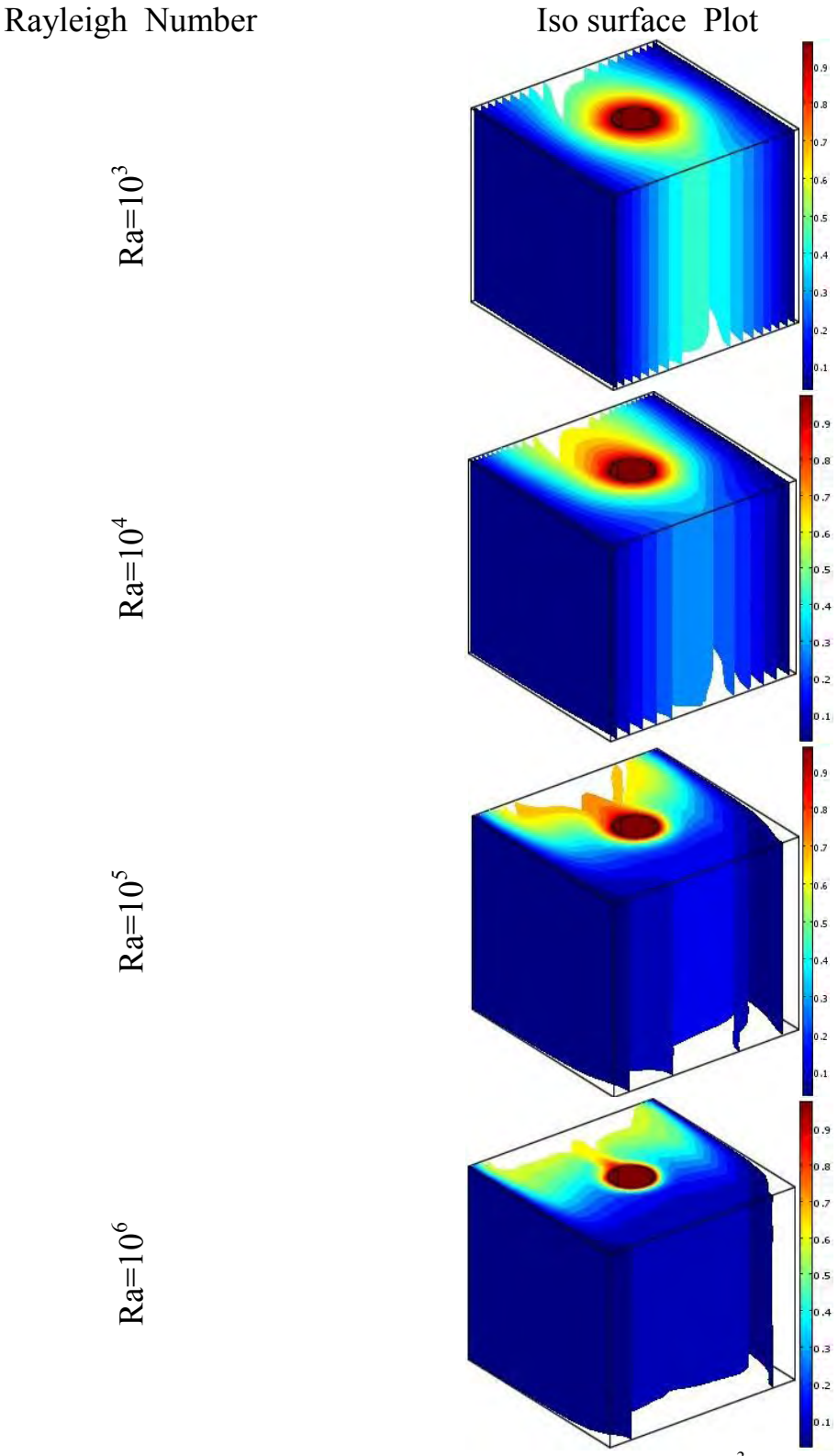

Fig. 6.10: Iso surface Plot of Cu-water nanofluid for Ra = 10^3 - Ra= 10^6 at φ=0.1

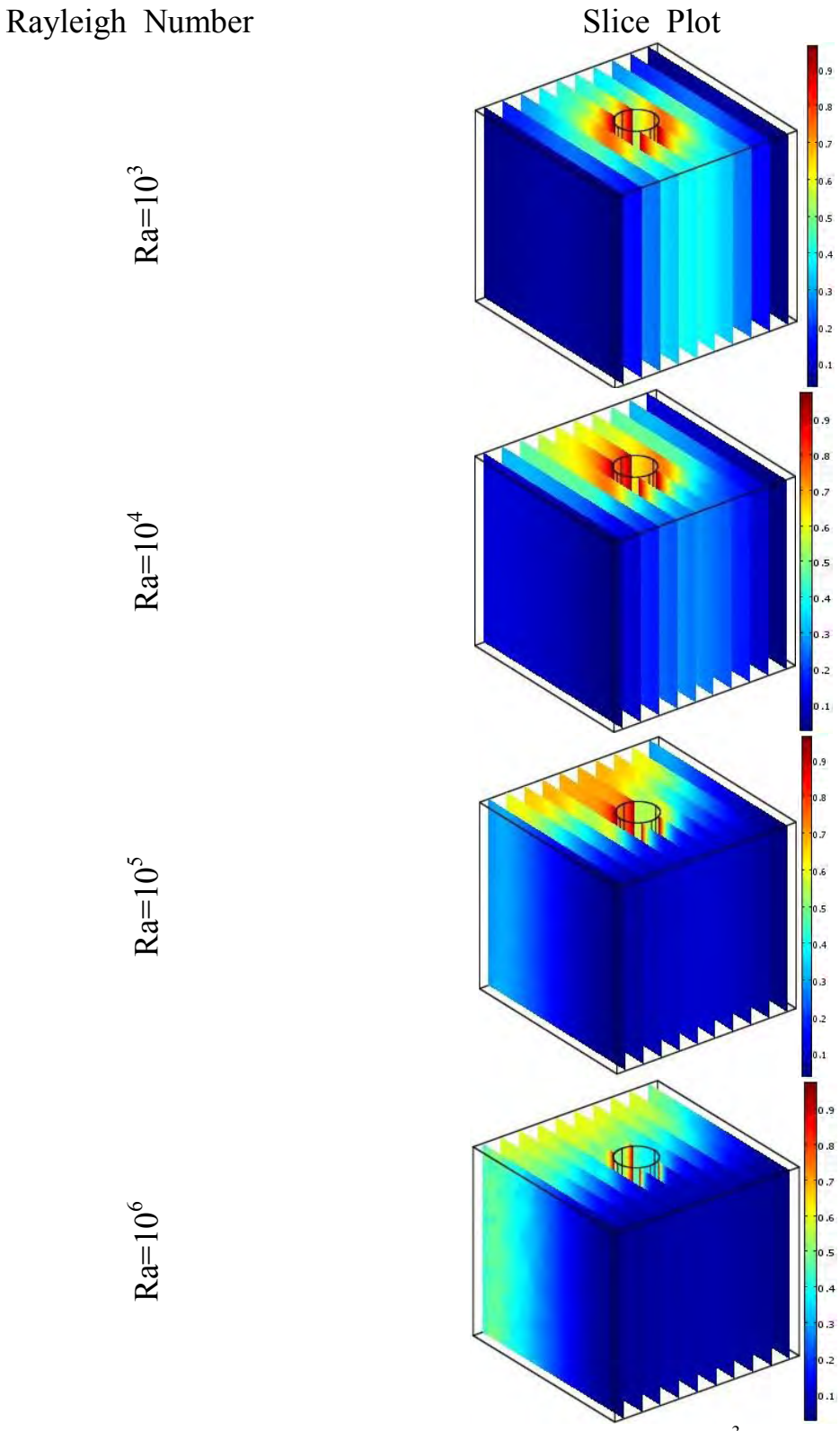

Fig. 6.11: Iso surface Plot of Cu-water nanofluid for Ra = 10^3 - Ra= 10^6 at φ=0.05

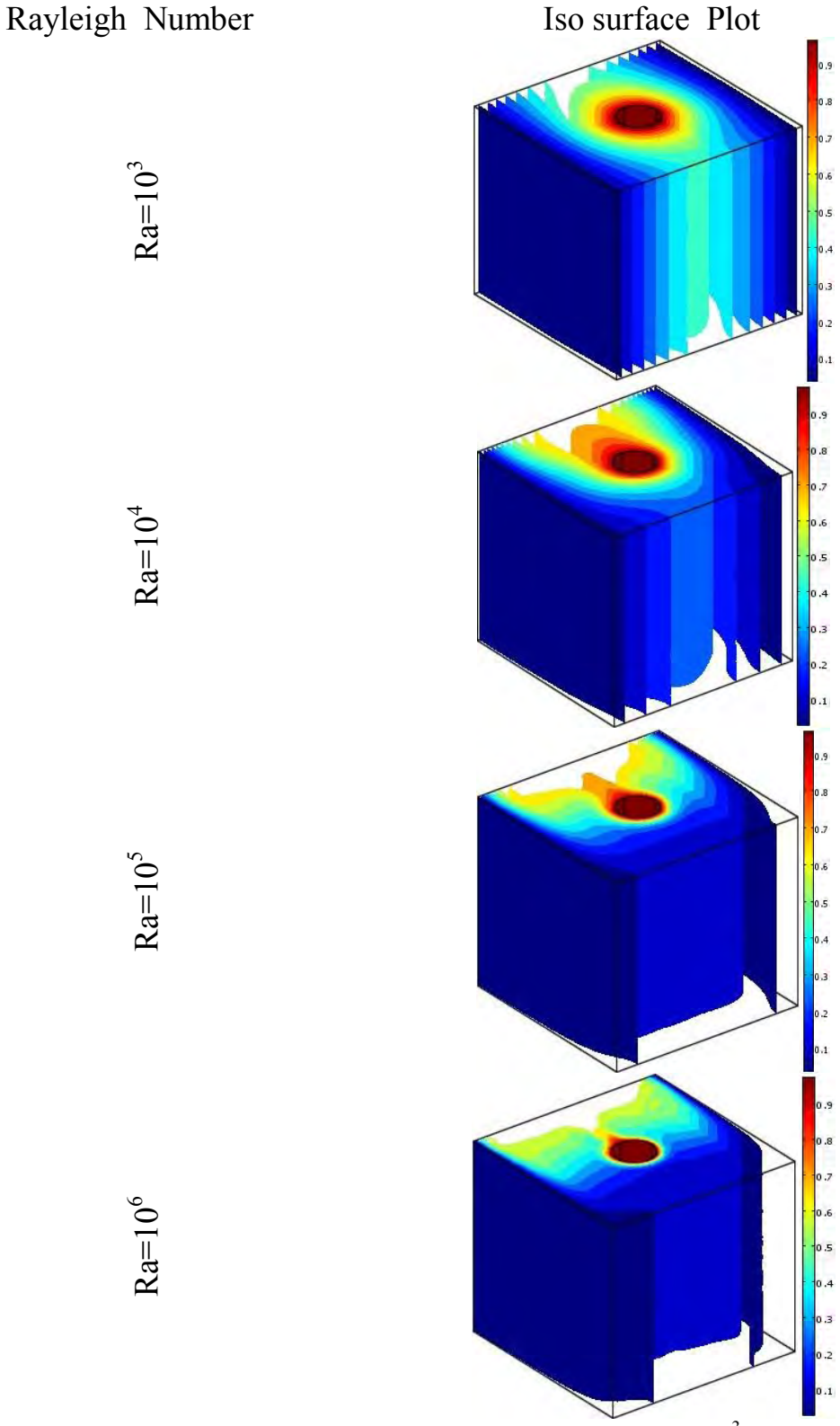

Fig. 6.12: Iso surface Plot of Cu-water nanofluid for Ra = 10^3 - Ra= 10^6 at φ=0.05

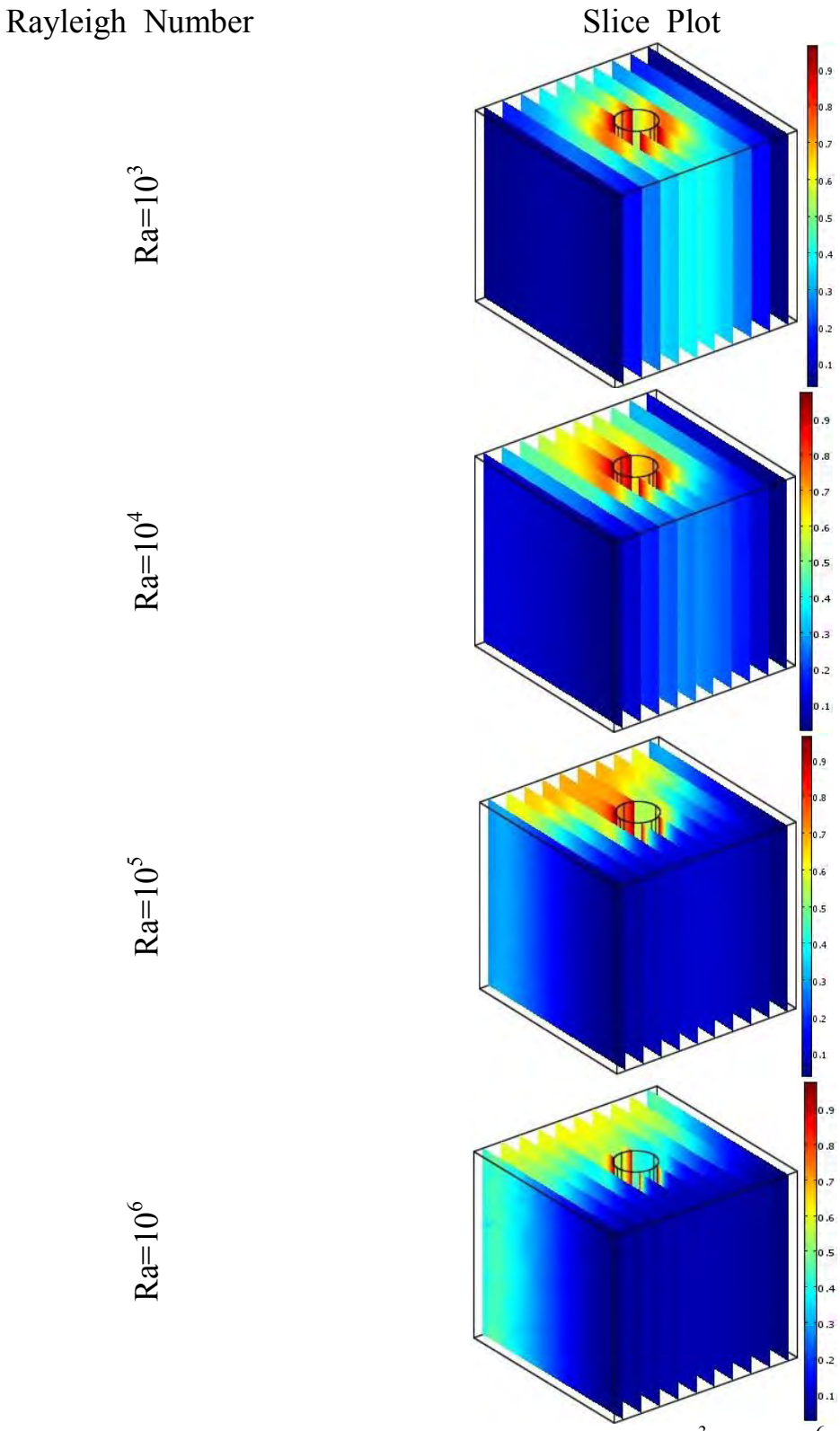

Fig. 6.13: Slice Plot of Cu-water nanofluid for Ra = 10^3 - Ra= 10^6 at φ=0.08

Rayleigh Number

Iso surface Plot

$Ra=10^3$

$Ra=10^4$

$Ra=10^5$

$Ra=10^6$

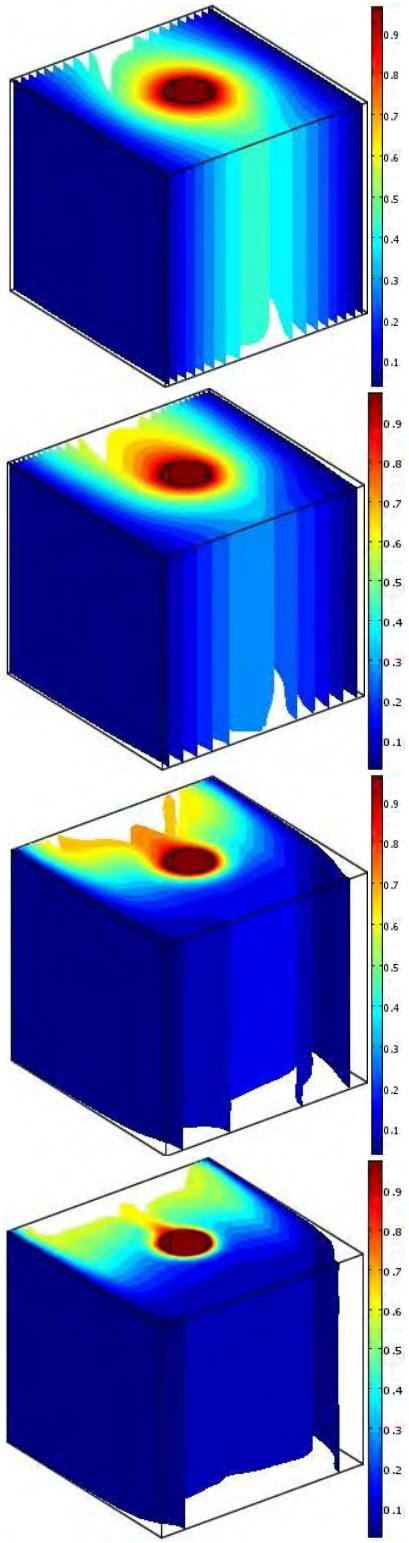

Fig. 6.14: Iso surface Plot of Cu-water nanofluid for Ra = 10^3 - Ra= 10^6 at φ=0.08

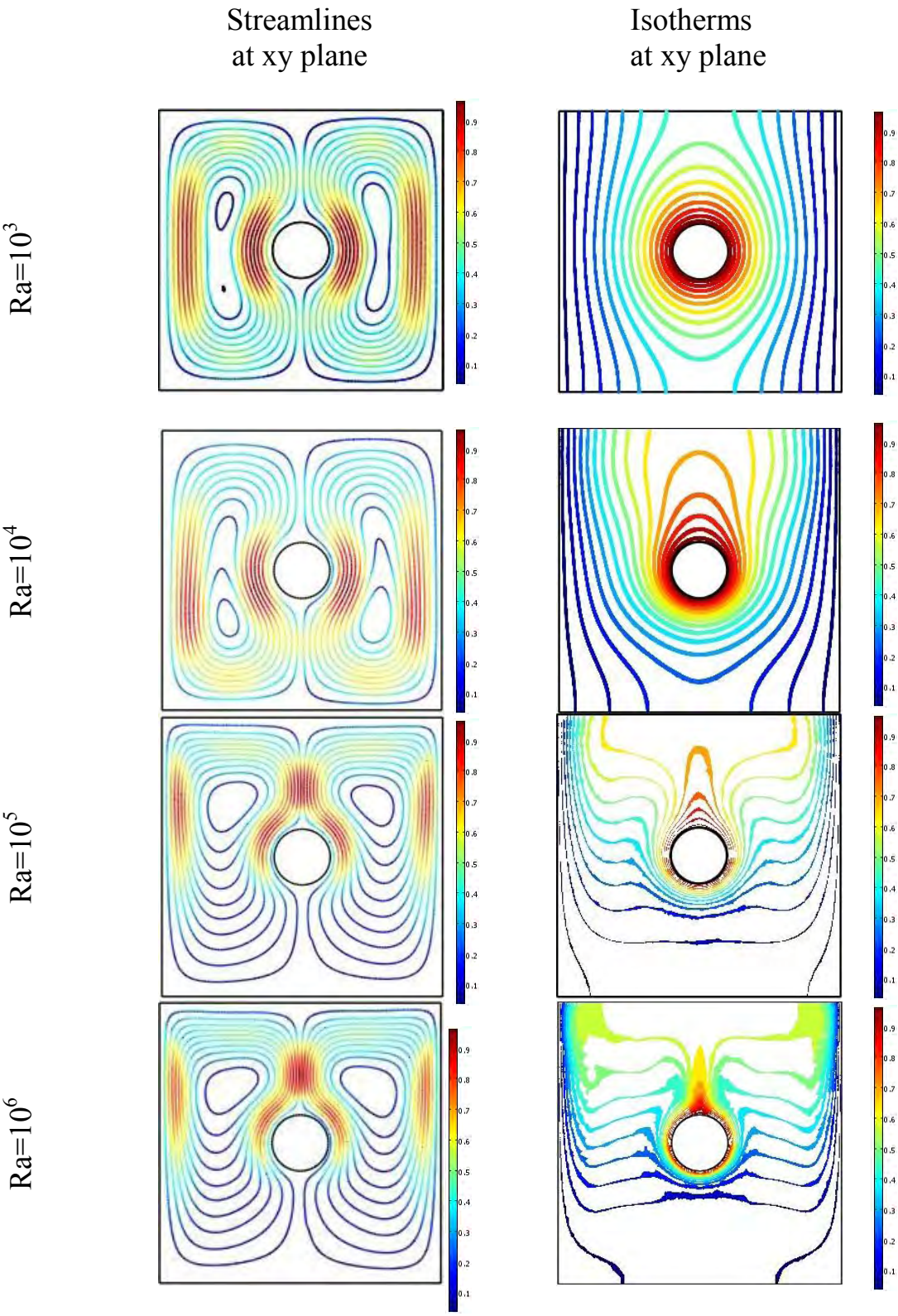

Fig. 6.15: Streamlines and Isotherms Plot of Cu-water nanofluid for Ra = 10^3 - Ra= 10^6 at φ=0.1

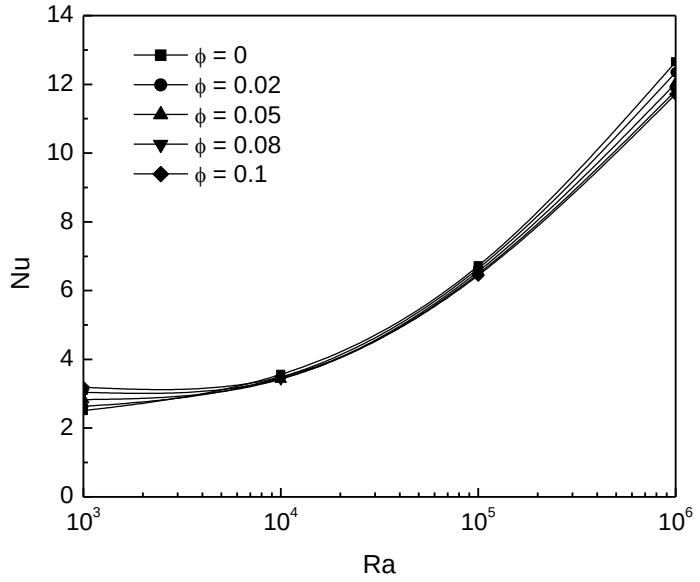

Fig.6.16. Variation of average Nusselt number for different volume fractions φ = 0, 0.02, 0.05, 0.08, 0.1 with Rayleigh numbers Ra = 10^3, 10^4, 10^5, 10^6.

CHAPTER 7

MHD Natural Convection of Cu-Water Nanofluid in Cubical Cavity with Circular Cylinder

7.1 Introduction

A schematic view of a cubical enclosure with circular disk considered in the present study is shown in Fig. 7.1. Side wall are the heated surfaces (hot and cold walls). Top and bottom walls with remaining walls of the enclosure and the circumference of cylinder are assumed to be adiabatic. The problem is considered three-dimensional. A uniform magnetic field strength of B_0 is considered in the horizontal direction. The enclosure is filled with Cu-water nanofluid ($Pr = 6.2$) and the thermophysical properties of Cu nanoparticles and water as base fluid are listed in Table 3.4. The nanofluid is considered to be Newtonian and the nanofluid flow is assumed to be laminar and incompressible. It is assumed that nanoparticles and base fluid are in thermal equilibrium and there is no slip between them.

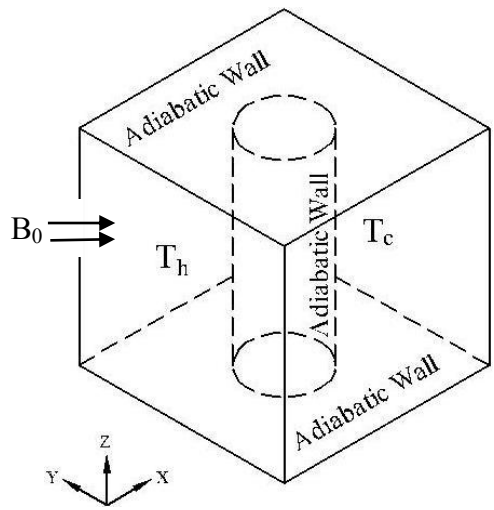

Fig.7.1: Schematic diagram of Cubical cavity with adiabatic cylinder

7.2 Results and discussion

No-slip condition is imposed on all surfaces. Thermal boundary conditions are $T = T_h$ for the left hot wall, $T = T_c$ for the right cold wall and $\partial T/\partial n = 0$ for the top, bottom and adiabatic cylinder's walls. The following boundary conditions are used.

On the hot wall: $U = V = W = 0$; $\theta = 1$

On the cold wall: $U = V = W = 0$; $\theta = 0$

On the adiabatic walls $U = V = W = 0$;

In this study, natural convection heat transfer in cubical enclosure with a circular cylinder in the presence of a magnetic field is investigated numerically using Finite Element Method. Calculations are made for the value of the Hartmann number Ha = 10 and various Rayleigh numbers Ra = 10^3, 10^4, 10^5 and 10^6. With each value of the Rayleigh number (Ra), the streamlines and the temperature iso-surfaces of the Cu–water nanofluid, with a volume fraction of φ = 0, 0.02, 0.05, 0.08 and 0.1 at Hartmann number Ha=10 are shown in Fig.7.2 to Fig.7.11 respectively. In the absence of the nanoparticle ($\varphi = 0$) and at a low value of the Rayleigh number, the dynamic field is plotted. In Fig. 7.2 the axis of rotation is parallel to the Z coordinate which can be related to the imposed thermal gradient. According to the 3-D presentation, the later is found unaccomplished. In fact, the flow field is divided into two symmetrical rolls, separated by the Z = 0.5 plane. In each side of the Z midplane, we denote a uniform circular motion of the nanofluid.

The increase in the Rayleigh number leads to the rolls elongation towards the two opposite top and bottom edges that are parallel to the axis of rotation. At Ra = 10^5, the convection mechanism starts to be more pronounced and then the rotation cells become more large near the active walls. By going far in the Rayleigh number value,

i.e., Ra = 10^6, the convection mechanism becomes more pronounced. The two symmetrical rolls are, then, merged to form a single one all along the rotation axis Z . Regarding the thermal field inside the cubical inclosure, the temperature iso-surfaces at various values of the Rayleigh number are visualized in Fig. 7.3. For the conductive mode, i.e., Ra = 10^3, the temperature iso-surfaces are uniformly distributed inside the cube, revealing a dominated-conduction heat transfer regime. Using an upper visualization, these iso-surfaces are found parallel to the rotation axis Z which explains then the topology of flow structures in the enclosure. As the Rayleigh number increases over than 10^4, the natural convection effect turns out to be dominant, and then, the isotherms are distributed in a stratified manner with an horizontal profile in the middle of the enclosure, whereas thin thermal boundary layers are shaped all along the active walls, indicating a large temperature gradient along these surfaces.Getting back to the upper visualization, the temperature iso-surfaces are found to be curved far from the center of the rotation axis. This seems to be in a great agreement with the previous flow predictions.The effect of the Cu nanoparticles volume fraction on the fluid and temperature fields is also investigated. Unlike the streamlines,where the same fluid motion is observed, the inspection of the isotherms at φ = 0.1 shows the decrease in the thermal boundary layer thickness to be less compact near the active walls, due to the high thermal conductivity of the considered nanoparticles. The increase in the magnitude of each velocity by increasing the Rayleigh number is a clear indication of a strong buoyant flow within the enclosure. The heat transfer mechanism is, therefore, expected to be due to convection when the conduction is responsible for the heat transfer at low Rayleigh number, i.e., $Ra \leq 10^4$.

Fig.7.12. represents that the heat transfer rate increases with an increase of the Rayleigh number but the increment of the nanofluid volume fraction leads to enhancement or deterioration of the heat transfer performance depending on the value of solid volume fraction of nanofluids and Rayleigh numbers.

Rayleigh Number	Slice Plot
$Ra=10^3$	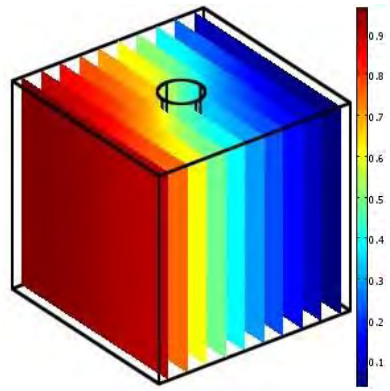
$Ra=10^4$	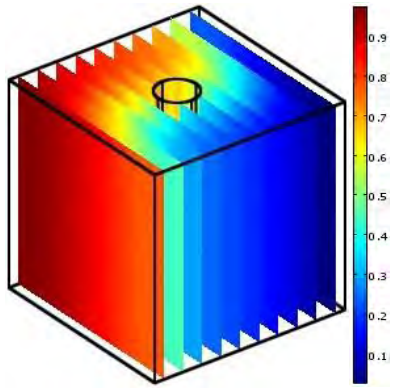
$Ra=10^5$	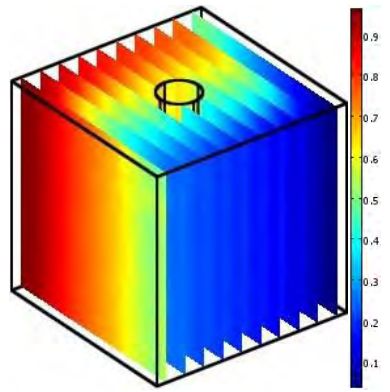
$Ra=10^6$	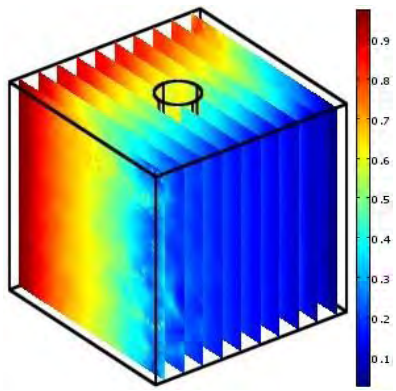

Fig.7.2: Slice Plot of pure water for Ra = 10^3 - Ra= 10^6 at φ=0

Rayleigh Number

Iso surface Plot

$Ra=10^3$

$Ra=10^4$

$Ra=10^5$

$Ra=10^6$

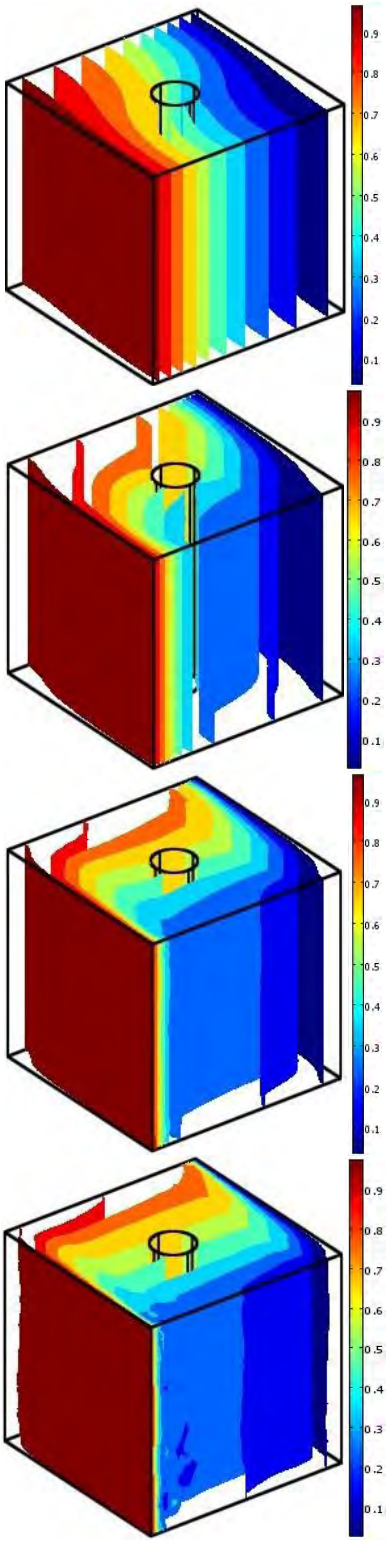

Fig 7.3: Iso surface Plot of Pure water for Ra = 10^3 - Ra= 10^6 at φ=0.

Rayleigh Number

Slice Plot

$Ra=10^3$

$Ra=10^4$

$Ra=10^5$

$Ra=10^6$

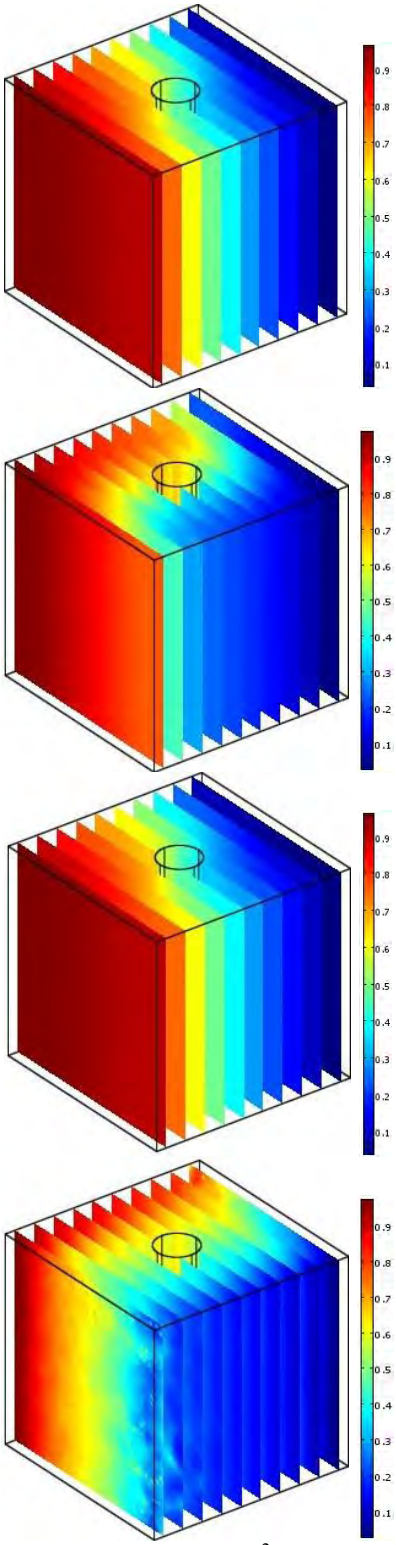

Fig 7.4: Slice Plot of Cu-water nanofluid for Ra = 10^3 - Ra= 10^6 at φ=0.02

Rayleigh Number

Iso surface Plot

$Ra=10^3$

$Ra=10^4$

$Ra=10^5$

$Ra=10^6$

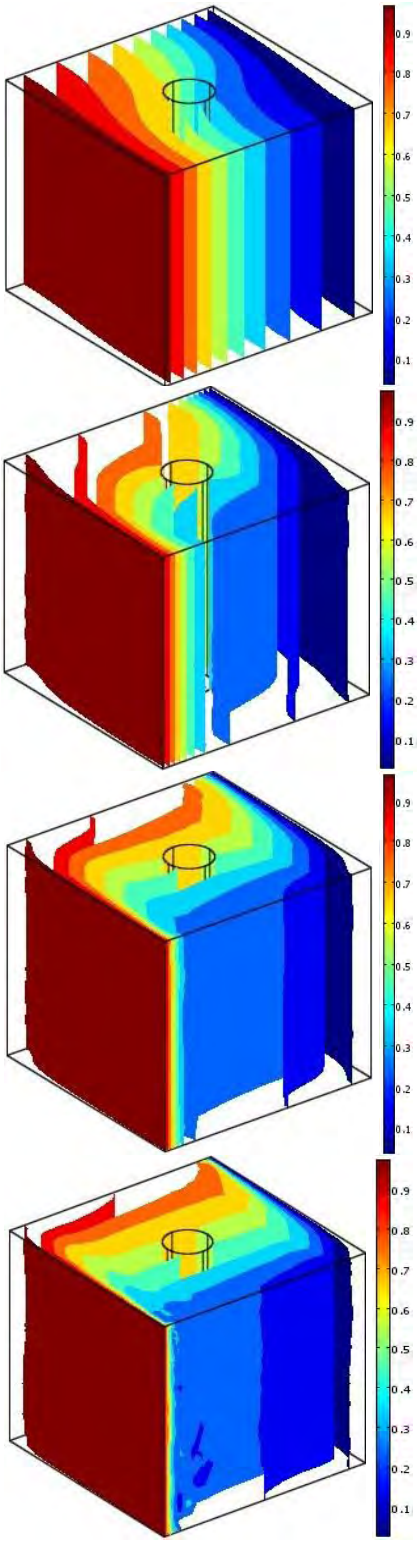

Fig 7.5: Iso surface Plot of Cu-water nanofluid for Ra = 10^3 - Ra= 10^6 at φ=0.02

Rayleigh Number

Slice Plot

$Ra=10^3$

$Ra=10^4$

$Ra=10^5$

$Ra=10^6$

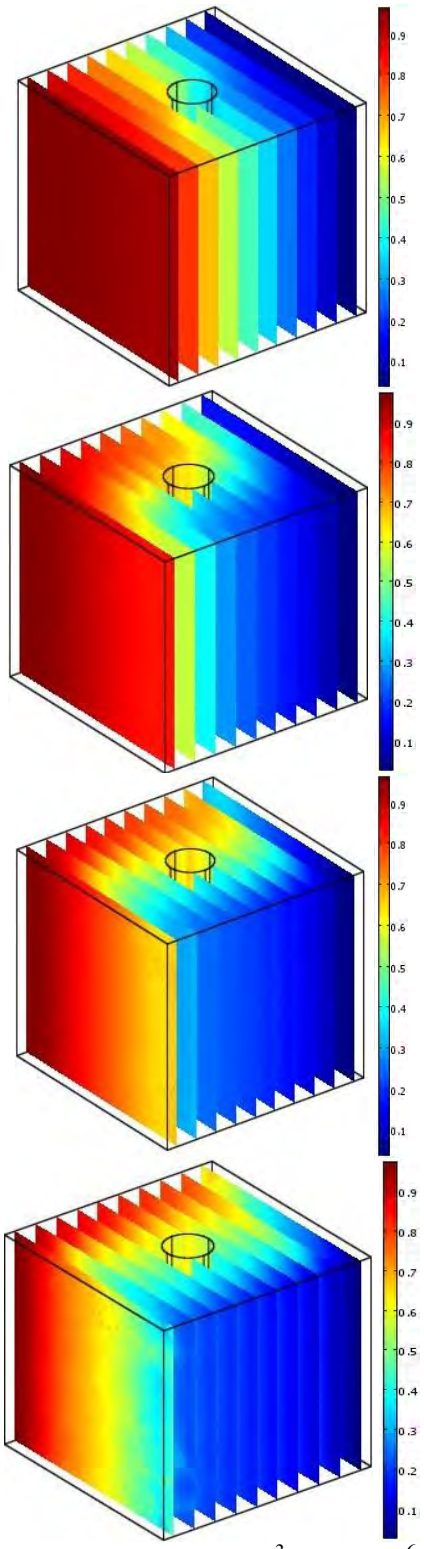

Fig 7.6: Slice Plot of Cu-water nanofluid for Ra = 10^3 - Ra= 10^6 at φ=0.05

Rayleigh Number

Iso surface Plot

$Ra=10^3$

$Ra=10^4$

$Ra=10^5$

$Ra=10^6$

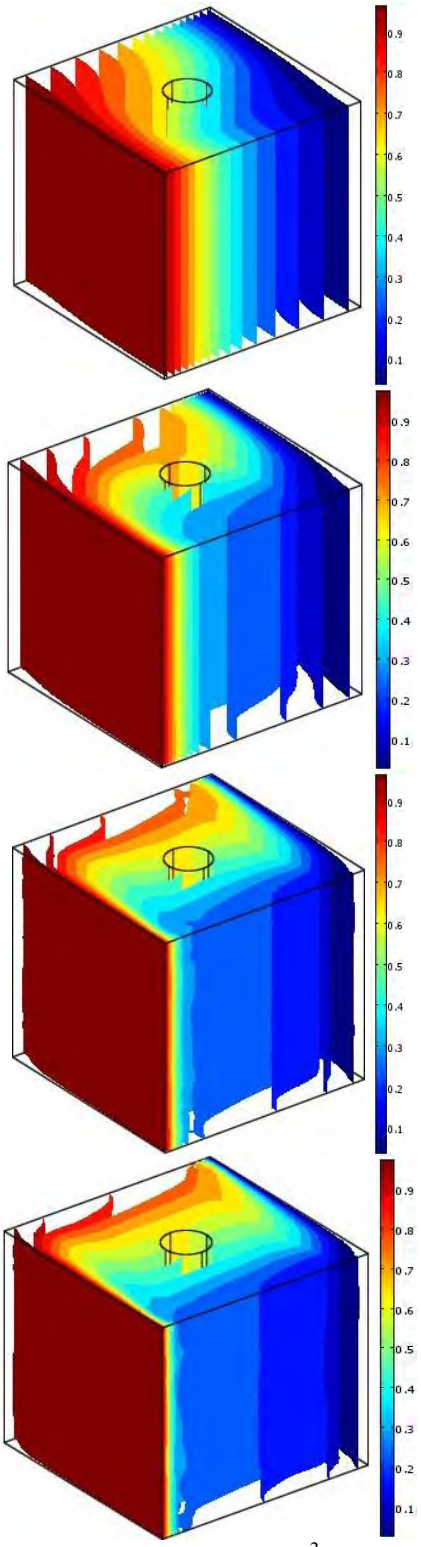

Fig 7.7: Iso surface Plot of Cu-water nanofluid for Ra = 10^3 - Ra= 10^6 at φ=0.05

Rayleigh Number

Slice Plot

$Ra=10^3$

$Ra=10^4$

$Ra=10^5$

$Ra=10^6$

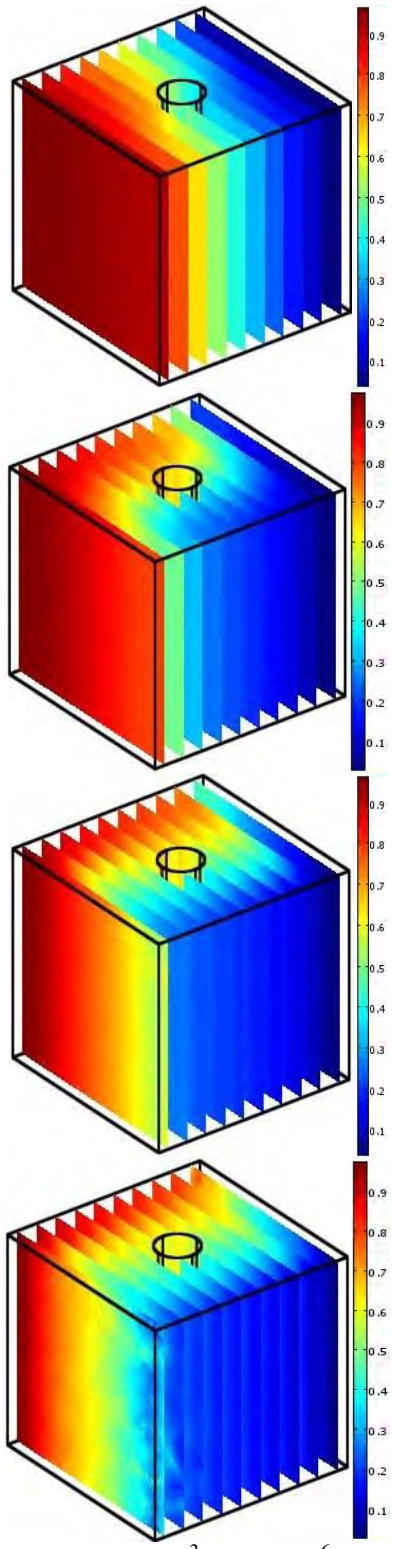

Fig 7.8: Slice Plot of Cu-water nanofluid for Ra = 10^3 - Ra= 10^6 at φ=0.08

Rayleigh Number

Iso surface Plot

$Ra=10^3$

$Ra=10^4$

$Ra=10^5$

$Ra=10^6$

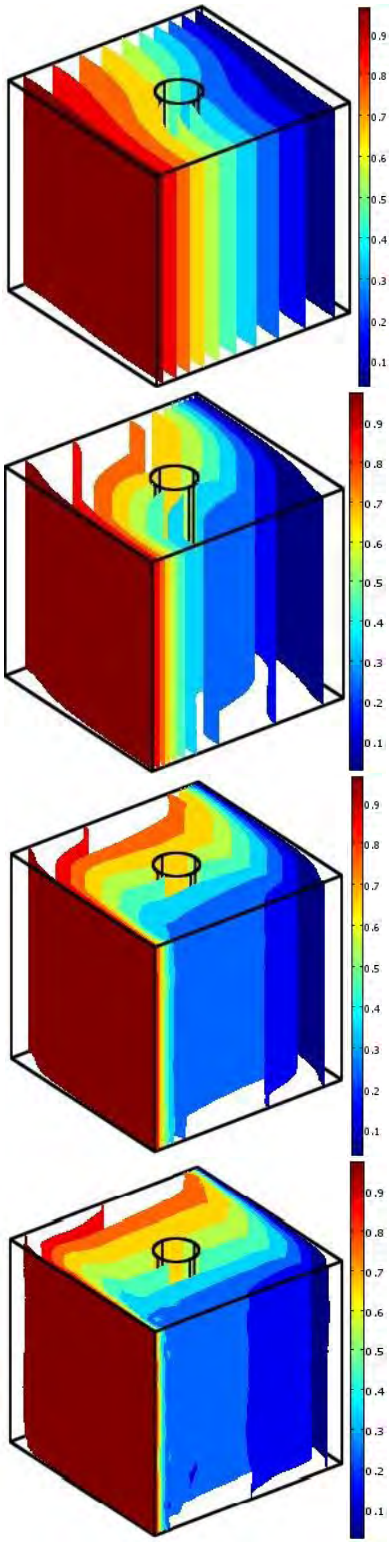

Fig 7.9: Iso surface Plot of Cu-water nanofluid for Ra = 10^3 - Ra= 10^6 at φ=0.08

Rayleigh Number

Slice Plot

$Ra=10^3$

$Ra=10^4$

$Ra=10^5$

$Ra=10^6$

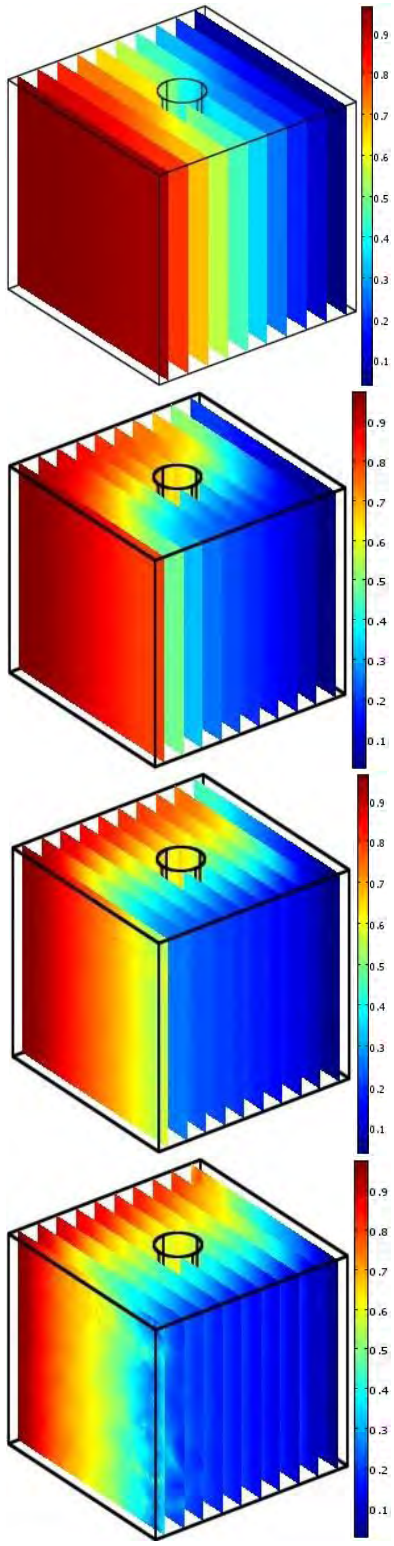

Fig 7.10: Slice Plot of Cu-water nanofluid for Ra = 10^3 - Ra= 10^6 at φ=0.1

Rayleigh Number

Iso surface Plot

$Ra=10^3$

$Ra=10^4$

$Ra=10^5$

$Ra=10^6$

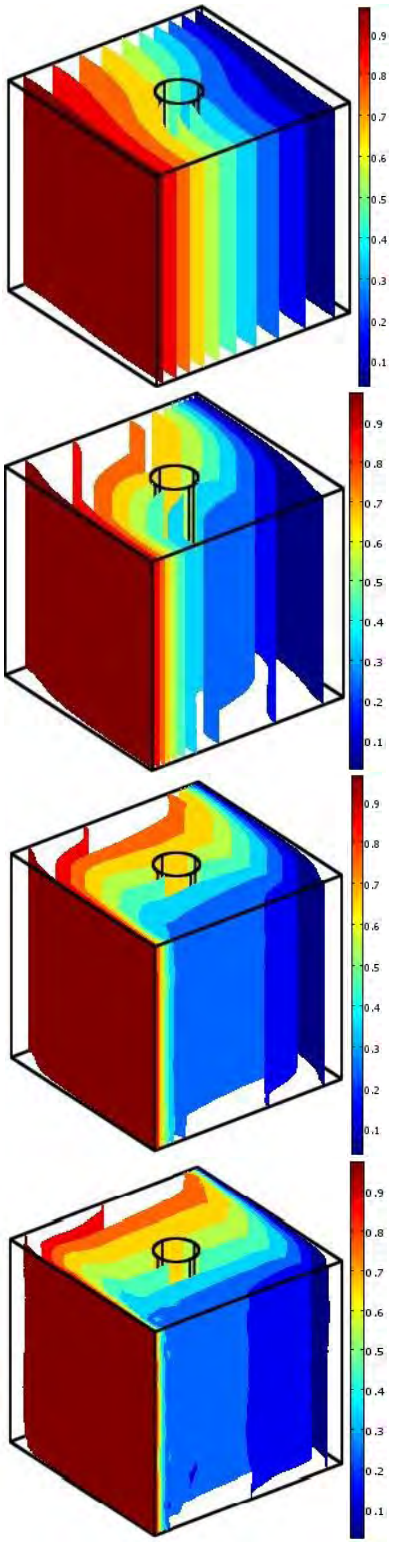

Fig 7.11: Iso surface Plot of Cu-water nanofluid for Ra = 10^3 - Ra= 10^6 at φ=0.1

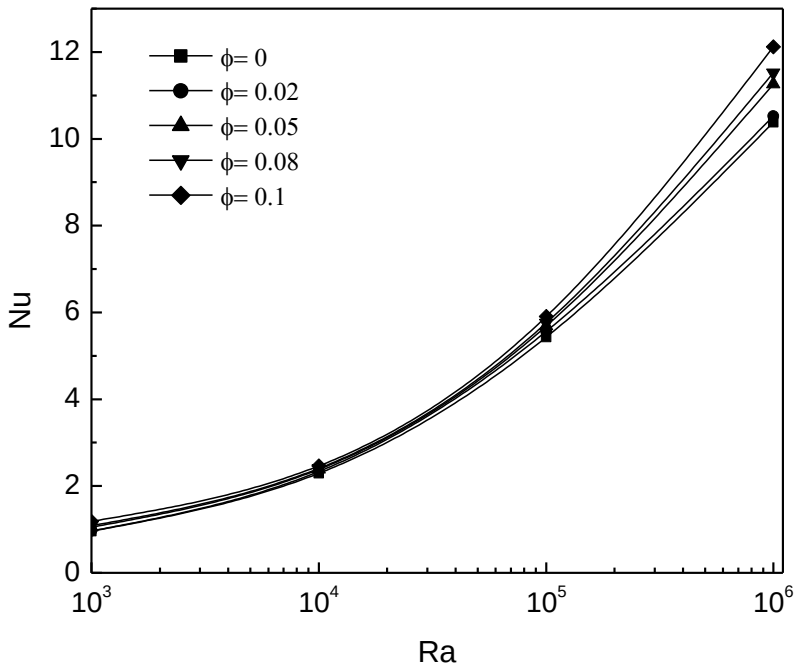

Fig.7.12. Variation of average Nusselt number for different volume fractions $\varphi = 0, 0.02, 0.05, 0.08, 0.1$ with Rayleigh number $Ra = 10^3, 10^4, 10^5, 10^6$.

CHAPTER 8

Conclusions

In the present paper a numerical investigation concerning the effects of average Nusselt number Nu_{avg}, the solid volume fraction φ of nanoparticle using different values of Rayleigh number Ra on velocity and temperature field in the square cavity is accounted. The subsequent findings can be seen from the current numerical analysis:

- Ra and φ significantly affect the configuration of the streamlines and isotherms within the square cavity.
- It is clear from the figures that the presence of the nanoparticle plays a significant role to increase the heat transfer.
- At high Rayleigh number maximum average Nusselt number has been found. Flow structures are sensitive to solid-particle concentration value.

In chapter 4, the effect of nanofluid on natural convection at a square cavity in the presence of a magnetic field is numerically studied. The cavity is filled with Cu-water nanofluid. The results were presented for Ra = 10^3, 10^4, 10^5, 10^6 with Ha = 0, 10 ,30, 50,100 and φ = 0, 0.05, 0.1, 0.15, 0.2. The results show that the solid volume fraction of the nanoparticles certainly enhances the heat transfer rate. An increase in Rayleigh number greatly enhances the heat transfer. The influence of the magnetic field is also studied and deduced that it has a remarkable effect on the heat transfer and flow field in the cavity. Overall Nusselt number is significantly decreased with Hartman number especially at high Rayleigh number.

The main conclusions of the analysis are:

- Use of nanofluid enhances heat transfer in most cases, where the majority of the heat is transferred by conduction. In cases, where convection is the dominant heat transfer mechanism, the heat transfer enhancement due to the use of a nanofluid is lower.
- Comparing the adiabatic and heated circular cylinders we observe similar heat transfer characteristics with the heated case yielding slightly better heat transfer rates.

- The increase is small in flows, where conduction dominates, while it is larger in convection dominated flows.
- Comparison of 2-D and 3-D simulations shows, that 3-D simulations yield slightly lower heat transfer rates. The difference is very small for conduction dominated flows, while in convection dominated flows it is larger. As the differences are small, 2-D simulations may be used to analyse such problems.
- A numerical study of MHD natural convection of Cu-water nanofluid filled in cubical enclosure with a circular cylinder has been performed. Following conclusions can be drawn from the numerical simulation results:
- The presence of the magnetic field retard the velocity field and isotherms profile.
- Averaged heat heat transfer decreases with increasing Hartmann number Ha.
- Magnetic field can be used to control the local heat transfer since magnetic field acts in a way to increase the heat transfer towards the right end of the bottom wall.
- When the solid volume fraction of nanoparticle is increased, heat transfer increases due to increase in effective thermal conductivity of the nanofluid which results in better thermal transport of the fluid.

Three dimensional natural convection investigation of Cu–water nanofluid has been performed through this paper. Effects of the Rayleigh number, the nanoparticles volume fraction and the average Nusselt numbers have been widely analyzed. The results may resume as follows:

- For low Rayleigh numbers ($Ra < 10^4$), the flow motion seems to be weak and the heat transfer is dominated by conduction.
- The increase in Rayleigh number over this limit, expressing a domination of the convection mode, leads to a lengthening of the flow cell near the insulated walls, with an ascent and a descent of the nanofluid along the hot and cold walls, respectively.
- The mean Nusselt number is found to be an increasing function of the nanoparticles volume fraction with respect to the Rayleigh number, especially in the convective regime, what makes the use of such nanoparticles recommended to improve heat exchange.

- The effect of nanoparticles volume fraction can be a key factor to increase (or decrease) the heat transfer.

8.1Extension of this work

The present work may be extended for consideration of following cases:

- Temperature dependent physical properties like viscosity, thermal conductivity and Prandtl number with different physics like heat generation/absorption, viscous dissipation, radiation effect, stress work and pressure work may be considered.
- Considering non-uniform cavity, porous medium and unsteady flow this work can be extended.
- Mixed and forced convection can also be considered through including the governing equation of concentration conservation.
- The study can be extended for turbulent flow using different fluids like, Newtonian or non-Newtonian fluid and different thermal boundary conditions such as heat flux.
- Considering critical behavior of the flow may extend this problem.

References

Abu-Nada, E., (2008): “Application of nanofluids for heat transfer enhancement of separated flows encountered in a backward facing step”, Int. J. Heat Fluid Flow, Vol. 29, pp. 242–249.

Abu-Nada, E., Oztop, H. F., (2009): “Effect of inclination angle on natural convection in enclosures filled with Cu-water nanofluid”, Int. J. Heat Fluid Flow, Vol. 30, pp. 669-678

Ahmed, G. R., Yovanovich, M. M., (1992): “Numerical study of natural convection from discrete heat sources in a vertical square enclosure”, Journal of Thermo Physics, Vol. 6, pp.121-127.

Alchaar, S., Vasseur, P., Bilgen, E., (1995): “Natural convection heat transfer in a rectangular enclosure with a transverse magnetic field”, Journal of Heat Transfer, Vol. 117, pp. 668–673

Alloui Z., Vasseur P. and Reggio M., (2011): “Natural convection of nanofluids in a shallow cavity heated from below”, Int. J. Therm. Sci., Vol. 50, No. 3, pp. 385–393.

Aminossadati S.M. and Ghasemi B., (2009): “Natural convection cooling of a localized heat source at the bottom of a nanofluid-filled enclosure”, Eur. J. Mech. B Fluids, Vol. 28, pp. 630-640.

Aminossadati, S. M., Ghasemi, B., (2005): “The Effects of Orientation of an Inclined Enclosure on Laminar Natural Convection”, Int. J. Heat Tech., Vol. 23, No. 2, pp. 43–49

Amara, S. B., Laguerrea, O., Mojtabi, M. C. C., Lartigue, B., Flick, D., (2008): “PIV measurement of the flow field in a domestic refrigerator model: Comparison with 3D simulations”, International Journal of Refrigeration, Vol. 31, pp. 1328-1340.

Basak, T., Roy, S., Bal Krishnan, A.R., (2006): “Effects of thermal boundary conditions on natural convection flows within a square cavity”, Department of Chemical Engineering, Vol. 49, pp. 4525–4535.

Barakos, G., Mitsoulis, E., Assimacopoulos, D., (1994): “Natural convection flow in a square cavity revisited: Laminar and turbulent models with wall functions", International Journal for Numerical Methods in Fluids, Vol. 18, pp. 695-719

Bejan, A., (2004): Convection heat transfer, John Wiley & Sons, Inc., Hoboken, New Jersey,USA.

Bilgen, E., (2005): “Natural convection in cavities with a thin fin on the hot wall”, International Journal of Heat and Mass Transfer, Vol. 48, pp. 3493–3505

Brinkman, H.C., (1952): “The viscosity of concentrated suspensions and solution”, Journal of Chemical Physics, Vol. 20, pp. 571–581

Cheikh, N.B., Campo A., Ouertatani N., Lili T., (2010): “Three-dimensional study of heat and fluid flow of air and dielectric liquids filling containers partially heated from below and entirely cooled from above”, Int. J. Heat Transfer., Vol. 37, pp. 449–456

Choi, S.U.S., (1995): “Enhancing Thermal Conductivity of Fluids with Nanoparticles”, ASME. Fluids Engineering Division, Vol. 231, pp. 99–105

Comini, G., Cortella, G., Manzan M., (1995): “Stream function-vorticity-based finite element formulation for laminar convection”, Numerical Heat Transfer, Part B, Vol. 28, pp. 1-22.

Das, S., Choi, S., Patel, H., (2006): Heat Transfer in Nanofluids-A review”, Heat Transfer Engineering, Vol. 27, pp. 3–19.

Davis, G.D.V., (1983): “Natural convection of air in a square cavity: A bench mark numerical solution, International Journal for Numerical Methods in Fluids”, Vol. 3, pp. 249-264 .

Ece, M.C., Buyuk, E., (2006): “Natural-convection flow under a magnetic field in an inclined rectangular enclosure heated and cooled on adjacent walls”, Fluid Dynamics Research, Vol. 38, pp. 564–590.

Frederick, R. L., Quiroz, F., (2000): “On the transition from conduction to convection regime in a cubical enclosure with a partially heated wall”, International Journal of Heat and Mass Transfer, Vol.44, pp, 1699-1709.

Fusegi, T., Hyun, J.M., Kuwahara, K., Farouk, B., (1991): “A numerical study of three-dimensional natural convection in a differentially heated cubical enclosure”, Int. J. Heat Mass Transfer, Vol. 34, pp. 1543–1557.

Garandet, J.P., Alboussiere, T., Moreau, R., (1992): “Buoyancy driven convection in a rectangular enclosure with a transverse magnetic field”, International Journal of Heat and Mass Transfer, Vol. 35, pp. 741–748.

Ghasemi, B., Aminossadati, S.M., Raisi, A., (2011): “Magnetic field effect on natural convection in a nanofluid-filled square enclosure”, International Journal of Thermal Sciences, Vol. 50, pp. 1748–1756.

Guiet, J., Reggio, M., Vasseur, P., (2012): “Natural Convection of Nanofluids in a Square Enclosure with a Protruding Heater”, Hindawi publishing corporation Advances in Mechanical engineering, Vol. 2012, pp. 1-11

Ha, M.Y., Jung, M. J., (2000): “A numerical study on three-dimensional conjugate heat transfer of natural convection and conduction in a differentially heated cubic

enclosure with a heat generating cubic conducting body", International Journal of Heat and Mass Transfer, Vol. 43, pp. 4229-4248.

Hattab, M.E.I., Mir, R., Hammami, Y.E.I., (2014): "Numerical Simulation of Natural Convection of Nanofluid in a Square Enclosure with a Protruding Isothermal Heater", International Journal on Heat and Mass Transfer - Theory and Applications (IREHEAT) Vol. 2 No.1, pp. 1–8

Jou, R.Y., Tzeng, S.C., (2006): "Numerical Research of Nature Convective Heat Transfer Enhancement Filled with Nanofluids in Rectangular Enclosures", International Communications in Heat and Mass Transfer, Vol. 33, pp. 727–736

Kakarantzas, S.C., Sarris, I.E., Grecos, A.P. and Vlachos, N.S. (2009): "Magnetohydrodynamic natural convection in a vertical cylindrical cavity with sinusoidal upper wall temperature," International Journal of Heat and Mass Transfer, vol. 52, pp. 250–259.

Khanafer, K., Vafai, K., Lightstone, M., (2003): "Buoyancy-driven Heat Transfer Enhancement in a Two-dimensional Enclosure Utilizing Nanofluids", International Journal of Heat and Mass Transfer, Vol. 46, pp. 3639–3653.

Kim, B. S., Lee, D. S., Ha M. Y. and Yoon, H. S. (2008): "A numerical study of natural convection in a square enclosure with a circular cylinder at different vertical locations", Int. J. Heat Mass Transfer, Vol. 51, pp, 1888–1906.

Koca, A., Oztop, H.F., Varol, Y., (2007), "The effects of Prandtl number on natural convection in triangular enclosures with localized heating from below", Int. Comm. Heat Mass Transfer Vol.34, 511–519.

Lee, J.R., Ha, M.Y., (2005): "A numerical study of natural convection in a horizontal enclosure with a conducting body", Int. J. of Heat Mass Transf., Vol. 48, pp. 3308-3318.

Mahian O., Kianifar A., Kalogirou S.A., Pop I. and Wongwises S., (2013): "A review of the applications of nanofluids in solar energy", International Journal of Heat and Mass Transfer, , Vol. 57, pp. 582-594.

Mahmoodi M., (2011): "Numerical Simulation of Free Convection of a Nanofluid in L-Shaped Cavities", International Journal of Thermal Sciences, Vol. 50, No. 9, pp. 1731-1740.

Mahmoudi, A.H., Pop, I., Shahi, M., (2012): "Effect ofmagnetic field on natural convection in a triangular enclosure filled with nanofluid", Int. J. Therm. Sci. Vol. 59, pp. 126–140.

Mahdy, A., Elshehabey, H.M., (2012): “Uncertainties in physical property effects on viscous flow and heat transfer over a nonlinearly stretching sheet with nanofluids”, Int. Commun. Heat Mass Transfer, Vol. 39, No. 5, pp. 713–719.

Maxwell, J., (1904): “A Treatise on Electricity and Magnetism”, second ed. Oxford University Press, Cambridge, UK.

Nasrin, R., Alim, M.A., Chamkha, A.J., (2012): “Combined convection flow in triangular wavy chamber filled with water-CuO nanofluid: Effect of viscosity models”, Int. Commun. In Heat and Mass Transf. Vol. 39, No. 8, pp. 1226-1236.

Nithyadevi, N., Yang, R., (2009): “Magnetoconvection in an enclosure of water near its densitymaximum with Soret and Dufour effects”, Int. J. Heat Mass Transfer, Vol. 52, pp. 1667–1676.

Ogut, E.B. (2009): “Natural convection of water-based nanofluids in an inclined enclosure with a heat source”, International Journal of Thermal Sciences, Vol.48, pp. 2063-2073.

Ostrach, S., (1998): “Natural convection in enclosures”, Int. J. Heat Transfer, Vol. 110, pp. 1175–1190.

Oztop, H.F., Abu-Nada, E., (2008): “Numerical Study of Natural Convection in Partially Heated Rectangular Enclosure Filled with Nanofluids”, International Journal of Heat and Fluid Flow, Vol. 29, pp. 1326–1336.

Ozoe, H., Okada, K., (1989): “The effect of the direction of the external magnetic field on the three dimensional natural convection in a cubical enclosure”, International Journal of Heat and Mass Transfer, Vol. 32, pp. 1939–1954.

Parvin, S., Nasrin, R., Alim, M.A., Hossain, N.F., Chamkha, A.J., (2012): “Thermal conductivity variation on natural convection flow of water-alumina nanofluid in an annulus”, Int. J. of Heat and Mass Transf., Vol. 55, No. 19-20, pp. 5268-5274.

Pak, B. C., Cho, Y. I., (1998): Hydrodynamic and Heat Transfer Study of Dispersed Fluids with Submicron Metallic Oxide Particles,” Exp. Heat Transfer, Vol. 11, No. 2, pp. 151-170.

Patankar S.V., (1980): "Numerical Heat Transfer and Fluid Flow", McGraw-Hill, New Yor Pirmohammadi, M., Ghassemi, M., (2009): “Effect of magnetic field on convection heat transfer inside a tilted square enclosure”, International Communications in Heat and Mass Transfer, Vol. 36, pp. 776–780.

Patankar, S.V., (1980):”Numerical Heat Transfer and Fluid Flow”, Hemisphere Publishing Corporation, New York, Taylor and Francis Group

Phelan, P.E., Bhattacharya, P., Prasher, R.S., (2005): “Nanofluids for Heat Transfer Applications”, Annual Review of Heat Transfer, Vol. 14, pp, 255–275.

Ravnik, J., Skerget, L., Hribersek, M., (2010): “Analysis of three-dimensional natural convection of nanofluids by BEM”, Engineering Analysis with Boundary Elements, Vol. 34, pp. 1018-1030.

Roslan, R., Saleh, H., Hashim, I., (2011): “Buoyuancy driven heat transfer in a naonofluid filled trapezoidal enclosure with variable thermal conductivity and viscosity”, Numerical Heat Transfer, Vol. 60, No. 10, pp. 867-882.

Rudraiah, N., Barron, R.M., Venkatachalappa, M., Subbaraya, C.K., (1995): “Effect of a magnetic field on free convection in a rectangular enclosure”, International Journal of Engineering Science, Vol. 33, pp. 1075–1084.

Sheikholeslami, M. , Gorji-Bandpay, M.and Ganji, D. D. (2012):“Magnetic field effects on natural convection around a horizontal circular cylinder inside a square enclosure filled with nanofluid,” International Communications in Heat and Mass Transfer, vol. 39, no. 7, pp. 978–986.

Sheikhzadeh, G. A., Arefmanesh, A., Kheirkhah, M. H., Abdollahi, R., (2011): Natural convection of Cu–water nanofluid in a cavity with partially active side walls”, Eur. J.Mech. B-Fluid, Vol. 30, No. 2, pp. 166-176.

Sivasankaran, S., Ho, C.J., (2008): “Effect of temperature dependent properties on MHD convection of water near its density maximum in a square cavity”, International Journal of Thermal Sciences, Vol. 47, pp. 1184–1194.

Sourtiji, E., Hosseinizadeh S.F., (2012): “Heat transfer augmentation of magneto hydrodynamic natural convection in L-shaped cavities utilizing nanofluids”, Thermal Science, Vol. 16, pp. 489-501.

Teamah, M. A., El-Maghlany W.M., (2012): “Augmentation of natural convective heat transfer in square cavity by utilizing nanofluids in the presence of magnetic field and uniform heat generation/absorption”, International Journal of Thermal Sciences, Vol. 58, pp. 130-142.

Tiwari, R.K., Das, M.K.(2007): “Heat transfer augmentation in a two-sided lid-driven differentially heated square cavity utilizing nanofluids”, International Journal of Heat and Mass Transfer,Vol. pp.2002–2018.

Trisaksri, V., Wongwises, S., (2007): “Critical review of Heat Transfer Characteristics of Nanofluids”, Renewable and Sustainable Energy Reviews, Vol. 11, pp. 512–523.

Valencia, A., Frederick, R.L., (1998): “Heat transfer in square cavities with partially active vertical walls”, Int. J. Heat Mass Transfer, Vol. 32, pp. 1567–1574.

Venkatachalappa, M., Subbaraya, C.K., (1993): “Natural convection in a rectangular enclosure in the presence of a magnetic field with uniform heat flux from the side walls”, Acta Mechanica, Vol. 96, pp. 13–26.

Wang, X.Q., Mujumdar, A.S., (2007): “Heat Transfer Characteristics of Nanofluids: A review”, International Journal of Thermal Sciences, Vol. 46, pp. 1–19.

Xuan, Y., Roetzel, W., (2000), “Conception for Heat Transfer Correlation of Nanofluids”, International Journal of Heat and Mass Transfer, Vol. 19, pp. 3701–3707.

Xuan Y.M., Li, Q, (2000): “Heat transfer enhancement of nanofluids”, Int. J. Heat Fluid Flow, Vol. 21, pp. 58–64.